Journal of Geoscience and Environment Protection, 2026, 14(6), 169-224
https://www.scirp.org/journal/gep
ISSN Online: 2327-4344
ISSN Print: 2327-4336

A Pragmatic Approach for Using Conventional Electron Microprobe Analyses to Obtain Reliable Formulae for Differentiated Alkali Igneous Rock Amphiboles by Assessing the Possible Presence of Oxy-Amphibole Components

C. Michael B. Henderson[1], Roger H. Mitchell[2]

[1]School of Earth and Environmental Sciences, Williamson Research Laboratories, University of Manchester, Manchester, UK
[2]Department of Geology, Lakehead University, Thunder Bay, Canada
Email: michael.henderson@manchester.ac.uk

How to cite this paper: Henderson, C. M. B., & Mitchell, R. H. (2026). A Pragmatic Approach for Using Conventional Electron Microprobe Analyses to Obtain Reliable Formulae for Differentiated Alkali Igneous Rock Amphiboles by Assessing the Possible Presence of Oxy-Amphibole Components. *Journal of Geoscience and Environment Protection, 14,* 169-224.
https://doi.org/10.4236/gep.2026.146010

Received: April 27, 2026
Accepted: June 23, 2026
Published: June 26, 2026

Abstract

Conventional electron probe microanalysis (EPMA) provides major and minor element data that lack water and Fe valence information, requiring calculation of Fe^{3+}/Fe^{total} ratios based on amphibole stoichiometry. Amphibole compositions, particularly in alkaline rocks, show the presence of extra oxygen (denoted $^{W}O^{2-}$ here) replacing (OH) (i.e., the oxyamphibole molecule). Micro-analytical and spectroscopic published work provides 'full' analyses which allow refinement of protocols for modelling amphibole formulae and calculation of Fe^{3+}/Fe^{total} ratios for a wide-range of amphiboles in alkaline igneous rocks. In this paper formula calculation protocols are checked against the compositions of hypothetical stoichiometric amphiboles with chosen proportions of vacant sites and fixed values for Fe^{3+} and Fe^{2+}. A spreadsheet for EMP analyses of Ca- and Na-rich amphiboles in alkaline igneous rocks with any content of vacancies in A, is provided to calculate formulae on a stoichiometric (23 O + $^{W}O^{2-}$/2) formula basis, with Fe^{3+} estimated for a 13 cation calculation. Ca-Na amphiboles generally have higher $^{W}O^{2-}$ than Na-amphiboles requiring their $^{W}O^{2-}$ contents to be assessed if reliable Fe-oxidation states are to be estimated. The preferred $Fe^{3+}/\Sigma Fe$ calculation protocol is assessed for published amphibole compositions with Fe-valence values determined by Mössbauer spectroscopy confirming the earlier reports that many amphiboles, especially Ti-rich samples, have high extra-O and may possess excess cations in the C cation group. A scheme is developed to quantify this excess (denoted ΔC) giving the relation-

ship $\Sigma^{13}_{cations} = \Sigma^{16}_{cations} - \Sigma(Ca + Na + K) - \Delta C$. It is found that many amphiboles have relatively low $Fe^{3+}/\Sigma Fe$ values (0.1 - 0.3) consistent with equilibration near the QFM buffer.

Keywords

Amphibole Stoichiometry, Oxo-Amphiboles, Vacant Cation Sites, Ti-Rich Amphiboles, 24 Anion Calculation, $Fe^{3+}/\Delta Fe$ Modelling, Alkaline Rocks

1. Introduction

The compositions and crystal structures of natural amphiboles store important data regarding the formation conditions including, temperature, pressure, and volatile activities (H_2O, CO_2, F, Cl, possibly S), with the oxygen fugacity playing a key control on the 'equilibrium' Fe oxidation state (e.g., see Ridolfi & Renzuli, 2012). In addition, research on amphibole dehydration/dehydrogenation mechanisms is key to understanding igneous processes in different tectonic environments (e.g., Darby Dyar et al., 1993; Han et al., 2024; Della Ventura et al., 2024). Early Ca-amphibole analyses were determined using classical gravimetric, volumetric, and flame photometric methods; such fully-analysed data included determination of water and values for both FeO and Fe_2O_3, with formulae calculated for a 24 anion formula (e.g., Deer, 1938; Prider, 1939; Borley & Frost, 1963; Henderson, 1968); also see the published amphibole data reported in Table 12 (Deer et al., 1997). Thus, such compositions were effectively recalculated on a 24 (O, OH, F, Cl) basis but equivalent extra-O contents were not reported. Assuming stoichiometry (see below), extra-O would be calculated as $^{W}O^{2-} = 24 - 22 - (OH + F + Cl)$ atoms per formula unit (apfu). However, it has become common practice to report amphibole formuale on a basis with (OH, F, Cl) = 2.000 apfu if the water content is not known reliably (*cf.* Hawthorne et al., 2012); note that that approach sets $^{W}O^{2-}$ to zero.

In the 1970s, the use of the electron microprobe analyser (EMPA) provided mineral 'spot' analyses, on a scale of a few microns that revolutionised the study of rocks. Conventional EMP analysis cannot provide separate values for Fe^{3+} and Fe^{2+}; and H/H_2O cannot be measured although F, Cl, and S can be determined. This has led to the convention for anhydrous minerals (e.g., pyroxene, magnetite) of reporting all iron as FeO followed by calculation of model Fe^{3+} values assuming strict stoichiometry on the basis of fixed numbers of atoms of oxygen. Amphibole calculations are made assuming 'anhydrous' equivalent formulae for amphiboles with 23 oxygens (23 O); i.e., $AB_2C_5T_8O_{22}(OH)_2 = AB_2C_5T_8O_{23} + H_2O$. This approach implies that formulae must have fully-occupied cation (A-T) and anion (O, (OH)) sites, and this assumption has been a continuing problem for both amphiboles and micas in which vacant sites may occur in some species, particularly in micas. In addition, a further problem for these hydrous minerals is that extra-

O atoms (O^{2-}) might be present, replacing $(OH)^-$ anions at the O(3) site (Hallimond, 1941; Robinson et al., 1982; Robinson et al., 1997, Oberti et al., 2018) The anhydrous calculation assumes that all the hydroxyl sites are occupied by $(OH)^-$, F^- or Cl^-; the fact that all are univalent means that the presence of F or Cl could be ignored and any present treated only as OH (*cf.* Schumacher, 1991), but the extra valence on O^{2-} replacing $(OH)^{-1}$ means that extra-O must be identified and allowed for.

Some authors have advanced the understanding of this relationship for amphiboles and biotites e.g.: 1) H/H_2O values were obtained by ion probe (SIMS; Righter et al., 2002) or other advanced methods (Virgo & Popp, 2000); 2) Fe^{3+} and Fe^{2+} analyses were obtained by X-ray Absorption Near Edge analysis (XANES; Dyar et al., 2016), Mössbauer spectroscopy (Dyar et al., 1993; Righter et al., 2002), or less directly by involving X-ray single crystal diffraction scattering techniques and stoichiometric/charge balance considerations (e.g., Ventruti et al., 2020); 3) a modified EMP technique has been developed to obtain separate Fe valence data by analysing the flank structure of the Fe *L* peak (Li et al., 2019; Hezel et al., 2024). None of these methods is straightforward and might even require synchrotron facilities (Berry et al., 2010). For conventional EMP amphibole analyses, Microsoft EXCEL spreadsheets based on phases without specified extra-O (i.e. (OH + F) = 2) were published by Tindle & Webb (1994), while Locock (2014) used the relationship $2Ti = {}^{W}O^{2-}$ (Hawthorne et al., 2012) to subtract an estimated extra-O content from the W group to provide amphibole formulae on an (OH, F, Cl) = 2 basis (see later).

However, using data from multi-technique analytical approaches described above, Ridolfi et al. (2018) and Li et al. (2020a) recently published spreadsheets to obtain **full** formulae for amphiboles, with quantified extra-O parameters. In our work, the input data are conventional EMP analyses with all iron reported as FeO and lacking water determinations. Thus, in this paper we use an EXCEL spreadsheet to model different approaches for using conventional EMP analyses to obtain estimates for the Fe^{3+}, Fe^{2+} contents of amphiboles occurring commonly in alkaline igneous rocks (see spreadsheet attached as Supplementary Excel file 1). Note that a similar approach for biotite with extra-O was provided by Li et al. (2020b) which Henderson (2025) used as a basis for developing a calculation scheme for biotite from alkali igneous rocks.

Thus in this paper we extend the approach of Henderson (2025) by studying published Ca- and Na-rich amphiboles from world-wide alkali- rich igneous rocks including crustal intrusive complexes and upper mantle samples, especially those rich in TiO_2. The work is based on conventional EMP analyses of amphiboles, and is aimed at obtaining reliable Fe valence data by incorporating extra-O parameters obtained using the Li et al. (2020a) spreadsheet. Thus, we modify a conventional 23 O calculation to one involving an extra-O proportion of ${}^{W}O^{2-}$. We will also assess the formula calculation method used by many researchers who simply add sufficient water to a wt.% EMP anhydrous analysis to provide an amphibole for-

mula normalised to (OH + F + Cl) = 2.000 apfu, effectively setting a possible $^{W}O^{2-}$ component to zero, perhaps even for Ti-rich amphiboles (Tindle & Webb, 1994; also see Oberti et al., 1992; Andersen & Sørensen, 1993; Moreau et al., 1996; Möller & William-Jones, 2016).

This paper describes an empirical, stepwise approach to providing petrological users, having conventional EMP amphibole analyses, with a method for obtaining reliable Fe-valence estimates, particularly for Ca-rich amphiboles in differentiated, alkaline igneous rocks which may have oxy-amphibole components.

2. Amphibole Stoichiometry

The general 24 anion formula (Deer et al., 1997; Leake et al., 1997; Hawthorne et al., 2012; Ridolfi et al., 2018) for amphiboles can be written $A_{0\text{-}1}B_2C_5T_8O_{22}W_2$ where: A is occupied by Na^+, K^+ or a vacancy (□); B (2 *M*4 sites) contains Na^+, K^+, Ca^{2+}, (possibly Mn^{2+}, Fe^{2+}, Mg^{2+}); C (*M*1, *M*2, *M*3 with 2, 2 and 1 sites pfu, respectively) has Mg^{2+}, Fe^{2+}, Mn, Al^{3+}, Fe^{3+}, Cr^{3+} or Ti^{4+}; the tetrahedral T group (4 *T*1 and 4 *T*2 sites) is occupied by Si^{4+}, Al^{3+}, or Ti^{4+}; and W contains $(OH)^-$, F^-, Cl^-, O^{2-}. Note the assumed absence of vacancies in the B, C and T cation positions, and that the extra-O in W would indicate the presence of an oxo-amphibole molecule in solid solution with the extra-O in the *O*(3) which also contains F; indeed, note that both the *M*(1) and *M*(2) octahedral sites in the C group are bonded to two *O*(3) in W (Hawthorne et al., 2012; Oberti et al., 1992). In addition, any vacancies are generally assumed to be restricted to A (Hallimond, 1941; Stout, 1972; Robinson et al., 1982; Schumacher, 1991, 2007) and we will employ that relationship in calculating the possible Fe^{3+} content for amphiboles (see below). For a 'full analysis' of amphibole, and in the absence of a reliable method of obtaining precise analyses for extra-O, the cation proportions in the amphibole formula are normally calculated on the basis of 24 anions. Note that the formula defined to be the smallest unit required (Whittaker, 1981) to repeat the calcic- and sodic-amphibole structure (commonly space group C/2*m*) consists of 24 anions, one large cation A, two 6 - 8 fold B, 5 octahedral C, and 8 tetrahedral T. For strict stoichiometry the proportion of extra-O (denoted $^{W}O^{2-}$) is calculated as [24-(22-(OH)-F-Cl)] and the valence balance for the cations must match the actual charge on the anion network. Any enrichment of high valence cations (mainly Ti^{4+}, Al^{3+} and Fe^{3+}) replacing the more abundant divalent cations in C could be matched by: essential coupled vacancies; coupled inter-valent, inter-site exchange; or related to the presence of extra-O. In addition, some authors have suggested that secondary alteration processes could be accompanied by loss of H (dehydrogenation), leading to the presence of extra-O and oxidation of Fe^{2+} to Fe^{3+} (e.g., Darby Dyar et al., 1993; Underwood et al., 2012, 2013; Li et al., 2020b).

Hawthorne (1983) and Hawthorne et al. (2012) used published chemical analyses of natural hornblendes with data for H_2O, FeO and Fe_2O_3 (e.g., data from Binns, 1965; Deer et al., 1966), to show how 24 anion amphibole formulae could

be recalculated to assess possible maximum and minimum Fe^{3+} estimates based on different crystal chemical models (see below); apparent excesses for a particular crystallographic site would indicate the presence of Fe^{3+}. However, if reliable Fe^{3+} estimates are to be calculated for stoichiometric amphiboles, the presence of vacancies at the structural cation sites must be dealt with correctly. For analyses lacking reliable water data the standard practice is to calculate an anhydrous, stoichiometric formula (ideal formula $A_{0\text{-}1}B_2C_5T_8O_{23}$) on the basis of 16 cation plus vacancy sites and 23 oxygens; this assumes the presence of exactly $2(OH)^-$ anions including their F and Cl equivalents (see before). Where separately estimated Fe-valence values are not available, many mineralogists calculate model Fe^{3+} values based on an ideal stoichiometric formula with Fe valences balanced on the basis of either 16 or 13 cation formulae (Stout, 1972; Robinson et al., 1982; Droop, 1987; Schumacher, 1991, 2007 [see Excel Supplementary file 1, Folder II, this work]). However, it has also been suggested that the calculation can be made on a 15 cation basis with cation totals including Ca or even Ca + Na (Robinson et al., 1982; Hawthorne & Oberti, 2007; Hawthorne et al., 2012). This approach may have little general applicability for natural amphiboles which usually have mixed occupancy of the B group for both calcic and sodic amphiboles (Deer et al., 1997); but how is it possible to assess the amount of Ca (or Na) to be added to B before the Fe^{3+} value is known? In addition, the overall charge balance must be maintained for all the multivalent interactions, especially to quantify Fe^{3+} reliably. Some authors prefer to use a 13 cation calculation, perhaps reflecting the possibility that vacancies at A appear to be more common and easier to quantify than those in C and T (Woolley & Platt, 1986; Cosca et al., 1991; Worley & Cooper, 1995; Harris et al., 1999; Mogahed, 2016). Hawthorne et al. (2012) defined terms for the 'aggregate charges' for the A and C groups as $A^+ = (Na + K + 2Ca)$ and $C^+ = (Al + Fe^{3+} + 2Ti^{4+})$; these relationships are equivalent to assuming the presence of a matching vacant cation site for each Ca^{2+} replacing Na^+ at A and each Ti^{4+} replacing Al^{3+} at C following strict stoichiometry rules.

Some workers, including those developing a useful system to give names to important end-members in the chemically complex amphibole group, use conventional EMP analyses to calculate formulae 'normalised' to (OH, F) = 2.0 by simply 'adding' enough water to the wt% anhydrous analytical data, **effectively setting $^{W}O^{2-}$ to zero** (e.g., Oberti et al., 1992, 2007a, 2018; Hawthorne & Harlow, 2008). For example, an EMP analysis of an Al-rich amphibole lacking any water determination (K22-2, Oberti et al., 2007a) was modified by simply adding 1.87 wt% H_2O to the analysed data and reported a refined single-crystal X-ray structure SREF (all Fe as Fe^{2+}) with Fe^{3+} determined by charge balance. Thus a value of Fe^{3+} = 0.42 apfu in the C group *M*(1) site ($Fe^{3+}/\Sigma Fe = 0.19$) with $^{W}O^{2-} = 0.000$, and ΣT + C group cations is 13.07 apfu (13.11 was reported in their **Table 2**. In our spreadsheet (Supplementary file 1, Folder I, row 91) we give their **Table 2** input data with MgO = 7.39% (including the equivalent amount of ZnO). In our spreadsheet 1.877 H_2O% gives $^{W}O^{2-} = 0.000$ apfu with $Fe^{3+} = 0.412$ apfu and $Fe^{3+}/\Sigma Fe \sim 0.182$.

If only 1.8 % H_2O had been added, $^{W}O^{2-}$ would have increased to 0.203, the proportion of **all** atomic components would increase with Fe^{3+} = 0.414 apfu (see row 92) reflecting that an excess contents of C cations had increased from 0.107 to 0.164, displacing the extra amount from C to B (i.e., 0.057 apfu) More significantly, the Fe^{3+}/Σ Fe value would hardly change (~0.184); any small change simply reflects how the small *difference* in added water would modify the *original* value estimated for Fe^{3+-}. Thus, if a reliable estimate of Fe^{3+} is available for analyses with a full C cation group, decreasing the water added increases cation numbers proportionately and transfers excess C cations to B so should not change a 13 cation Fe^{3+}/ΣFe value significantly. A similar treatment using *all Fe as FeO* for this sample is shown in our spreadsheet, Folder I, rows 132 - 134) where the total amount of estimated Fe^{3+} for $^{W}O^{2-}$ = 0.000 (H_2O is 1.859 wt. %), gives a stoichiometrically calculated Fe^{3+} of 0.15 apfu (column CK), with ΔC = 0.225 apfu (column CH) and Fe^{3+}/Σ Fe = 0.065 (column CP). Decreasing added water to 1.75 (row 133) and 1.60% (row 134) increases ΔC to 0.255 and 0.297 pfu, Fe^{3+} to 0.26 and 0.41 apfu, and Fe^{3+}/Σ Fe to 0.11 and 0.18; we now see distinct changes in the oxidation state of the Fe!

We conclude that the approach of fixing (OH) to 2 atoms pfu has no general merit in dealing with the possible presence of extra-O in amphiboles with C > 5 apfu if reliable estimates for Fe valence (preferably Mössbauer) are not available (e.g., Robinson et al., 1997; Uvarova et al., 2007; Abdu & Hawthorne, 2009; Colombo et al., 2023). Indeed, Hawthorne et al. (2012) wisely pointed out that that approach is the same as a 23 O recalculation and is "probably not correct in the majority of cases". While the (OH, F) = 2.0 calculation appears to be acceptable for some amphibole compositions, we will see that it is less appropriate for amphiboles rich in Ti and octahedral Al in C (cf. Hawthorne et al., 2012). Thus, amphiboles with relatively low Ti and low $^{W}O^{2-}$ studied with single-crystal X-ray diffraction tend to have all Ti^{4+} and trivalent cations ordered at *M*(2) (e.g. Oberti et al., 2003, 2007b, 2016, 2018; Uvarova et al., 2007). However, Hawthorne et al., (2012) pointed out that amphiboles with high contents of extra-O in W also tended to show that any 'highly' charged Ti would be ordered at *M*(1) and/or *M*(3), both of which are bonded to *O*(3) at W. By contrast, Kitamura et al. (1975) used single-crystal neutron-diffraction to study a Ti-rich oxy-kaersutite and assigned Ti mainly to *M*(1) (i.e., *M*(1) 0.27, *M*(2) 0.02, *M*(3) 0.04 a.p.f.u.). Oberti et al. (1992) used X-ray single diffraction to suggest that richterites with TiO_2 up to 6.2 wt.% had all Ti ordered at *M*(1) with lower amounts at *M*(3) and low occupancy at *M*(3); that relationship was correlated with the occurrence of the extra-O at *O*(3). Hawthorne & Harlow (2008) studied two Al-rich, amphiboles with calculated water to give (OH + F) = 2.000; both samples have "significant" Ti contents with ~0.20 apfu assigned to *M*(2); they concluded that for Ti-rich samples (Ti > 0.2 apfu) Ti should be assigned to the *M*(1) site, via the interelement/intersite exchange $^{M(1)}Ti^{4+} + 2\ ^{O(3)}O^{2-} = {}^{M(1)}Mg^{2+} + 2\ ^{O(3)}(OH)^{2-}$ (Oberti et al. 1992), possibly leading to the approximation (OH, F, Cl) = (2 – 2Ti). That model, assuming $^{W}O^{2-}$ = 2Ti, would lead to the

maximum value for extra-O (Hawthorne et al., 2012); thus, the way that Ti is treated is **critical** for the calculated formula. Amphiboles and biotite micas in alkaline igneous rocks commonly have high proportions of oxo-components to match high Ti^{4+}, octahedral Al, and possibly Fe^{3+} substituting for divalent cations. These compositions appear to have crystallized as primary phases at high temperatures (and pressures?) from parental magmas, so any attempt to 'correct' for Ti contents in amphiboles in order to standardise anion formulae seems inappropriate petrologically (Darby Dyar et al., 1993; Righter et al., 2002; Henderson, 2025).

Hawthorne et al. (1998) studied a suite of Na-Ca zoned amphiboles from an alkaline ultramafic diatreme at Coyote Peak, California; these include Ti-rich samples, providing a suite with variable $^{W}O^{2-}$. Samples were analysed by EMP, ion probe for Li and H (error ~10%), and with Fe^{3+} estimated by single crystal XRD, coupled with stoichiometric reasoning. Formulae were calculated to 24 (O, OH, F, Cl) and show $^{W}O^{2-}$ ranging from 0 to 1.16 apfu, reflecting the presence of 0.12 to 0.75 Ti apfu; all Ti in the lowest Ti sample (0.12 apfu) was allocated to *M*(2), with each of the other samples having 0.13 apfu also allocated to that site. The remaining Ti was assigned to the *M*(1) site which is bonded to the two extra-O atoms substituted for (OH) in O(3). Figure 2 in Hawthorne et al. (1998) shows that a plot of Ti *vs* $^{O(3)}O^{2-}$ (our $^{W}O^{2-}$) has all data points for the Coyote samples falling close to the same linear fit ($Ti = 0.53^{W}O^{2-} + 0.13$), this has a smaller slope than the equivalent fit for the whole lithium-free amphibole database (Li et al., 2020a: $Ti = 0.65^{W}O^{2-} + 0.05$). Hawthorne et al. (1998) accounted for that overall relationship as $Ti^{4+} + 2O^{2-} = (Mg, Fe^{2+}) + 2(OH)^{-}$ and pointed out this exchange "is not site-specific". We will consider below if the Ti-rich amphiboles in other differentiated alkaline igneous rocks follow the same relationship. In addition, Hawthorne et al. (1998) considered atomic proportions of the calculated formulae for these Coyote Ti-bearing amphiboles and states "the fact that all values are systematically low indicates that this feature is also the result of inappropriate method of normalization". For example, Oberti et al. (1992) calculated formulae for a Ti-rich amphibole (sample R(5) with 6.54 TiO_2) for (OH + F) = 0 and assigned Ti = 0.343 apfu to the tetrahedral site; our approach, assuming a feasible $^{W}O^{2-}$ of ~0.70 pfu, leads to higher proportions for all cations, reducing Ti in *T* to ~0.22 pfu. This is the same situation found in Ti- and Ba- rich biotites which have high oxo-molecule contents and lack significant cation site vacancies (Righter et al., 2002; Henderson & Foland, 1996; Henderson, 2025).

We will consider the possible problems dealing with high quality, fully analysed high-Ti amphiboles below (Section 4), paying particular attention to doing that in the context of including the extra-O component as a primary oxo- amphibole component in calculating 24 anion formulae. The aim is to use the end result to provide reliable $Fe^{3+}/\Sigma Fe$ ratios with charge balance over full T, C, B, A groups rather than attempting to involve ordering over separate *M*(1), *M*(2), *M*(3), *M*(4) sites within B and C.

3. Amphibole Formula Calculation Protocol Development

Henderson (2025) stressed that, for complete study of stoichiometric micas, each site vacancy must be considered a primary component of the formula (cf. Oberti et al., (2007b) for amphiboles). End-member formulae calculated to 22 oxygens were assessed to develop 'rules' for assessing mica formulae. The same approach is instructive for hypothetical, end-member amphiboles, with the equivalent formula based on 23 O pfu.

3.1. Calculations for Hypothetical Amphiboles

In the present work the wt.% oxide compositions are calculated for a set of hypothetical end-members and solid-solution, stoichiometric amphibole compositions with fixed vacancies, Fe valences, excess oxygen proportions (O^{2-}), and $(OH)^-$ in W. Details of the compositions are given in the Supplementary Excel spreadsheet file 1, Folder I. The examples used are chosen to test how calculation protocols can be developed to deal with different types of crystal chemical challenges. Different stages of formula calculation are shown and are intended to be detailed enough for mainstream petrologist readers to follow.

Table 1. Calculation of Fe^{3+} on a 23 O basis for hypothetical vacancy-present and oxo-end-member amphibole molecules.

(a)								
	1a	1b	2	3a	3b	4	5a	5b
Wt.%	Glaucophane		Ferro-glaucoph	Mg-ferri-hornblende		Ferri-tschermakite	Riebeckite	
							Fe^{3+} & Fe^{2+}	All Fe^{2+}*
SiO_2	61.35	61.35	54.74	49.90	49.90	41.28	51.36	51.36
TiO_2								
Al_2O_3	13.01	13.01	11.61	6.05	6.05	11.68		
MgO	15.43	15.43		19.13	19.13	13.85		
Fe_2O_3				9.47			17.06	
FeO			24.54		8.52	16.46	23.03	38.38
CaO					13.31	12.84		
Na_2O	7.91	7.91	7.06				6.62	6.62
H_2O	2.30	2.30	2.05	2.14	2.14	2.06	1.92	1.92
Fe_2O_3	0	0	0	9.47	9.47	18.29		17.06
FeO	0	0	24.54		0	0		23.03
Cell formulae.	24 anion & 16 $\Sigma_{cat+vac}$	23 O & 16 $\Sigma_{cat+vac}$	23 O & 16 $\Sigma_{cat+vac}$	24 anion & 16 $\Sigma_{cat+vac}$	23 O & 16 $\Sigma_{cat+vac}$	23 O & 16 $\Sigma_{cat+vac}$	24 anion & 16 $\Sigma_{cat+vac}$	23 O & 16 $\Sigma_{cat+vac}$
Si	8.000	8.000	8.000	7.000	7.155	6.273	8.000	8.364
Ti								
Al	2.000	2.000	2.000	1.000	1.022	2.091		
Mg	3.000	3.000		4.000	4.089	3.136		
Fe^{3+}				1.000			2.000	

Continued

Fe^{2+}			2.999		1.022	2.091	3.000	5.227
Ca				2.000	2.045	2.091		
Na	2.000	2.000	2.001				2.000	2.090
(OH)	2.000			2.000			2.000	
(a) $*\Sigma^{23}_{cats}$ (no □ included)	15.000	15.000	15.000	15.000	15.333	15.682	15.000	15.681
Vacancies	1.000	1.000	1.000	1.000	1.000	1.000	1.000	1.000
Total cats + vac	16.000	16.000	16.000	16.000	16.333	16.682	16.000	16.681
(b) Fe^{3+}calc. to 16 (cats + □)	0.000	0.000	0.000	1.000	0.939	1.880	2.000	1.879
(c) Fe^{3+}calc. to 15 cats NO □	0.000	0.000	0.000	1.000	1.000	2.000	2.000	2.000
(d) Fe^{3+}calc. to 13 cats: Σcats NO □ − Σ(A + B)	0.000	0.000	0.000	1.000	1.000	2.000	2.000	2.000
Normalization factor Q[$] (e) X =13/[$\Sigma^{23}_{cats}$ − Σ(Na + Ca)]	1.000	1.000	1.000	1.000	0.978	0.957	1.000	0.956
Stoichiometric $^{w}O^{2-}$ pfu		0	0		0	0	0	0
Charge balance		46.0	46.0		46.0	46.0		46.0
$^{w}O^{2-}$ calc. Ridolfi et al. (2018) Spreadsheet		0	0		0	0.281		0
$^{w}O^{2-}$ calc. Ridolfi et al. (2018) eqn. 4a		-0.003	0		0	0.575		2.000
$^{w}O^{2-}$ calc. Li et al. (2020a)		0	0		0	0.280		0.094
Calc. Fe^{3+} Ridolfi et al. (2018) Sp.sh.[+]		0	0		0.357	0.700		2.000
Calc. Fe^{3+} Ridolfi et al. (2018) eqn. 4a		0	0.002		0.786	2.072		4.002
Calc. Fe^{3+}, Li et al. (2020a) Spreadsheet		0	0.10		0.328	0.712		1.036
Calc. Σ^{16}_{cats} Ridolfi et al. (2018) Sp.sh.		15.00	15.00		15.22	15.54		15/51
Calc. Σ^{16}_{cats} Li et al. (2020a) Spreadsheet		15.5	15.04		15.19	15.44		14.98

End-member and hypothetical amphibole cell formulae: 1) Glaucophane $\square Na_2(Mg_3Al_2)[Si_8]O_{22}(OH)_2$; 2) Ferroglaucophane $\square Na_2(Fe^{2+}{}_3Al_2)[Si_8]O_{22}(OH)_2$; 3) Magnesio-ferri-hornblende $\square Ca_2(Mg_4Fe^{3+})[Si_7Al]O_{22}(OH)_2$; 4) Ferri-tschermakite $\square Ca_2(Mg_3Fe^{3+}{}_2)[Si_6Al_2]O_{22}(OH)_2$; 5) Riebeckite $\square Na_2(Fe^{2+}{}_3Fe^{3+}{}_2)[Si_8]O_{22}(OH)_2$; $\Sigma cats^{23}$ is the total of cations for recalculating cell to 23 oxygens; [$]For these examples the only cations occupying A and B are Na and Ca; [+]Sp. Sh. Spreadsheet.

(b)

	6	7	8	9	10a	10b	10c	11a	11b
Wt. %	0.5 Rieb 0.5-ferri-taram	0.5 Mg-ferri-0.5-hb. ferro-taram	0.5 Mg-ferri hb-0.5 ferro taram +0.15 Mn for Ca	0.5 Mg-ferr-hb-0.5 ferro-taram; oxo with Ti and $\square^{Ti}$	Oxo-ferro-sadanagaite			0.25 Ferri-taram –0.25 riebeckite 0.5 oxo-Ferro-sadanagaite	
SiO_2	46.345	44.409	44.297	44.017	32.30			39.238	
TiO_2				4.502					
Al_2O_3	5.618	14.493	14.456	14.365	27.41			16.646	
MgO	6.662	9.166	9.148	6.814				3.291	
Fe_2O_3									
FeO	27.709	16.340	16.299	16.196	23.18			25.395	
MnO			1.207						

Continued

CaO	3.090	9.565	8.587	12.641	12.06			7.630	
Na_2O	6.829	3.524	3.515	1.015	3.33			5.059	
H_2O	1.985	2.049	2.043		0			0.980	
Fe_2O_3	17.596	4.540	4.428	4.500	17.17			17.381	
FeO	11.876	12.255	12.224	12.147	7.73			9.755	
Cell formulae.	23 O, $16\Sigma_{cat+vac}$	23 O $16\ \Sigma_{cat+vac}$	23 O $16\ \Sigma_{cat+vac}$	23.5 O	23 O	24 O	24 O normalized	23.5 O	23.5 normalized
Si	7.318	6.571	6.671	6.592	5.000	5.217	5.000	6.267	6.001
Ti			-	0.507					
Al	1.045	2.527	2.527	2.535	5.000	5.218	5.000	3.134	3.000
Mg	1.568	2.022	2.024	1.521				0.784	0.750
Fe^{3+}							2.002		1.997
Fe^{2+}	3.659	2.022	2.022	2.028	3.000	3.131	0.999	3.392	1.252
Mn			0.150						
Ca	0.523	1.516	1.365	1.949	2.000	2.087	2.000	1.326	1.250
Na	2.091	1.011	1.011	0	1.000	1.043	0.999	1.567	1.500
(a) $^*\Sigma^{23}_{cats}$ (no □ included)	16.205	15.670	15.671	15.133	16.000	16.696	16.000	16.449	15.750
Vacancies in A	0.500	0.500	0.500	1.0	0			0.250	0.250
Total cats +vac	16.705	16.170	16.171	6.133	16.000	16.696		16.699	
(b) Fe^{3+}calc. 16 (cats + □)	1.940	0.484	0.486	0.380	0.000	2.000		1.968	
(c) Fe^{3+}calc. 15 cats NO□	3.420	1.968	1.970	0.405	3.000	4.874		4.78	
(d) Fe^{3+}calc. to 13 cats: Σcats NO □ − Σ(A + B)	2.000	0.500	0.500 -CNK + Mn	0.656	0.000	2.002		1.994	
Normalization factor Q$^{\$}$ (e) X =13/[Σ^{23}_{cat} − Σ(Na + Ca)]	0.956	0.989	0.989	0.986	1.000	0.9584		0.9575	
Stoichiometric $^wO^{2-}$ pfu	0	0	0	0.998		2.000		1.000	
Charge balance	46.0	46.0	46.0	47.0			47.0		47.0
$^wO^{2-}$ calc. Ridolfi et al. (2018) Spreadsheet	0	0				0.311		0.003	
$^wO^{2-}$ calc. Ridolfi, eqn. 4	1.674	0				0.052		1.161	
$^wO^{2-}$ calc. Li et al. (2020a)	0.128	0				0.134		0.131	
Calc. Fe^{3+} Ridolfi, Sp.sh.	0.976	0.493				0.312		0.742	
Calc. Fe^{3+} Ridolfi, eqn. 4	2.65	0.493				0.004		1.90	
Calc. Fe^{3+}, Li et al. (2020a)	1.012	0.342				0.340		0.672	
Calc. Σ^{16}_{cats} Ridolfi et al. (2018)	15.86	15.50				16.00		15.84	
Calc. Σ^{16}_{cats} Li et al. (2020a)	15.78	15.53				16.21		15.95	

End-member and hypothetical amphibole cell formulae: 6) 0.5 Riebeckite:0.5 Ferri-taramite $\square_{0.5}Na_{0.5}(Na_{1.5}Ca_{0.5})\ (Mg_{1.5}Fe^{2+}{}_{1.5}Fe^{3+}{}_2)$-$[Si_7Al]O_{22}(OH)_2$; 7) 0.5Mg-ferri-hornblende-0.5ferro-taramite $\square_{0.5}Na_{0.5}(Na_{0.5}Ca_{1.5})\ (Mg_2Fe^{2+}{}_{1.5}Fe^{3+}{}_{0.5}Al)[Si_{6.5}Al_{1.5}]O_{22}(OH)_2$; 8) 0.5Mg-ferri-hornblende-0.5ferro-taramite $\square_{0.5}Na_{0.5}(Na_{0.5}Ca_{1.35}Mn_{0.15})\ (Mg_2Fe^{2+}{}_{1.5}Fe^{3+}{}_{0.5}Al)[Si_{6.5}Al_{1.5}]O_{22}(OH)_2$; 9) $\square_{0.5}\square_{Ti0.5}$ $-(Ca_2)(Mg_{1.5}Ti_{0.5}Fe^{2+}{}_{1.5}Fe^{3+}{}_{0.5}Al)[Si_{6.5}Al_{1.5}]O_{23}(OH)$; note oxo with 23.5.O cell; 10) Oxo-ferrosadanagaite $NaCa_2(Fe^{2+}Fe^{3+}{}_2Al_2)[Si_5Al_3]O_{22}O_2$; 11) 0.25 Ferritaramite-0.25riebeckite- 0.5oxo-ferro-sadanagaite $\square_{0.25}Na_{0.75}(Na_{0.75}Ca_{1.25})(Mg_{0.75}Fe^{2+}{}_{1.25}Fe^{3+}{}_2Al)[Si_6Al_2]O_{22}(OH)O$. $^*\Sigma cats^{23}$ is total cations for recalculating cell to 23 oxygens; $^{\$}$For these examples the only cations occupying A and B are Na and Ca.

Table 1 (this work) gives the wt. % oxides of these hypothetical amphiboles, with total Fe calculated as wt.% FeO; structural water is also given with the wt% calculated compositions with the equivalent values for FeO and Fe_2O_3 just below. Table 1 includes both anhydrous 23 O calculations dealing with the full amphibole formula with fixed 16 cation + vacancy formulae, but the availability of values for FeO, Fe_2O_3 and H_2O in Table 1 allows the full 24 anion data to be calculated for these ideal compositions if required. The first example considered is the iron-free ideal glaucophane ($\square Na_2(Mg_3Al_2)Si_8O_{22}(OH)_2$) with a vacancy at A, 2 Na^+ cations occurring in B, a total of 5 atoms at C (3 Mg^{2+} and 2 Al^{3+}), 8 Si^{4+} cations at T ; positive charges for the different sites are 0, 2, 12, 32 consecutively, totalling +46. These are balanced electrostatically by 22 O^{2-} in the amphibole double chain sheet framework and 2$(OH)^-$ forming the hydroxyl group at W, totalling −46. Note that (OH) is chosen to occupy W in most of the ideal amphiboles considered initially, and this cation charge is fixed by stoichiometry for amphiboles without excess O. Also note that the cation plus vacancy total is 16 which is fixed by the amphibole stoichiometry. In the amphibole spreadsheet used here the first stage is to calculate the atomic proportions of oxygen and then of the cation numbers from Si to H (Na for the amphiboles in Table 1) following (Deer et al., 1966; Schumacher, 1991); in Table 1 (column 1a) the water content is included as the first calculation is on a 24 anion hydrous basis with a zero Fe component. The atomic proportions for the cations and for H as (OH) exactly match the molecular formula shown above; the cation sum (denoted Σ^{24}_{cats}) equals 15.000 per formula unit (pfu), and as the stoichiometric formula must have 16 possible sites, the vacancy number ($\square$, $\square^A$ in this case) must be 1.000. Table 1 column 1b shows the data for the same sample without an H component; thus the stoichiometric proportion of (OH) is assumed. The calculation here is to sum the oxygen for a 23 O formula on an anhydrous basis (Σ^{23}_O = 2.935pfu) and to incorporate it into the cation correction factor (denoted *Y*) to calculate the cation proportions on the basis of 23 O, which we define as $Y = 23/\Sigma^{23}_O$; for ideal glaucophane $Y = 7.836$, but for most amphiboles would lie within an extended range from ~8 - 10. This factor is then used to calculate the numbers for all the cations and thus a value for the total Σ_{cats}. The 23 O cation values for glaucophane (Table 1, column 1b) match those calculated for the stoichiometric, 24 anion formula (1a); all the components show the stoichiometric values expected for the formula defined, with a cation total (Σ^{23}_{cats}) of 15.000. While all the cation data at this stage look complete, they only refer to a 23 O formula and we know that stoichiometric amphibole has 24 anions, 22 in the sheet and 2(OH) at W which shares oxygens with the sheet. However the 24 anions must be related to 16 possible cation sites and the actual cation plus vacancy total has been shown to be 16 so the stoichiometry normalisation factor to convert the 23 O proportions is simply $(16^{stoic.})/(\Sigma^{23}_{cats}$ + vacancies) [denoted *Q* here]; note that this type of correction factor is denoted the 'ferric normalization factor' (*FNF*) by Schumacher (1991). $Q = 16/16 = 1$ for ideal glaucophane, and the final stoichiometric 24 anion formula for the cations remains the same as for the

23 O formula. The calculation of these values seems straightforward but that reflects the absence of Fe^{3+}, indeed for end-member glaucophane there is no Fe at all.

The same approach is followed for ferroglaucophane where Fe^{2+} replaces Mg ($\square Na_2(Fe^{2+}{}_3Al_2)Si_8O_{22}(OH_2)$) as there is no valence difference between Fe^{2+} and the Mg it 'replaces'. The wt. % oxide values with all iron as FeO and the stoichiometric data for ferroglaucophane are given in Table 1, column 2, although correct oxide amounts for Fe_2O_3 and FeO are given in italics at the bottom of the oxide data; for this amphibole only FeO is present. The calculated oxide data with separate Fe_2O_3 and FeO values, including H_2O, would give exact stoichiometric atomic values where calculated on a 24 anion basis with cation sums of 16.000 atoms, **as long as vacancy values are included as essential empty stoichiometric cation sites;** note that for the 24 anion calculation the Droop (1987) formula used to model the Fe vacancy values must use a 24 O value.

The 23 O formula calculation gives exactly the same cation proportions (Table 1, column 2) as the 23 O formula for glaucophane (and to the 24 anion calculation), as long as all Fe is present as Fe^{2+}, but now the Droop (1987) formula basis is defined by requiring a 23 O value. Thus following Droop, the calculation to obtain the Fe^{3+} in the 24 anion formula is shown as Equation (1) below:

$$F = 2X(1 - T/S) \quad (1)$$

where Droop defined F as the number of Fe^{3+} ions per X oxygens, T as the ideal number of cations per formula and S as the observed cation total per X oxygens; T is denoted Σ^{stoic} here (usually either 16 or 13 total cations) and S is denoted $\Sigma^{23}{}_{cats}$; for strict stoichiometry both Σ^{stoic} and $\Sigma^{23}{}_{cats}$ should include vacancy values but we will see later that it may be convenient (simpler) to ignore a vacancy altogether as long as it occurs at A, which is normally the case for amphiboles (see above). The next stage in producing a full 24 anion formulaformula would be to convert the 23 O cation proportions to the full formula on the basis of either 16 cation or 13 cations proportions. Thus, for ferroglaucophane, 1 vacancy is required to be added to each calculation leading to the calculated apparent Fe^{3+} values of $2 \times 23 \times (1 - 16/16)$ (Table 1, column 2, row 2b) and $2 \times 23 \times (1 - 13/13)$, respectively. In each case the apparent Fe^{3+} is zero, as required by the ideal formula. The final 24 correct anion proportions would therefore be the same as for the first stage 23 O values. However, another second stage approach might be to accept that ferroglaucophane has one vacancy and therefore the cation sum ratios could be defined simply as 15/15 which gives the correct calculation for Fe^{3+} of 0.0 (Table 1, column 2, row 2c). Indeed, the presence of a vacancy could be ignored with the 23 O cation sum alone totalling 15 atoms ($\Sigma^{23}{}_{cats}$) to be corrected by subtracting the stoichiometric 23 O, B category content ($2Na^B$ ignoring the vacancy), to also give Fe^{3+} = 0.0 for the 13/13 correction (Table 1, column 2d); thus both the 16 and 13 cation corrections give exactly the same zero Fe^{3+} as required by the strict stoichiometry of the input data. The 23 O cation values for all the elements multiplied by the stoichiometry correction factor (denoted Q) which for this sample has the value

Q = 13/13 = 1.000 (Table 1, column 2 row e); the final formula values would now match all the stoichiometric cation proportions with 3 Fe^{2+} and zero Fe^{3+} pfu (see formula given above and in Table 1 footnote).

The next example is an end-member with a fixed Fe^{3+} content together with a single vacancy, e.g., magnesio-ferri-hornblende ($(\square Ca_2(Mg_4Fe^{3+})[Si_7Al]O_{22}(OH)_2$); for a 23 O calculation the Fe_2O_3 content of that end-member (9.47 wt.%) is input to the amphibole spreadsheet as an anhydrous amphibole (0% H_2O) with 8.52 wt% FeO. However, as this is the first of our examples to have ferric Fe, the first calculation considered is for the full 24 anion formula with Fe_2O_3 and H_2O included (Table 1, column 3a). The 24 anion cation values shown match those for the stoichiometric formula (see above and Table 1 footnote), with 15 cations and 1 vacancy giving Si = 7.000, Fe^{3+} = 1.000 and (OH) = 2.000. The 23 O calculation is shown in column 3b with Fe input as FeO and without the water value. The $\Sigma^{23}{}_{O}$ cation values now show higher cation proportions than for those shown for the 24 anion cations (column 3a) and with those in the molecular formula; for example, Si = 7.1555 pfu compared with the required 24 anion value of 7.000 pfu (see above formula); each element, including the bulk Fe value, shows the same excess proportion with a total cation sum for $\Sigma^{23}{}_{cats}$ = 15.3335 pfu. These values are too high because not enough O is present in the calculation due to the total iron being reported only as FeO. The Σ_{cats} = 15.3335 is used to convert a proportion of the input Fe^{2+} to the known stoichiometric value for Fe^{3+} following the Droop method, as explained above with Equation (1). The '16' cation calculation must include the vacancy of 1.0 pfu so that Fe^{3+} = 2 × 23 × (1 − 16/16.3335) = 0.939 pfu (Table 1, column 3, row b); that value is slightly less than the known Fe^{3+} amount of 1.000 atom pfu. The deficiency reflects the fact that the value calculated for 16 cations has used cation data calculated on a 23 O basis with a cation total of 15 cations. However, the presence of one vacant site increases the effective *total* site occupancy to 16 leading to a correction factor of 16/15 increasing the Fe^{3+} content to 1.0 (0.939 × 16/15 = 1.00), the known Fe^{3+} content. Note that the equation adds a known vacancy to obtain a 16 cation plus vacancy total for a stoichiometric amphibole, then subtracts this vacancy value to convert to a 13 cation basis! Thus, a numerically correct and simpler approach is to ignore the vacancy at A, to use the $\Sigma^{23}{}_{cats}$ of 15.3335 without the vacancy value, and to subtract the $\Sigma^{23}{}_{Ca}$ value (2.045) to give Q = 13/13.2886 and thus Fe^{3+} = 1.000; this formulation now defines step (d) in the amphibole spreadsheet for the Fe^{3+} calculation. Thus step (b) described above depends on knowing the exact vacancy contents and *only* works if the vacancy is restricted to A. However, the final 13 cation (d) correction factor could be used to deliver the preferred Fe^{3+} cation values for the full formula for any stoichiometric amphiboles containing vacancies at A; indeed, it **would work for any** vacancy content without the requirement of the value being known exactly (see later). In addition, if the cation count is taken to be exactly 15 for the '16' cation calculation and 13 for the 13 cation calculation exactly the same Fe^{3+} is given reflecting the exact stoichiometry of the input data (see above for ferroglaucophane). In effect, ignoring the known vacancy at A fol-

lows the usual practice of researchers who choose the 13 cation calculation for amphiboles (rather than a 16 cation calculation) to give a more reliable Fe^{3+} estimate; it seems that although ignoring a known vacancy content is counter-intuitive it is valid for stoichiometric amphiboles. However, if the essential vacancy is ignored, the basic amphibole spreadsheet for a 16 cation formula would calculate an apparent Fe^{3+} for magnesio-ferri-hornblende as $2 \times 23 \times (1 - 16/15.3335)$, i.e., giving the non-physical value of **minus** 1.999 Fe^{3+} in a phase known to have one atom of Fe^{2+}; clearly that calculation is not valid (*cf.* Droop, 1987). The Li et al. (2020a) and Ridolfi et al. (2018) approaches are to set such a non-physical negative result for the model fitting parameters to **zero, leading to possible mismatches with charge balance!** Thus, it is crucial to match all the correction factors in terms of whether the vacancy values are included, or not. Further examples below will test how reliability for this approach.

The end-member ferri-tschermakite (**Table 1**, column 4) contains a vacant A and only Fe^{3+} i.e. twice that of the hornblende matched by a higher substitution of Al for Si in the *T* site; hence the name. As expected, the 23 O cation values are higher than the stoichiometric values (Si = 6.273 rather than 6, total cations + vacancy = 16.682) and the calculated Fe^{3+} estimates show the expected characteristics (**Table 1**, column 4 row b $1.880 \times 16/15 = 2.004$, and column 4 rows c ans d = 2.000); the Q factors to correct the 23 O cation data to the full 24 anion formula are similar for ferri-hornblende and ferri-tschermakite at 0.978 and 0.957, respectively (**Table 1** column 3 row **e** and column 4 row e).

Ideal riebeckite ($\square Na_2(Fe^{2+}{}_3Fe^{3+}{}_2)Si_8O_{22}(OH)^-{}_2$) has a vacancy at A while C contains both iron Fe oxidation states (**Table 1**, column 5); this is the first example of our ideal amphiboles with this feature. **Table 1**, column 5a shows the complete 24 anion data for the hydrous phase with both Fe_2O_3 and FeO values declared. The 24 anion cation proportions match the stoichiometric formula with Si = 8.000, Fe^{3+} = 2.000, Fe^{2+} = 3.000, $\Sigma^{23}{}_{cats}$ = 15.000. The anhydrous 23 O formula (**Table 1**, column 5b) is calculated with all Fe as FeO (30.96 wt.%) giving cation values larger than those in 5a with Si = 8.364, Fe = 5.227 and $\Sigma^{23}{}_{cats}$ = 15.681 plus 1 vacancy. Calculated Fe^{3+} values are 1.879 (**Table 1** 5a, row b) and 2.000 (**Table 1** column 5b, rows d and e). The multiplication of all the 23 O cation values by the 24 anion correction factor (Q) of 0.956 (row e) now gives the correct stoichiometric formula values with Si = 8.000, Fe^{3+} = 2.000 and Fe^{2+} = 3.000. Thus, stoichiometric amphiboles with vacant A groups and with only Fe^{3+} or with mixed Fe valence components have the same calculation characteristics.

The following examples are for more complex hypothetical amphibole compositions including solid solutions with variable vacancy contents, Ti-bearing, and oxo-amphibole compositions. **Table 1** (continued), columns 6 and 7 show data for solid solutions which show the presence of 0.5 vacancies at A. The binary solid solutions chosen are 0.5 ideal riebeckite: 0.5 ferri-taramite ($\square_{0.5}Na_{0.5}(Na_{1.5}Ca_{0.5})(Mg_{1.5}Fe^{2+}{}_{1.5}Fe^{3+}{}_2)[Si_7Al]O_{22}(OH)^-{}_2$) (column 6) and 0.5 Mg-ferrihornblende: 0.5 ferro-taramite ($\square_{0.5}Na_{0.5}(Na_{0.5}Ca_{1.5})(Mg_{2.0}Fe^{2+}{}_{1.5}Fe^{3+}{}_{0.5}Al)[Si_{6.5}Al_{1.5}]O_{22}(OH)^-{}_2$) (columns 7). As expected, both have 23 O atom cation totals

greater than the stoichiometric values with total cation values of 16.205 + $\square_{0.5}$ and 15.670 + $\square_{0.5}$, Fe^{3+} contents of 1.940, 2.000 (column 6 row b and 6 row d) compared with 0.484, 0.500 (column 7 row b and 7 row d), and *Q* correction factors of 0.956 and 0.989 (columns 6 row e and 7 row e); application of those *Q* values results in 24 anion formulas that match the stoichiometric formulae. However, the data for row (c) are invalid (highlighted in the Table) because the parameter was developed specifically for compositions with 1 vacant site. *The main conclusion is that the* Fe^{3+} *estimations described can be used for any vacancy content as long as it can be* ***restricted*** *to Roman* A. The amphiboles in Table 1 (continued), columns 8 and 9 will be dealt with within the context of some natural amphibole compositions.

Calculation of formulae for end-member oxo amphiboles is considered for ideal oxo-ferro-ferri-sadanagaite $NaCa_2(Fe^{2+}Fe^{3+}{}_2Al_2)[Si_5Al_3]O_{22}O_2$ (Table 1 continued, column 10a). A 23 O calculation for the analytical data with all Fe as FeO gives the correct cation proportions (column 10a) but that cannot be valid because the whole basis of the 23 O model assumes a stoichiometric amphibole with 22 O atoms and 2(OH) per 24 anion formula and this amphibole is (OH) free. Thus the standard Fe^{3+} calculations give values of 0, 3.0 and 0 (column 10 rows a, c, d), none of which are correct. End-member oxo-amphiboles all require a 24 O calculation (i.e., 23 + $^{W}O^{2-}/2$) to obtain the meaningful cation contents shown in column 10b. All of these values are higher than the correct values and correction by the factor 0.9584 (column 10b row c) reduces the cation values shown for Si to Na provides the correct 24 anion values for all elements including Fe^{3+} and Fe^{2+} values. Thus, both 16 cation (column 10b, row (b) and 13 atom calculations (row (c) provide correct values for Fe^{3+} of 2.000 pfu but the value of 4.874 in column 10b, row (c) is nonsense and has no validity for a formula with no vacancies and no (OH). It was mentioned above that many natural amphiboles show the presence of oxo-amphibole components; thus, calculation of meaningful formulae requires quantification of the $^{W}O^{2-}$, correction factor.

The composition given in Table 1, continued (column 11) is for a hypothetical amphibole solid solution with 25% ferri-taramite, 25% riebeckite and 50% oxo-ferro-sadanagaite (i.e., with 0.25 A vacancies and 1 $^{W}O^{2-}$ and 1 $(OH)^-$ pfu (ideal formula $\square_{0.25}Na_{0.75}(Na_{0.75}Ca_{1.25})(Mg_{0.75}Fe^{2+}{}_{1.25}Fe^{3+}{}_2Al)[Si_6Al_2]O_{22}(OH)O$. In Table 1 examples 1 to 8 are all stoichiometric amphiboles having the required formulae with 2 $(OH)^-$ pfu; however, examples 10 and 11 involve amphibole formulae with oxo-components requiring the first stage in the recalculation to be carried out on a recalculation defined by (23 + $^{W}O^{2-}/2$) rather than 23 O. Thus, the presence of 50% oxo molecule (e.g., example 11) would require the formula to be corrected on a 23.5 O basis, which delivers cation proportions larger than the stoichiometric values. Calculation of the Fe^{3+} values using the standard calculations gives the values 1.968 for column 11a row (b) (note that 1.968 × 16/15.75 = 2.000), 4.78 for row c, and 2.000 for row d. It is clear that the calculation for column 11, row c is not valid for such samples; it was developed to deal with amphiboles having a fixed

vacancy total of 1.000 atoms pfu. Thus, that calculation basis involves normalisation to 15 cations, but the correct normalising values should be 16 minus the known vacancy count, a total of 15.75 in this case. The 13 atom calculation defines the value of $Q = 0.9575$ for recalculating the correct cation atomic proportions for 24 anions and the corrected values are shown in Column 11b. *Based on all of the examples discussed here, the most reliable calculation for assessing the Fe valence proportions is that for row* (*d*) *in* **Table 1**, *which gives the data for a* 13 *cation count for* 23 *O calculations for normal amphiboles with* 2(*OH*) *and for amphiboles with a proportion of oxo-amphibole components in solid solution using a* (23 + $^{W}O^{2-}$/2) *calculation*.

3.2. Developing the Formula Calculation Protocol

The main requirement for dealing with EMP analyses of amphiboles is to quantify the oxy-amphibole component; Ridolfi et al. (2018) and Li et al. (2020a) provide a better basis for this approach. Those databases include data of well analysed amphiboles to provide reference 'standards' with reliable EMP data, H/(OH) values estimated with SIMS/vibrational spectroscopy, and separate values for Fe^{2+} and Fe^{3+} obtained by chemical, Mössbauer, XANES, or from single crystal refined X-ray data with Fe^{3+} based on charge balance (SREF). The compositional, crystal chemical and structural information for key samples in the Ridolfi et al. (2018) database were analysed using multivariate regression analysis, while Li et al. (2020a) applied a machine-learning method based on principal component regression analysis. Note that we only use those papers to estimate $^{W}O^{2-}$ for new and published analyses that lack data for H_2O. In their databases, we have checked if the regressions have significantly modified the original atomic proportions of the reference samples (e.g., Dyar et al., 1993, 2016) and are satisfied that the calculated model $^{W}O^{2-}$ values are generally within ~5% - 10% of the original 'analysed' values. Thus we will apply our own crystal chemical calculations to obtain atomic proportions **constrained by strict stoichiometry**, with the possibility of a small uncertainty in the estimated $Fe^{3+}/\Sigma Fe$ at that level.

Our calculation protocol provides atomic formulae for conventional EMP amphibole analyses with all Fe reported as FeO, and which lack H_2O/(OH) data. We prefer to assess the reliability of Fe^{3+} estimates against reference samples with Fe valence values determined by chemical analysis, or by Mössbauer / XAS methods rather than single crystal XRD refinement (SREF). Indeed, least squares regression analyses (SREF) for chemically-complex amphiboles involve assessing how valence, size, molecular mass, and electron density properties for key elements (e.g., Mn, Fe, Mg, Al, Ti, Cr, Ni, Zn, Li) might be used to predict cation-site occupancies, especially ordering between the 4 distinct sites containing C and B group cations. This is difficult enough for **pairs** of competing elements in multi-site crystal structures, but multi-element structural interactions are even more difficult to predict as discussed by Hawthorne (1983) and Oberti et al. (2007b). Thus, it is difficult to assess the results summarised in the Li et al. (2020a) spreadsheet, but it is our objective to use a simple model aimed at obtaining reliable Fe^{3+}/total Fe

ratios ($Fe^{3+}/\Sigma Fe$) based on the overall charge distribution over the whole structure on the basis of calculating Fe^{3+} for 16 (T + C + B + A) and 13 (T + C) cation + vacancy formulae. Fortunately in most amphiboles, any vacancies occur in A (see above).

The $^{W}O^{2-}$ values calculated for the amphibole database assembled here using both the Ridolfi et al. (2018) and Li et al. (2020a) spreadsheets provide similar sets of results. However, the Ridolfi et al. (2018) paper also provides a formula (their equation 3) for calculating a value for all elements from Si to K, and another formula (equation 4a) approximates a $^{W}O^{2-}$ value based on the atomic proportions of Ti and Fe^{3+} in C and of (Na+K) in A. The coefficients for the dependent variables in those equations are based on the standard amphibole dataset some of which provide high positive or even high non-physical negative $^{W}O^{2-}$ values; however, atomic proportions for the latter are returned as zero values and, thus, we do not use either of those equations. In addition, some end-member and hypothetical amphibole compositions with vacancies (e.g., tremolite and glaucophane) return very small, or even negative, $^{W}O^{2-}$ values; indeed estimated $^{W}O^{2-}$ values show significant differences to the known values for some Al-rich compositions (see bottommost rows in **Table 1**). Indeed, care is needed in considering the reliability of such estimates for certain amphibole compositions and related model Fe^{3+} and $\Sigma^{16}{}_{cats}$ data, but small $^{W}O^{2-}$ values will have little effect on a 23 O formula calculation (see below).

In this work, the $^{W}O^{2-}$ values incorporated used are those obtained using the Li et al. (2020a) spreadsheet with folder 'Dataset of Li-free AMPH'; the quality of Li-et al. estimated $^{W}O^{2-}$ values are checked against the values obtained for high quality, fully-analysed samples (e.g., Dyar et al., 1993, Satoh et al., 2004) and are found to be within 5% - 10% relative (see above). Our approach is to obtain amphibole compositions from the published literature, and to test whether these follow rigorous stoichiometry with reliable 16-cation plus vacancy, and 24 anion formulae. We have shown above that using the 13 cation calculation provides reliable Fe^{3+} values irrespective of vacancy content as long as they only occupy A (see above). Thus, we normalize cation proportions using the factor $(23 + {}^{W}O^{2-}/2)/\Sigma O$; *note that half of the determined 'extra oxygen' is required to supply the extra charge provided by* O^{2-} *compared to* $(OH)^{-}$.

The hypothetical amphibole examples used have had exact stoichiometries and vary depending on the presence or absence of vacancies and on the proportions of extra oxygen values. As long as such information is available the correct amount of Fe^{3+} can be calculated with the **same value** being returned on the basis of calculation to **either** 16 **or** 13 cations pfu. Well-analysed natural amphiboles would be expected to show some departure from this ideal situation reflecting the level of analytical error on individual chemical components, especially for the reliable estimation of the $^{W}O^{2-}$ value; in addition the analyses must include all the essential amphibole major elements and possible minor elements including, for example Cr, V, Ni, Sr, Ba, Zr and Li. If such information is not available, it would be even more difficult to deal with the presence of vacancies when the amount of Fe^{3+} is

being estimated for conventional EMP analyses.

4. Application of the Preferred Formula Calculation Method to Natural Amphiboles

The next step is to assess recalculation of amphiboles from different petrological environments, including examples with substantial extra-oxygen-components and variable Fe^{3+} contents. High-quality 'fully analysed' samples, having both water/OH determinations and separate analyses for both Fe^{3+} and Fe^{2+} will provide the means to assess the reliability of our approach [Dyar et al. (1993, 2016); Uvarova et al. (2007); Della Ventura et al. (2016); Zaitsev et al. (2013)].

Table 2. Cell formulae of fully-analysed Ca-, Ca-Na-, and Na- amphiboles.

	1a	1b	1c	1d	1e	2	3	4
	Zaitsev et al. (2013) Oxo-Mg-hastingsites*, Gregory rift alkaline rocks					Dyar et al. (1993)	Uvarova et al. (2007)	DellaVentura et al. (2016)
	OL 22	OL 313	OL 246	OL -/11	LL 5, 4, 3 /4, OL165	Mantle kaersutites	Metamorph. Mg- hornbl.	Synthetic richterite
	Av. 17	Av. 7	Av. 9	Av. 14	Av. 34	Av of 20	Av of 7	One analysis
SiO_2	41.89	42.06	40.29	42.16	40.42	39.85	44.06	48.88
TiO_2	3.96	3.92	4.34	3.94	4.31	4.50	0.83	-
Al_2O_3	10.75	10.99	11.88	10.75	12.01	14.47	10.89	-
FeO	10.12	9.14	12.21	9.33	10.49	11.75	18.25	38.11
MnO	0.08	0.09	0.12	0.09	0.10	0.14	0.28	-
MgO	14.79	15.06	13.09	15.74	14.40	12.47	9.20	-
CaO	11.76	11.79	11.80	11.85	11.99	10.47	11.71	2.96
Na_2O	2.84	2.71	2.76	2.83	2.64	2.80	1.27	7.57
K_2O	1.74	1.74	1.66	1.72	1.74	1.43	0.75	-
H_2O	0.61	1.40	1.30	1.03	1.49			
Total	99.67	99.24	99.94	99.44	99.71	97.88	97.25	97.25
$^{W}O^{2-}$. Li et al. (2020a) pfu	0.565	0.539	0.674	0.593	0.679	0.836	0.109	0
$Fe^{3+}/\Sigma Fe$ Mössbauer	1.00	0.33	0.34			0.41 (16)	0.15 (02)	0.07
Unit cell atomic proportions, pfu	(23 + $^{W}O^{2-}$/2) 13 cations					(23 + $^{W}O^{2-}$/2) 16 cations	(23 + $^{W}O^{2-}$/2) 13 cations	(23 + $^{W}O^{2-}$/2) 13 cations
(i) Total cats Σ^{16}	16.207	16.147	16.256	16.237	16.283	16.166	15.569	16.182
(ii) $Fe^{3+}/\Sigma Fe$	0.48	0.38	0.48	0.60	0.63	0.33	-0.56	0.10
(iii) $\Sigma^{13}_{noCNK} = \Sigma^{16} - CaNaK$	13.169	13.148	13.215	13.215	13.231	13.383	13.143	13.253
(iv) $Fe^{3+}/\Sigma Fe$	0.48	0.46	0.50	0.67	0.63	0.93	0.22	0.17
(v) $\Sigma^{13}_{noCNK} - \Delta C^*$	13.104	13.091	13.132	13.133	13.142	13.236	13.088	13.156
(vi) $\Delta C^* = (\Sigma^{13}_{noCNK} - 13)^*5/13$	0.065	0.057	0.083	0.083	0.089	0.147	0.055	0.097
(vii) $Fe^{3+}/\Sigma Fe$	0.30	0.28	0.31	0.41	0.39	0.57	0.14	0.11

Continued

(viii) $\Sigma^{13}_{noCNK} - \Delta C^{corrected}$	13.082	13.072	13.104	13.104	13.112	13.186	13.069	13.123
(ix) $\Delta C^{corr} = (\Sigma^{13}_{noCNK} - 13)*6.7/13$	0.087	0.076	0.111	0.111	0.119	0.197	0.074	0.130
(x) $Fe^{3+}/\Sigma Fe$	0.23	0.23	0.24	0.32	0.31	0.45	0.11	0.083
Si	6.211	6.230	6.032	6.188	6.002	5.943	6.628	7.927
Al	1.789	1.770	1.968	1.812	1.998	2.057	1.372	0.073 (Fe^{3+})
Ti	-	-	-	-	-			
Z	8.000	8.000	8.000	8.000	8.000	8.000	8.000	8.000
Al_{IV}	0.090	0.145	0.129	0.048	0.103	0.487	0.565	
Ti_{VI}	0.442	0.437	0.489	0.435	0.482	0.504	0.094	
Fe^{3+}	0.370	0.323	0.470	0.470	0.505	0.480	0.319	0.481
Fe^{2+}	0.884	0.809	1.059	0.675	0.797	0.986	1.985	4.625
Mn	0.010	0.013	0.015	0.011	0.013	0.018	0.036	
Mg	3.269	3.326	2.921	3.444	3.187	2.772	2.057	
C	5.005	5.053	5.083	5.083	5.087	5.247	5.056	
Ca	1.868	1.871	1.893	1.863	1.908	1.673	1.889	0.514
Na	0.816	0.778	0.801	0.805	0.760	0.809	0.372	2.380
K	0.329	0.329	0.317	0.322	0.351	0.273	0.145	
AB	2.999	2.978	3.011	2.990	3.019	2.755	2.406	2.891
OH								
This work								
mg#	0.72	0.74	0.65	0.75	0.71	0.65	0.47	0
13cat calc.	16.08	16.04	16.09	16.07	16.11	15.88	15.46	15.99
$Fe^{3+}/\Sigma Fe$	0.23	0.23	0.24	0. 32	0.31	0.45	0.11	0. 083
16 cat calc	16.00	16.00	16.00	16.00	16.00	16.00	16.00	16.00
$Fe^{3+}/\Sigma Fe$	0.48	0.38	0.48	0.60	0.63	0.33	-ve Fe^{3+}	-ve Fe^{3+}
Zaitsev et al. (2013)								
mg#	0.72	0.75	0.65					
$Fe^{3+}/\Sigma Fe$	1.00	0.334	0.337					
Σ_{cats}	16.06	16.04	16.09					
Li et al. (2020a)								
$Fe^{3+}/\Sigma Fe$	0.26	0.26	0.24	0.30	0.26	0.26	0.19	0.2
Σ_{cats}	16.06	16.01	16.12	16.08	16.14	16.02	15.40	15.60
Ridolfi et al. (2018)								
$Fe^{3+}/\Sigma Fe$	0.5	0.33	0.5	0.6	0.66	0.30	0.20	0.03
Σ_{cats}	16.00	15.04	16.00	16.00	16.00	16.00	15.41	16.14

*Magnesian hornblendes and hastingsites.

4.1. Fully Analysed Amphiboles from Mantle-Derived Peridotites, Kaersutite Megacrysts, Kola Hastingsites, and Synthetic Richterites

The first samples discussed are Ti-rich 'ferri-kaersutites' from northern Tanzania (Zaitsev et al., 2013); which were renamed as 'oxo-magnesio-hastingsites' (end-member $NaCa_2Mg_2Fe^{3+}{}_3[Si_6Al_2]O_{22}O_2$) by Zaitsev et al. (2013). Zaitsev et al. report EMP analyses for 8 amphiboles; three have Fe-valence values determined by Mössbauer spectroscopy and all have water values reported. The three amphiboles with measured Fe valence show formulae calculated to 24 anions apfu as shown in **Table 2** in Zaitsev et al. (2013). We deal with the three samples analysed by Mössbauer (OL 22, OL 313 and OL 246), together with another sample from the same locality as OL 22 (DT -/11), and an average for the four other samples (LL 1/5, LL -/4, LL 3/4 and OL 165) (**Table 2** this work). For all of those samples the wt.% values with all Fe as FeO have been recalculated as anhydrous formulae on the basis of (23 + $^{W}O^{2-}/2$) with $^{w}O^{2-}$ obtained from the Li et al. (2020a) spreadsheet. The initial cation totals with all Fe as Fe^{2+} are shown at the top of the data columns (denoted Σ^{16}; **Table 2** row (i)) All show values with totals > 16 atom pfu reflecting the presence of Fe^{3+}. The calculated $Fe^{3+}/\Sigma Fe$ ratios are given in **Table 2** row (ii); these values might be reliable as the Σ^{16} are so high that the proportions of any vacant cation sites could be small. Row (iii) of **Table 2** gives the total cation values for the 13 cation formulae defined as Σ^{16} – (Ca + Na + K) in B and A (here denoted $\Sigma^{13}{}_{noCNK}$). We have shown earlier (Section 2) that stoichiometric amphiboles should give very similar values for estimated model Fe^{3+} without vacant sites having any effect. Indeed, the first two estimates (Σ^{16} and $\Sigma^{13}{}_{noCNK}$; rows (ii) and (iv) for all 5 samples show good agreement suggesting high Fe^{3+}. Except for OL 22, calculated estimates are much more oxidising than Mössbauer values for OL 313 and OL246 (**Table 2**, columns 1b and 1c). These analyses show significant amounts of C-type atoms greater than the limit of 5.0 atoms pfu with the excess over 5.00 termed ΔC following Ridolfi et al. (2018); we define this excess as $\Delta C = \Sigma^{13}{}_{noCNK} - 13$; however, that value still has the enhanced values for all the T and C components due to the presence of all Fe as Fe^{2+} coupled to the absence of the extra O defining the amount of Fe^{3+} present. For OL 22 that initial excess ΔC = 0.169 and that amount is firstly distributed based on the stoichiometric amphibole T and C (8 and 5, respectively). Thus, an initial value is calculated as $\Delta C^* = (\Sigma^{13}{}_{noCNK} - 13) \times 5/13$ (row (vi)) and the estimated $Fe^{3+}/\Sigma Fe$ all show lower ratios reflecting the different calculated ΔC^* values. The estimated oxidation states for OL 313 and OL 246 are similar to the Mössbauer analyses suggesting that this ΔC calculation might be reliable. However, when dealing with other published data sources it soon became clear that this method for modelling the value for ΔC* tended to give estimated Fe^{3+} that appeared to be too high so it was decided to define the composition for a hypothetical amphibole with a chosen proportion of component that might occur in either C or B. Thus a fixed proportion of the Ca in the ideal amphibole 0.5 Mg-ferri-hornblende – 0.5 ferrotaramite of composition $\square_{0.5}Na_{0.5}(Na_{0.5}Ca_{1.5})(Mg_2Fe^{2+}{}_{1.5}Fe^{3+}{}_{0.5}Al)[Si_{6.5}Al_{1.5}]O_{22}(OH)_2$ (see our

Table 1, column 7) is replaced with 0.15 atoms Mn to give the composition $\square_{0.5}Na_{0.5}(Na_{0.5}Ca_{1.35}Mn_{0.15})$ $(Mg_2Fe^{2+}{}_{1.5}Fe^{3+}{}_{0.5}Al)[Si_{6.5}Al_{1.5}]O_{22}(OH)_2$ (Table 1, column 8); note that both compositions have the same Fe^{3+} - Fe^{2+} contents. Recalculation of the new composition with the spreadsheet (Folders I, III) with the Mn component gives a $\Sigma^{13}{}_{noCNK}$ (i.e. all Mn included with Mg and Fe) estimated Fe^{3+} of 0.632 rather than the known value of 0.500 pfu with all the element proportions being slightly smaller than the known values (e.g. Si 6.481 instead of 6.500 pfu!). Thus the excess C calculation has been varied by trial and error to provide the new calculation defined as $\Delta C^{corrected} = (\Sigma^{13}{}_{noCNK} - 13) \times 6.7/13$. This calculation now gives Fe^{3+} = 0.500 pfu for the Mn amphibole chosen to calibrate a feasible 'correction' method; note that the final formula data (Table 1, column 8 and attached spreadsheet Folder I) show a $\Sigma^{13}{}_{noCNK}$ value of 13.15 **without** any Mn; thus Mn = 0.15 pfu clearly belongs to B as shown in its ideal formula. Thus, the new values for the Zaitsev amphiboles using the $\Delta C^{corredted}$ factor are shown in Table 2 and columns 1a to 1e.

The same crystal chemical reasoning has been used for the other samples in Table 2 (rows (vii – x)), columns 1b-1e and in all cases the formulae show that the 13 cation formulas with the recalibrated $\Delta C^{corrected}$ component added to the B + A term have much less oxidised Fe valence ratios. All have similar calculated values for the $Fe^{3+}/\Sigma Fe$ ratios (range 0.23 - 0.32) which are slightly lower than the analysed $Fe^{3+}/\Sigma Fe$ Mössbauer values for samples OL 313 and OL 246 (0.33 and 0.34; Zaitsev et al., 2013). However, the calculated crystal chemical $Fe^{3+}/\Sigma Fe$ value for OL 22 is completely different to that from the Mössbauer study results which showed only peak pairs for Fe^{3+} (Zaitsev et al., 2013). It is possible that the sample used for that study was more altered than the others but it is clear that the estimated $^{W}O^{2-}$ values for amphibole are dependent on the whole mineral composition, especially the coupled Si-Al-Ti relationships which are much more difficult to reset than a simple and much more rapid Fe^{2+} oxidation which can occur very rapidly by an electron shuttle mechanism for micas, amphiboles and spinels (*cf.* Dyar et al., 1993; Righter, et al., 2002; Henderson et al., 2016; Della Ventura et al., 2018; Bernardini et al., 2023; Henderson, 2025). At the bottom of Table 2 the *mg#*, total cation numbers and $Fe^{3+}/\Sigma Fe$ ratios are summarised for 13 and 16 cation formulae with data from this work, Zaitsev et al. (2013), and for data obtained using the Li et al. (2020a) and Ridolfi et al. (2018) spreadsheets.

The work of Dyar and colleagues on Ti- bearing kaersutite amphiboles is very relevant to this paper, the element specific Mössbauer (Dyar et al., 1993) and X-ray absorption spectroscopic (XAS, Dyar et al., 2016) techniques were used to determine Fe-valences directly. Table 2 (column 2) shows the average composition for 20 samples from their Table 5 (Dyar et al., 1993) with all Fe input as FeO and on an anhydrous basis. In addition, another publication repeats the data for some of 1993 samples as well as giving XAS pre-edge and XANES K-edge data for new samples in good agreement with Mössbauer $Fe^{3+}/\Sigma Fe$ results (Dyar et al., 2016). The average data reported here (our Table 2, column 2) give the data in the same

format as for the 5 Zaitsev et al. (2013) samples. The average 16 cation formula gives a total cation sum of 16.165 equivalent to a $Fe^{3+}/\Sigma Fe$ ratio of 0.32 [**Table 2**, (ii) (range 0.15 - 0.46 for the 20 individual samples], while the uncorrected 13 cation formula (only Ca, Na, and K at B and A) totals 13.388 with a $Fe^{3+}/\Sigma Fe$ ratio of 0.94 (row (iv)) (range 0.8 - 1.9!). The first estimate is only slightly smaller than the Dyar et al. (1993) average (0.41 ± 0.14) while the second is clearly incorrect because the assumed A + B occupancy by Ca + Na + K is only 2.755 which could reflect the presence of unanalysed components such as Sr or Ba. Note that a cation shortfall cannot be explained by the presence of vacancies (see above), however, the Dyar et al. (1993) samples show that large proportions of C-type cations occupy B. Thus, the first calculation we have used to estimate the ΔC content gives a value of 0.149 pfu (row (vi)) leading to an A + B occupancy of 2.93, a 13 total cation sum of 13.239 (row (v)) and an $Fe^{3+}/\Sigma Fe$ ratio of 0.58 (range 0.42 - 0.96) for the average composition (**Table 2**, column 2, row (vii)). The preferred $\Delta C^{corrected}$ – Σ^{13} cation calculation (row (viii-x)) now gives an average $Fe^{3+}/\Sigma Fe$ of 0.45, within error of the Dyar et al. (1993) average Mössbauer composition (0.41 (16)). Our data for 9 representative samples from the Dyar et al. (2016) paper shows a similar level of agreement but note that two heated samples with very high proportions of Fe^{3+} (>0.9) both show $Fe^{3+}/\Sigma Fe$ estimates < 0.2; this confirms our earlier suggestion that the overall crystal chemistry estimate of $^{W}O^{2-}$ appears to be coupled to the overall Si-Al-Ti composition which leads to lower $Fe^{3+}/\Sigma Fe$ ratios consistent with primary amphibole crystallization conditions, or mantle heterogeneities, rather than those of later dehydroxylation and rapid Fe-oxidation reactions (Graham et al., 1984; Dyar et al., 1993; cf. Ba-Ti-rich micas, Righter et al., 2002; Henderson, 2025).

Uvarova et al. (2007) reported analysis, with Fe valence determined by Mössbauer techniques, of hornblendes and hastingsites. The average composition for 7 samples (**Table 2**, column 3) shows atomic proportions for a 13 cation formula. The '16 cation' total is < 16.0 pfu (row (i)) so negative Fe^{3+} contents are implied; however an uncorrected 13 cation formula gives 13.151 cations pfu giving a model $Fe^{3+}/\Sigma Fe$ = 0.23 (rows (iii-iv)). The initial calculated ΔC value is 0.055 (row (vi)) giving a corrected B + A occupancy of 2.413 and a lower 13 cation total of 13.088 leading to a $Fe^{3+}/\Sigma Fe$ = 0.14 (rows (v, vii)); the equivalent values for the $\Delta C^{corrected}$ – Σ^{13} cation formula are 2.48, 13.069 and 0.11 (rows (viii, x); both the Σ^{13} cation formula estimates are close to the spectroscopically determined value of 0.15 (2) (Uvarova et al., 2007). The final dataset (our **Table 2**, column 4) is for a single sample of a synthetically prepared richterite (Della Ventura et al., 2016). For this sample our calculated data are reported mainly for a 13 cation formula but the full 16 cation total is 16.182 atoms pfu ($Fe^{3+}/\Sigma Fe$ = 0.10) and the uncorrected 13 cation total is 13.253 pfu with a higher $Fe^{3+}/\Sigma Fe$ = 0.17. The calculated ΔC^{*} value is 0.097 leading to a recalculated $Fe^{3+}/\Sigma Fe$ = 0.11 (column 3, rows (vi, vii)) and the equivalent calculated $\Delta C^{corrected}$ values are 0.130 and 0.083 (**Table 2**, column 4, rows (ix, x)).

We have shown that calculation of Fe valences depends on correctly dealing with the possibility of significant vacancy proportions. Amongst others, Hawthorne

(1983), Dyar et al. (1993), and Hawthorne & Oberti (2007) have pointed out that there might not be any significant correlation between calculated and measured amounts, however, it is possible that other workers might not have developed sufficiently robust of ways of quantifying, or approximating, the vacancy count. We have attempted to do that and we conclude that, depending on the amphibole species, the most reliable calculation for the atomic proportions is for a 13 cation calculation with a robust treatment of the possible presence of a C-group excess over 5 for the small divalent cations species (mainly Mn and Fe^{2+}). This preferred approach is denoted here as the ($\Delta C^{corrected}$, Σ^{13}) cation calculation. Other workers have published Fe valence data which shows mixed agreement with our approach as demonstrated in the next section. Indeed, the most useful calculation mode found for amphiboles in the work is that defined by $\Sigma^{13} - (Ca + Na + K) - \Delta C^{corrected}$ with $\Delta C^{corrected}$ having the empirical 6.7/13 factor and the numerical details are shown in the attached spreadsheet, Folder III. Calculation details for Σ^{16} formulas are shown in Folder II as the first set of labelled final formula data and for $\Sigma^{13} - (Ca + Na + K)$ ($\Delta C = 0$) as the second labelled set of final data.

4.2. Other Published Ca/Na Amphiboles with Fe Valence and Water/H Determinations

Mössbauer spectroscopy Fe values are preferred (Taran et al., 1999; Enders et al., 2000; Popp et al., 2006; Ishida et al., 2002; Abdu & Hawthorne, 2009); followed by chemical analysis for Fe valence (Satoh et al., 2004); Fe-X-ray Absorption Spectroscopy data (Bonadiman et al., 2014; Dyar et al., 2016); and indirect Fe^{3+} estimation from single crystal diffraction methods (e.g., Hawthorne et al., 1998; Gatta et al., 2017). Particular attention was paid to Ti-rich amphiboles (e.g., Oberti et al., 1992; Hawthorne et al., 1998; Bonadiman et al., 2014). Our approach deals with averaged data for each source paper, but additional samples are included in the amphibole spreadsheet (Folders II to IV). Thus, **Table 3** summarises the best approaches for calculating formulae for Ca-rich or Na-rich amphiboles for 24 anion ($23O + {}^{W}O^{2-}/2$) formulae, followed by (i) 13 cation $\Sigma^{13} = \Sigma^{16} - \Sigma(Ca + Na + K)$ (denoted $\Delta C = 0$) or (ii) as $\Sigma^{13} = \Sigma^{16} - \Sigma Ca + Na + K - \Delta C^{corr}$ (correction parameter 6.7/13). Ca-rich amphiboles are best fitted using (ii) and Na-rich by method (i). Ca-rich compositions in columns 1 - 5 show how maximum and minimum Fe^{3+} contents could be estimated.

Hawthorne and colleagues used two chemically analysed data sets (Binns, 1965; Deer et al., 1966) to discuss how amphibole analyses could be modelled based on different cation totals to estimate the lower and higher possible Fe^{3+} contents. The first two columns in **Table 3** show the source chemical data for those amphiboles; method (ii, above) column 1 shows that with $\Delta C^{corr} = 0.176$ our calculated $Fe^{3+}/\Sigma Fe$ of 0.20 is in excellent agreement with the Binns (1965) chemical analysis (0.21); while that for column 2 is only slightly higher than for the Deer et al. (1966) analysis (0.36 and 0.30, respectively). For further comparison, an early reliable chemical analysis of a Glenelg hornblende with $H_2O+ = 2.05$ wt. % (equivalent to

Table 3. Amphibole formula checks for published analyses with Fe-valence determined or estimated.

(a)							
	1	2	3	4	5	6	7
	Hawthorne (1983) Binns Chem anal.	Hawthorne et al. (2012) Deer Chem. anal.	Tilley & Vincent (1937), Chem anal.	Schumacher (2007), Hb Av. of 1252 chem. anals	Stout (1972), EMP Hb 161A	Deer et al. (1997) Kaersutite Tble 21 #13	Nasir & Al-Rawas (2006) Ferri-kaersut Av o 5
SiO_2	40.85	51.63	42.28	44.08	45.4	39.98	40.40
TiO_2	0.65	-	0.66	1.12	0.0	5.68	5.98
Al_2O_3	14.45	7.39	17.24	11.65	23.3	14.17	14.69
FeO	23.56	7.55	11.75	15.66	12.7	13.03	9.48
MnO	0.35	0.17	0.12	0.27	0.3	0.13	0.054
MgO	5.11	18.09	11.91	11.23	13.8	10.45	13.49
CaO	10.86	12.32	11.06	11.16	11.2	9.68	10.79
Na_2O	1.48	0.61	1.73	1.69	1.6	3.49	2.62
K_2O	0.61	-	0.81	0.65	0.0	1.52	1.71
Total	97.92	97.76	97.56	97.51	98.3	98.13	99.21
$^{W}O^{2-}$ source	0.345	0.000	0.02			0.95	1.73
$^{W}O^{2-}$ Li et al. (2020a)				0.218	0.141	0.915	1.044
ΔC^{corr} this work	0.176	0.096	0.124	0.138	0.205	0.134	0.183
				23 O + ($^{W}O^{2-}$/2), ΔC^{corr} with factor 6.7/13			
Si	6.259	7.211	6.112	6.527	6.478	5.998	5.897
Al	1.741	0.789	1.888	1.473	1.522	2.002	2.103
T total	8.000	8.000	8.000	8.000	8.000	8.000	8.000
Al (VI)	0.870	0.428	1.049	0.560	0.715	0.503	0.424
Ti (VI)	0.075	-	0.072	0.125	0	0.641	0.657
Fe^{3+}	0.590	0.318	0.409	0.458	0.675	0.449	0.613
Fe^{2+}	2.429	0.564	1.012	1.481	0.840	1.186	0.544
Mn	0.045	0.020	0.015	0.034	0.036	0.017	0.007
Mg	1.167	3.766	2.567	2.479	2.935	2.337	2.935
C total	5.176	5.096	5.124	5.137	5.201	5.133	5.180
ΔC	0.176	0.096	0.124	0.137	0.201	0.133	0.180
Ca	1.783	1.844	1.713	1.771	1.712	1.556	1.687
Na	0.041	0.060	0.163	0.092	0.087	0.311	0.133
B total	2.000	2.000	2.000	2.000	2.000	2.000	2.000
Na (A)	0.399	0.105	0.322	0.393	0.361	0.704	0.610
K	0.119	-	0.148	0.123	0	0.291	0.318
A Total	0.518	0.105	0.470	0.516	0.361	0.995	0.928
$Fe^{3+}/\Sigma Fe\ \Delta C^{corrected}$	0.20	0.36	0.29	0.24	0.44	0.27	0.53
Charge balance	46.35	46.00	46.02	46.22	46.14	46.92	47.04

Continued

Ma.x Fe^{3+-} source calc, 13 cat	0.652 pfu	0.86 pfu	0.836 pfu	0.718 pfu	1.23 pfu	0.92	0.20
Minm Fe^{3+} source calc 15 to Ca	0.132 pfu	0.12 pfu	0	0	0.27 pfu	0	1.25
$Fe^{3+}/\Sigma Fe$, source data	0.21 (chem.)	0.30 (chem.)	0.21 (chem.)	0.19 (av calc)	Source preferred 0.18	0.69	1.0

1) Hawthorne (1983) with Binns (1965) data; 2) Hawthorne et al. (2012) with Deer (1938) data; 3) Tilley & Vincent (1937); 4) Schumacher (2007); 5) Stout (1972); 6) Deer et al. (1997), Kaersutite, Table 21, analysis #13; 7) Nasir & Al-Rawas, Ferri-kaersutute average of 5 megaxts and upper mantle samples.

(b)

	8	9	10	11	12	13	14	15	16
	Taran et al (1999) Av. 17	Popp (2006)/ Gatta et al. (2017) Av. 2	Satoh et al. (2004) Av 7	Hawthorne et al. (1998) Ca-Na Av. 8	Hawthorne et al. (1998) Na amp Av. 3	Enders et al. (2000) Na amph Av. 12	Colombo et al. (2023) Ferro-ferri kataphorite	Bonadiman et al. (2014) Av 6	Tiepolo et al. (1999) Sample K(1)
SiO_2	41.08	39.35	42.27	53.77	54.27	55.78	43.08	42.64	42.86
TiO_2	3.88	6.48	4.39	2.83	3.45	0.30	2.84	4.46	3.96
Al_2O_3	13.88	12.63	10.70	0.71	0.18	6.79	8.76	13.96	14.70
Cr_2O_3	0.10	0.01	-	-	-	0.03	0	0.47	0.02
FeO	10.77	9.73	14.59	12.03	16.11	18.99	22.26	6.05	
MnO	0.12	0.12	0.48	0.26	0.21	0.12	0.43	0.07	
MgO	12.99	13.35	10.65	14.73	11.74	7.61	6.91	15.25	19.28
Li_2O	-			0.018	0.080				
CaO	11.27	12.34	10.73	5.16	2.37	0.51	6.58	10.99	10.86
Na_2O	2.50	2.51	2.87	6.28	7.91	7.34	5.55	2.79	3.19
K_2O	1.51	0.97	1.65	1.94	1.81	0.17	1.18	0.90	1.08
Total	98.10	97.49	98.33	97.73	98.15	97.64	97.59	97.58	96.04
$^{W}O^{2}$ source		0.862	0.698	0.337	0.489	0.030	0.61	0.866	0.62
$^{W}O^{2-}$ Li et al.	0.608		0.457	0.142	0.242	0.01	0.423	0.623	0.55
ΔC^{corr}	0.116	0.090	0.077	0	0	0	0.138	0.103	0.124
	23O + $^{W}O^{2-}/2$; ΔC^{corr} with 6.7/13 factor; attached spreadsheet Folder III			23O + $^{W}O^{2-}/2$; $\Delta C = 0$; see spreadsheet II, Σ^{13} cation cell (Σ^{13}_{noCNK})				23O + $^{W}O^{2-}/2$; ΔC^{corr} 6.7/13 Folder III	23O + $^{W}O^{2-}/2$ 16 cations Folder II
Si	6.083	5.902	6.379	7.851	7.968	7.939	6.603	6.163	6.167
Al	1.917	2.100	1.621	0.123	0.032	0.061	1.397	1.832	1.833
Ti	-	-	-	0.026	-				
T total	8.000	8.000	8.000	8.000	8.000	8.000	8.000	8.000	8.000
Al (VI)	0.453	0.134	0.282	-	-	1.076	0.185	0.546	0.675
Ti (VI)	0.432	0.731	0.498	0.284	0.381	0.033	0.327	0.485	0.429
Cr	0.012	0.001	-	-	-	0.003	-	0.051	0.002
Fe^{3+}	0.386	0.302	0.259	0.150	0.471	0.734	0.940	0.343	
Fe^{2+}	0.948	0.9191	1.581	1.318	1.507	1.527	1.914	0.388	
Mn	0.014	0.017	0.061	0.032	0.026	0.014	0.056	0.009	
Mg	2.868	2.984	2.395	3.206	2.569	1.614	1.579	3.285	4.235

Continued

Li				0.010	0.047				
C total	5.113	5.088	5.076	5.000	5.001	5.001	5.001	5.107	5.124
ΔC	0.113	0.088	0.076	0	0.003	0.000	0.001	0.107	0.124
Ca	1.783	1.912	1.735	0.807	0.373	0.078	1.081	1.702	1.674
Na	0.089	-	0.185	1.193	1.624	1.922	0.918	0.191	0.202
B total	2.000	2.000	2.000	2.000	2.000	2.000	2.000	2.000	2.000
Ca (A)		0.071							
Na (A)	0.628	0.730	0.655	0.584	0.629	0.105	0.731	0.591	0.688
K	0.286	0.185	0.318	0.362	0.340	0.031	0.231	0.165	0.198
A Total	0.914	0.986	0.973	0.946	0.969	0.136	0.962	0.756	0.836
Charge balan	46.61	46.26	46.70	46.33	46.44	46.03	46.42	46.62	46.6
$Fe^{3+}/\Sigma Fe$ corrected	0.29	0.25	0.14	0.10	0.24	0.32	0.33	0.47 0.18	n.a.
%Ti as $\square^{Ti}$								~19%	
$Fe^{3+}/\Sigma Fe$ source data	0.38	0.25	0.13	0.11	0.18	0.31	0.38 Mössbauer	0.17	

8) Taran et al. (1999); 9) Popp et al. (2006) and Gatta et al. (2017); 10) Satoh et al. (2004); 11-12) Hawthorne et al. (1998); 13) Enders et al. (2000); 14) Colombo et al. (2023); 15) Bonadiman et al. (2014); 16) Tiepolo et al. (1999); includes H_2O 1.356 wt%, F 0.03, C 0.03 wt% all by SIMS.

0.02 $^{W}O^{2-}$ pfu) and $Fe^{3+}/\Sigma Fe = 0.21$ (Tilley & Vincent, 1937) gives a slightly higher calculated 13 cation $Fe^{3+}/\Sigma Fe = 0.29$ ($\Delta C^{corr} = 0.124$, this work) (see **Table 3**, column 3). We also show the recommended estimated minimum and maximum $Fe^{3+}/\Sigma Fe$ from the source references. Columns 4 and 5 show similar data for key amphibole papers (Schumacher, 2007; Stout, 1972). For all 5 published Ca-amphibole examples we suggest that our estimated Fe oxidation ratios are more useful for petrologists than those recommended previously based on model calculations for maximum and minimum Fe^{3+} contents (e.g., Schumacher, 1991; Hawthorne et al., 2012) and for those obtained with Locock (2014) corrected by subtracting 2Ti from the atomic O values to obtain a corrected value without any estimated $^{W}O^{2-}$ component. The same format is adopted to test how the spreadsheet deals will Ti-rich kaersutite compositions (see Folder III, rows 363 and 281-286); **Table 3** column 6 shows our data for a chemically analysed sample (Deer et al., 1997) and column 7 an EMP analysis with Fe-valence determined using Mössbauer spectrocscopy (Nasir & Al-Rawas, 2006).

Taran et al., (1999) [**Table 3**] studied upper mantle Fe- and Ti-bearing Ca amphiboles, with 13 samples with Mössbauer Fe valence data. We calculated Fe^{3+} for 15 analyses based on formulae calculated using Li et al. $^{W}O^{2-}$ with 13 cations and $\Delta C^{corr} = 0.116$ (**Table 3**, column 8). The model $Fe^{3+}/\Sigma Fe$ ratio is 0.29 slightly smaller than the average Mössbauer value for 12 samples of 0.38 (range 0.13 - 1.0). However, two of the samples show very high Fe^{3+} ratios (1.0 and 0.54) which are not matched by high calculated $^{W}O^{2-}$, in line with our earlier suggestion that it is much easier to oxidise Fe during later sample alteration than to equilibrate the

bulk composition of the Ti and other components coupled with a high extra-O content (see above). Without the two higher-Fe^{3+} samples the average $Fe^{3+}/\Sigma Fe$ ratio for 10 samples is 0.30(8), in excellent agreement with our model value. Both Popp et al. (2006) and Gatta et al. (2017) studied the crystal chemistry of kaersutite from the same Greenland locality with H determined by manometry (Popp) or SIMS (Gatta). Mössbauer (^{57}Fe, Popp) and stoichiometry plus SC X-ray and neutron diffraction (Gatta) were used to determine the Fe-valence data giving published $Fe^{3+}/\Sigma Fe$ of 0.22 (Popp et al., 2006) and 0.28 (Gatta et al., 2017). The coupled high $^{W}O^{2-}$ and Ti-Ca-rich composition has $\Delta C^{corrected} = 0.090$ leading to a model Fe^{3+} content of 0.302 apfu and $Fe^{3+}/\Sigma Fe = 0.25$ matching the average of the Popp and Gatta estimates. Satoh et al. (2004) studied Ti-Fe-rich calcic amphiboles (edenite to kaersutite) with Fe^{2+} determined chemically, and H and O data by mass spectrometry. We report atomic proportions for the average of 7 samples (**Table 3**, column 10) with $^{W}O^{2-}$ values from the source paper (0.698 pfu). These samples are Ca-Ti-rich with high $^{W}O^{2-}$ leading to cation totals higher than 16, and very high 13 cation totals refection C >> 5. The atomic proportions are therefore calculated on the basis of $\Sigma^{13}_{noCNS} - \Delta C^{corrected}$ (**Table 3**, column 10). The calculated $Fe^{3+}/\Sigma Fe$ for the sample average composition is 0.14 (range for 7 samples 0.09 - 0.23) in excellent agreement with the chemically-determined ratio of 0.13 (range 0.07 - 0.17).

The next 4 examples (**Table 3**, columns 11 to 14) are for Na-rich amphiboles which are best calculated using method (i) described above (i.e. $\Delta C = 0$). Enders et al. (2000) studied Na-rich amphiboles (variable Fe and low Ca and Ti), all with Fe Mössbauer spectroscopy, and microchemical analysis for lithium and H_2O (1.9 - 2.7 wt.%). We report average data for the 12 samples (**Table 3** column 13) with 24 anion formulae (Li et al. $^{W}O^{2-}$ values), all of which have very low values typical of sodic amphiboles. (low $^{W}O^{2-}$, low Ti and with cation totals (Σ^{16}) < 16.000 requiring the Fe valence values to be calculated on a 13 cation formula simply defined as Σ^{16} – Ca + Na + K (denoted Σ^{13}_{noCNS}) (see attached spreadsheet Folder II). The atomic proportions have a model $Fe^{3+}/\Sigma Fe$ value of 0.32 (range 0.07 - 0.69) matching measured Mössbauer values of 0.31 (range 0.07 - 0.52). Our calculation method confirms the stoichiometric approach of Enders et al. (2000) where their Mössbauer results show good agreement with those obtained using an EMP high-resolution, microanalytical flank method (Höfer et al., 2000).

A similar approach was used to calculate formulae and Fe valence data for amphiboles in metasomatised sandstone xenoliths (Hawthorne et al., 1998). In that work, EMP and H-ion probe analyses of 11 samples were studied with Fe^{3+} values estimated from single-crystal X-ray data. Hawthorne et al. (1998) showed that Ti and $^{W}O^{2-}$ values are very closely correlated ($2Ti = {}^{W}O^{2}$); this type of relationship is commonly found in amphiboles and biotite micas (Henderson, 2025). We divided the samples into Na-Ca-rich and Na-rich groups and used $^{W}O^{2-}$ values from Hawthorne et al. (1998) rather than Li et al. $^{W}O^{2-}$ values, which are much smaller for the Ti rich samples. However, the Ridolfi et al. (2018) $^{W}O^{2-}$ values agree with

the Hawthorne data, except for the most sodic sample. Our 13 cation formula results are shown in **Table 3**, (columns 11 and 12) where the atomic proportions and Fe valence values are calculated relative to Σ^{16} – (Ca + Na + K) (i.e., Σ_{noCNK}; attached spreadsheet II). These results support the conclusion of Hawthorne et al. (1998) that the formula are best for calculated with $\Delta C = 0$. The $Fe^{3+}/\Sigma Fe$ ratio for the Ca-Na average is 0.10 (range 0.06 - 0.11) and that for the Na-amphibole is 0.24 (range 0.18 - 0.26). These values are only slightly different to the SREF estimates reported by Hawthorne et al., i.e 0 - 0.11 and 0.13 - 0.24, respectively.

Column 14 gives data for a Ti-rich ferro-ferri-kataphorite (Colombo et al., 2023) with Fe-valence determined with Mössbauer methods and extra-O being modelled on SREF Fe-valence and on a Ti – O3 relationship similar to that discussed above (extra-O = 2Ti). The Folder II calculation (Folder II, row 275) uses the Li et al. estimated $^{W}O^{2-}$ and the full formula is very similar to that reported in the first column of **Table 2** published in (Colombo et al., 2023) with our $Fe^{3+}/\Sigma Fe$ = 0.33, only slightly smaller than the Mössbauer value of 0.38 (our **Table 3**, column 14) which, in turn, is lower than the value of 0.43 obtained using SREF (Colombo et al., 2023).

Table 3 column 15 data gives calculated $Fe^{3+}/\Sigma Fe$ ratios significantly larger than those of the published values which are difficult to reproduce using our adopted calculation protocols, but we will draw attention to possible problems. Thus, Bonadiman et al. (2014) studied Ti-rich calcic amphiboles within metasomatised lherzolites. Analytical results are reported for 6 samples, including SIMS for H, single crystal XRD, together with pre-edge X-ray absorption spectroscopy (XAS) for two samples to estimate $Fe^{3+}/\Sigma Fe$ values of 0.21(5) and 0.16(5). Formulae for these samples (**Table 3**, column 15) are reported for a 24 O formula with $Fe^{3+}/\Sigma Fe$ varying from 0.14 to 0.24 (average 0.17(4)). We have recalculated those analyses with all Fe input as FeO using $^{W}O^{2-}$ values from Bonadiman et al. (2014), ranging 0.499 - 0.994 (average 0.866). Our formula proportions for these Ca-rich amphiboles are calculated on the basis of $\Sigma^{13}{}_{noCNS} - \Delta C^{corrected}$ (average $\Delta^{corrected} = 0.138$); we report an average $Fe^{3+}/\Sigma Fe$ of 0.63 (range 0.5 - 0.8) much more oxidising than the Bonadiman et al. (2014) values. Model $^{W}O^{2-}$ values obtained from the Li et al. spreadsheet are smaller ranging 0.372 - 0.756 (average 0.623) which provide lower $Fe^{3+}/\Sigma Fe$ ratios of 0.39 - 0.61 (average 0.47). We will consider below the possibility that the XAS-determined values for $Fe^{3+}/\Sigma Fe$ values could be overestimates.

Bonadiman et al. (2014) calibrated the $Fe^{3+}/\Sigma Fe$ values for their samples using the positions of the pre-edge feature in the XANES spectrum (e.g., Wilke et al., 2001). The peaks resolved at the absorption edge show some support for low oxidation values but post-edge features are much more similar to more oxidised compositions. Indeed, amphibole XANES spectra in Hawthorne & Oberti (2007) and Dyar et al. (2016) have amphiboles with $Fe^{3+}/\Sigma Fe$ ratios as high as 0.4 - 0.5 show XANES features consistent with those for the Bonadiman samples (cf. data for a Ba-Ti rich mica, Henderson & Foland, 1996). Indeed, it has been shown that using

particular XANES energies to deduce $Fe^{3+}/\Sigma Fe$ values could provide more robust data than PE refinements (e.g., amphiboles (Dyar et al., 2016); garnets (Berry et al., 2010; Dyar et al., 2012)). We have tested the suggestion that some Ti content might involve a coupled Ti-vacancy in the A site ($^{A}\square^{Ti}$) by using a hypothetical amphibole molecule based on the solid solution 0.5-ferrihornblende – 0.5ferrotaramite (our **Table 1**, column 7: $\square_{0.5}Na_{0.5}(Na_{0.5}Ca_{1.5})$ $(Mg_2Fe^{2+}{}_{1.5}Fe^{3+}{}_{0.5}Al)[Si_{6.5}Al_{1.5}]O_{22}(OH)_2$). The proportions of Fe^{2+} and Fe^{3+} are kept constant, as are those of Si and Al, but 0.5 atoms Ti are substituted for 0.5 atoms Mg at C leaving C full with a $Mg_{1.5}$ content; in addition the original vacant 0.5 apfu at A is substituted with an A vacancy related to Ti entry ($\square^{Ti}{}_{0.5}$). The result is that there is a cation and anion valence imbalance which is restored by substituting the Na content at B with Ca and with one oxygen replacing hydroxyl to cope with the molecule now having 47 positive charges. This amphibole now has 50% amphibole in solid solution with the overall formula $\square_{0.5}\square^{Ti}{}_{0.5}(Ca_2)(Mg_{1.5}Ti_{0.5}Fe^{2+}{}_{1.5}Fe^{3+}{}_{0.5}Al)[Si_{6.5}Al_{1.5}]O_{23}(OH)$) requiring the formula to be recalculated to 23.5 oxygens pfu (*cf.* our **Table 1**, column 9). With this approach the phase has a cation total of 15.1574 not including the known vacancy account of 1.0 apfu; as shown above in this case the Fe^{3+} could be calculated on the basis of a 15 cation calculation and this gives a value of 0.488 pfu for Fe^{3+}, close to the known input value. The 23.5O Σ^{13} cation formula calculated from $\Sigma^{16}{}_{\text{no vacancy}}$ – ΣCaNaK gives the value 15.1574 – 2.019 = 12.633, with Fe^{3+} = 12/12.63 = 2.52 apfu, 5 times too high. Calculation of a possible value for Fe^{3+} can only be made using a 'cation' sum of 12.5 with the value for the $\square^{Ti}$ of 0.5 apfu counted as a coupled, essential virtual Ti cation rather than a real vacancy, thus Fe^{3+} = 12.5/12.633 = 0.495 pfu, the known value within error. It is clear that this approach could be used for dealing crystal-chemical problems with Ti-rich amphiboles.

We conclude that our calculation method is robust for stoichiometric amphiboles; however, if the Bonadiman et al. (2014) amphiboles are indeed reduced, we can only suggest that some of the Ti in C must be present associated with a matching vacancy at A. Thus, if 19 % of the Ti is present coupled to a matching vacancy (see earlier), that would reduce the average $Fe^{3+}/\Sigma Fe$ from 0.63 to 0.18, to match the published values (Bonadiman et al., 2014)! See the attached spreadsheet Folder III for the numerical details. The last dataset in **Table 3**, column 16 is for a synthetic Al-rich,Fe-free kaersutite (sample (K(1) Tiepolo et al., 1999) with water, F and Cl measured using SIMS. The calculated 24 anion formula (Supplementary file 1, Column I) has a moderate $^{W}O^{2-}$ value of 0.62 apfu mainly reflecting the high Ti and Al contents (*cf*, a Li et al. spreadsheet vaue of 0.55 apfu). The formula shown in **Table 3** is calculated based on an O factor of (23 + $^{W}O^{2-}/2$) and 16 atoms (Supplementary file 1, Folder II). Those values and the equivalent data shown in Folders III and IV are all in close agreement with the 24 anion data (Folder I) with slightly smaller values for the anhydrous data calulations (e.g., ~1% for Si and ~0.2% for Mg (relative) for the column III data. The strcture determined by

Tiepolo et al. (1999) has Ti ordered at *M*(1) and Al at *M*(2).

Finally, the high quality analyses for Ca-amphiboles discussed above, with EMP TiO_2, Mössbauer or chemical Fe valence, and heat-extracted water reduced with U or SIMS H values (e.g., Cosca et al., 1991; Dyar et al., 1993; Satoh et al., 2004; Popp et al., 2006) all show a clear positive relationship between analytically estimated $^{W}O^{2-}$ and Ti content up to ~8% TiO_2 consistent with data for Coyote samples (Hawthorne et al., 1998; see above). Indeed, the common practice is to assume the relationship $2Ti = {}^{W}O^{2-}$ apfu, in effect with Ti as a proxy for $^{W}O^{2}$ (Hawthorne et al., 2012; Oberti et al., 2007b). Indeed, Oberti et al. (1992, 2007b) have also suggested that that relationship is site-specific for Ti occupying the *M*(1) octahedral site in the C cation group; that site is coordinated with 2 *O*(3) sites in the W position. Most crystallographers working on **low** Ti amphiboles have assigned Ti to *M*(2) together with trivalent cations (mainly Fe^{3+} with Cr if present) rather than (see above); higher Ti contents are ordered at *M*(1) (see above). However, most of that work has been done using single-crystal X-ray diffraction which shows poor scattering contrast for Ti with dominant Mg and Fe components but it is generally assumed that occupancy of *M*(3) is minor while that at *M*(2) is very low. However, Kitamura et al. (1975) studied a Ti-rich kaersutite by single-crystal neutron diffraction which shows high scattering contrast with (Ti cross section $b_c = -3.4$ fm), compared with Fe (9.45) and Mg (5.4); Kitamura found a strong preference for Ti in *M*(1) with 0.27 apfu and low occupancies at *M*(2) 0.02 and *M*(3) 0.04 apfu. Gatta et al. (2017) used X-ray and neutron scattering to study a Greenland kaersutite and reported 0.38 apfu Ti in *O*(1) with 0.16 apfu in **both** *O*(2) and *O*(3); thus $2Ti^{O(1)} = 0.76$ which is lower than measured $^{W}O^{2-}$ of 0.935 apfu (Gatta et al., 2017). However, *M*(3) also has 2 *O*(3) atoms as nearest neighbours so for this sample $2\ Ti^{O(1+3)} = 1.08$ apfu; however, Hawthorne et al. (1998) point out that the local geometry of the *M*(3) site in richterites is not favourable for the presence of Ti. Nevertheless, it appears that for Ti-rich, Ca amphiboles, the overall Ti distribution in the C group might indeed not follow a strict $^{M(1)}$Ti vs $^{W}O^{2-}$ but may involve a contribution from some Ti in *M*(3). Indeed, the more general relationship might be $Ti^{4+} + 2\ O^{2-} = (Mg, Fe^{2+}) + 2(OH)^{-}$, as suggested in Oberti et al. (1992) and Hawthorne et al. (1998).

This is the approach we will follow for the remainder of this paper. However, robust Fe^{3+} contents can only be obtained on a 16 cation basis if it is known that the vacancy count is very small. However, if Σ^{16} is >16.2 with Σ^{13} ~13.2 it is worth trying a 16 cation total calculation (see spreadsheet in Folder II of the attached EXCEL file). Nevertheless, if a '13 cation' total (Σ^{13}) at this stage is larger than ~13.20 to 13.25, a 13 cation calculation might be preferred calculated as $\Sigma^{13} = \Sigma^{16} - (Ca + Na + K) - \Delta C^{corr}$, where the Δ term includes the correction factor 6.7/13 (see above and supplementary file, Folder III, this work). However, many of the analyses shown here have Σ^{16} total less than, or only slightly larger, than 16; and may have ΔC^{corr} values < 0.05 - 0.1; thus, in this work these amphiboles have 13 cation atomic proportions on the basis of $\Delta C = 0$. However, if some particularly

Ti-rich samples cannot be reasonably treated using the above approaches, the possibility of some Ti being present coupled to essential 'virtual-Ti' vacancies should be considered. However, if the vacancy content and Fe valence ratio is not known from reliable analyses, that approach would not particularly useful for assessing robust Fe valence estimates.

In Table 2 and Table 3 we have compared our adopted estimates for Fe^{3+}/Fe with the analysed values (Mössbauer or chemical analyses) and reported generally good agreement for both Ca- and Na-rich amphiboles. We have also calculated the root-mean-square error (RMSE) for 16 samples and can report an average error of 0. 011 apfu for an average sample with $Fe^{3+}/\Sigma Fe = 0.25$ (i.e., 0.25 ± 0.011 apfu); this relative error is equivalent to a total error of 18% for $Fe^{3+}/\Sigma Fe$ values which is equivalent to the errors reported by Ridolfi et al. (2018) and Li et al. (2020a). However, the relative values and general trends for $Fe^{3+}/\Sigma Fe$ ratios found here for different samples will be more robust than calculated Fe^{3+} atomic proportions.

5. Formulae for Published Analyses for Marangudzi and Coldwell Intrusions

Our earlier published research on alkaline syenite igneous complexes includes work at Marangudzi, Zimbabwe (Henderson, 1968; Landoll et al., 1989) and Coldwell, Canada (Mitchell & Platt, 1978, 1982; Lukošius-Sanders, 1988). The first published analyses of minerals from Marangudzi magmatic rocks were obtained for 'pure' amphibole separates using 'classical techniques' (gravimetric, volumetric and spectroscopic). Thus, Borley & Frost (1963) reported 5 analyses of hastingsitic amphiboles from nepheline syenites; Henderson (1968) subsequently published data for amphiboles from 8 nepheline syenites and 5 quartz syenites, but neither of those papers gave values for an extra-O component. The original chemical analyses of Maranguzi amphiboles are given in supplementary file 1, Folder I, together with other crystal chemical calculations (this work). Landoll et al. (1989) gave EMP analyses of Marangudzi amphiboles from 5 nepheline syenites and 3 quartz syenites in a stepwise heating $^{40}Ar/^{39}Ar$ study which gave a reliable cooling age of 178.1 ± 1.8 Ma for the complex.

Most EMP analyses for minerals are averages of individual spot analyses for a given rock sample; such analyses would tend to average out random analytical errors. For many complexes the same mineral variety (e.g., hastingsite or arfvedsonite), has a range of *mg*# [Mg/(Mg + Mn + ΣFe)] atomic ratios, but also tends to show even larger ranges in the calculated Fe^{3+}/Fe^{total} ratios which are unlikely to result from random fluctuation of oxygen fugacity during fractionation. Indeed, very large variations in calculated Fe^{3+} could accumulate from very small analytical errors for the full element suite rather than reliable variations in model extra-O estimates. Thus, we use average compositions for amphibole varieties, and for parent rocks from a given igneous complex, to obtain more reliable average amphibole $Fe^{3+}/\Sigma Fe$ for different amphiboles in different types of parent alkaline complex.

Table 4. Amphibole analyses from Marangudzi alkaline complex, Zimbabwe.

	1a	1b	1c	2a	2b	2c	3a	3b
Wt.%	Chem. NS Av. 12	EMP Av. 5	EMP NS Av 27	Chem. QS Av. 4	EMP QS Av. 3	EMP QS Av. 14	Chem NM	EMP NM Av 7
SiO_2	36.97	38.13	38.02	40.15	40.28	40.89	36.59	38.53
TiO_2	1.61	1.85	1.83	1.89	1.82	1.85	2.81	2.10
Al_2O_3	12.23	12.44	12.47	8.01	7.72	8.06	14.51	13.60
Fe_2O_3	6.61			5.23			5.02	
FeO	19.50	24.04	23.34	24.07	29.90	28.72	16.99	20.12
MnO	0.92	0.81	0.82	0.74	0.80	0.72	0.38	0.37
MgO	4.56	5.11	5.64	4.12	2.87	3.93	6.35	7.38
CaO	11.02	10.94	11.24	10.11	10.08	10.40	11.75	11.55
Na_2O	2.50	2.33	2.25	2.15	2.31	2.07	2.09	2.04
K_2O	2.12	2.11	2.12	1. 41	1.26	1.35	2.25	2.27
H_2O	0.87	n.a.		0.77	n.a.		0.40	
F	0.95	n.a.		1.11	n.a.		0.8	
Cl	0.11	n.a.		n.a.	n.a.		n.a.	
O - F, Cl	0.42			0.47			0.34	
Total	99.53	97.75	97.73	99.28	97.04	97.99	99.60	97.96
Fe^{3+}/Fe^{total}, chemical anal.	0.23			0.16			0.21	
$^{W}O^{2-}$ Li et al. (2020a)	0.330	0.350	0.350	0.427	0. 320	0.368	0.546	0.386
Del C	0.120	0.114	0.110	0.183	0.144	0.159	0.117	0.095
Cell calculation	X = (23 + $^{W}O^{2-}$/2) 13 cations; Δ^{corr} 6.7/13 Cell calculated with all Fe input as FeO							
Si	5.955	6.054	6.025	6.466	6.559	6.540	5.742	5.985
Al_{iv}	2.045	1.946	1.975	1.521	1.441	temp	2.258	2.015
Ti_{iv}				0.013				
Z	8.000	8.000	8.000	8.000	8.000	8.000	8.000	8.000
Al_{vi}	0.245	0.383	0.354	-	0.041	0.060	0.426	0.476
Ti_{iv}	0.195	0.221	0.218	0.216	0.223	0.222	0.332	0.245
Fe^{3+}	0.398	0.379	0.378	0.605	0.479	0.528	0.390	0.334
Fe^{2+}	3.031	2.813	2.716	3.270	3.593	3.313	2.433	2.281
Mn	0.126	0.109	0.110	0.100	0.110	0.098	0.051	0.049
Mg	1.095	1.209	1.332	0.990	0.697	0.937	1.485	1.709
C	5.121	5.113	5.109	5.181	5.143	5.157	5.117	5.094
ΔC	0.121	0.113	0.109	0.181	0.143	0.157	0.117	0.094
Ca	1.902	1.861	1.909	1.745	1.759	1.776	1.976	1.921
Na	0.781	0.717	0.691	0.670	0.729	0.639	0.636	0.615
K	0.436	0.427	0.429	0.289	0.262	0.275	0.450	0.450

Continued

A + B	3.240	3.118	3.027	2.885	2.893	2.857	3.179	3.080
Total cats	16237	16.119	16.138	15.885	15.893	15.85	16.178	16.082
mg#	0.28	0.27	0.29	0.200	0.14	0.19	0.39	0.39
#(i) Fe^{3+}/Fe^{total} Σ^{13} (with ΔC^{corr})	0.12	0.12	0.12	**0.17**	**0.12**	**0.14**	0.15	0.13
(iia) Fe^{3+}/Fe^{total} Σ^{16}	0.32	**0.23**	**0.25**	0.07	0.04	0.03	0.32	**0.22**
(iib) Fe^{3+}/Fe^{total} Σ^{13}	**0.24**	**0.25**	**0.25**				**0.29**	**0.26**
(iii) Fe^{3+}/Fe^{total} Σ^{13} Ti cal.	0.12			0.11	0.12	0.13	0.14	0.12
(iv) Fe^{3+}/Fe^{total} Landoll		0.14			0.12			
Charge balance	46.28	46.35	46.35	46.32	46.32	46.37	46.49	46.39
Fe^{3+}/Fe^{tot}, Li et al. (2020a)	0.27	0.26	0.26	0.25	0.24	0.21	0.22	0.22
$\Sigma^{16}{}_{cats}$, Li et al. (2020a)	16.22	16.02	16.05	15.91	15.80	15.77	16.241	16.05
Fe^{3+}/Fe^{tot}, Ridolfi et al. (2018)	0.30	0.21	0.18	0.20	0.16	0.19	0.34	0.23
$\Sigma^{16}{}_{cats}$, Ridolfi et al. (2018)	16.00	15.97	16.00	15.82	15.77	15.73	16.00	16.00

Samples: **Table 4**, Marangudzi, Zimbabwe, 1a Average amph. for 13 nepheline syenites (Henderson, 1968); 1b EMP average analysis for 5 neph. syen. amphiboles (Landoll et al., 1989); 1c analysis for 27 neph. syen. amphiboles this work) 2a Average amph. for 4 quartz syen. amphiboles (Henderson, 1968); 2b EMP av. for 3 qtz. syen. amph. (Landoll et al., 1989); 2c, av. for 14 quartz syen. amph. (this work) 3a chem. anal. neph monzonite amph R174, 3b av. of 7 EMP neph mon amph (this work) $^{w}O^{2-}$ based on original chemical analyses, #Source Supp file (i) Folder C; (ii) Folder A, (iii) Folder D, (iv) Landoll et al. (1989) **Bold** typeface is shown for preferred values.

The data for Marangudzi intrusions are shown in **Table 4**. The initial chemically analysed data for Marangudzi amphiboles from 12 nepheline syenites (Henderson, 1968) show *mg*# ranging 0.31 to 0.10 (average 0.29) and $Fe^{3+}/\Sigma Fe$ from 0.19 to 0.29 (average 0.23); the equivalent ranges for 4 quartz syenite amphiboles are 0.11 - 0.33 (0.20) and 0 - 0.21 (0.16); note the lower oxidation states for the oversaturated rocks. EMP amphibole data for 5 nepheline syenites are *mg*# 0.45 - 0.17 (0.27) and $Fe^{3+}/\Sigma Fe$ 0.09 - 0.16 (0.12). The consistency of the chemically analysed Fe valence values for both the undersaturated and oversaturated syenite amphiboles are considered to be much more reliable than those estimated based on the stoichiometry of the EMP data for the same samples and we adopt the chemically determined $Fe^{3+}/\Sigma Fe$ ratios as the best values for the Fe valence states for the Marangudzi amphiboles. EMP analyses for a wide range of minerals from Marangudzi rocks are available (Henderson, in preparation) and those for amphiboles from nepheline monzonites, nepheline syenites and quartz syenites are used here. Averages of Fe-valence ratios show a significantly larger variation than those for the petrologically easily understood variation of evolving Fe/Mg ratio in genetically related, igneous rocks. In addition, study of individual EMP analyses for unaltered hastingsitic amphibole in Marangudzi mafic foyaite R17 shows this same relationship with $Fe^{3+}/\Sigma Fe$ variations double those shown for the *mg*# index. In addition, the use of averaged EMP data fits in with the results for Mössbauer Fe valence or H analyses being obtained on crushed bulk powders prepared from

mineral separates.

The first column in **Table 4** (1a) gives the average for the original chemical analyses for 12 hastingsitic amphiboles from Marangudzi nepheline syenites. Note that the chemically analysed $Fe^{3+}/\Sigma Fe$ values for the Marangudzi amphiboles are given in the upper part of **Table 4** along with the chemical wt.% oxide data. The 24 anion formula formula shown was calculated with our amphibole spreadsheet but the original F analyses were halved based on later studies of these samples. The chemical analysis has $^{W}O^{2-} = 0.569$ but the calculated $^{W}O^{2-}$ is 0.330 (Li et al., 2020a spreadsheet); the average chemical analysis has *mg*# = 0.28 and $Fe^{3+}/\Sigma Fe$ = 0.23 and the latter is adopted as the best available value for the Fe oxidation ratio (**Table 4**, 1a). The average chemical analysis calculated on an anhydrous basis with all iron as FeO is also calculated for a $(23 + {}^{W}O^{2-}/2)$ formula with $^{W}O^{2-} = 0.330$ (Li et al. spreadsheet); formulae are based on 13 cations (with $\Delta C = 0$) and 13 cations (with the $\Delta C^{corrected}$ parameter). Those calculations give $Fe^{3+}/\Sigma Fe = 0.32$ and 0.12 (**Table 4**, 1a, rows ((iia) and (i) respectively) for a cation total of 16.24 apfu. The average of EMP analyses for amphiboles from 5 Marangudzi nepheline syenites (Landoll et al., 1989) is calculated in the same way (**Table 4**, 1b) giving $Fe^{3+}/\Sigma Fe$ = 0.23 (16 cations) and 0.12 (13 cations) [**Table 4**, 1b, rows (iia) and (i) respectively], with cation total 16.12. Column 1c shows the mean composition for a wider range of 27 Marangudzi nepheline syenites (pulaskites, foyaites and juvites). They give very similar data to those in 1b with $Fe^{3+}/\Sigma Fe = 0.25$ (**Table 4**, 1c, (iia)) and 0.12 (c, (iii)) cation total of 16.14. Thus, for the average EMP analysed Marangudzi nepheline syenite amphiboles our $\Sigma^{13} - \Delta C^{corr}$ Fe valence estimates are half of those determined chemically which we have adopted as reliable. This underestimate is related to the standard procedure developed here for studying amphiboles which mainly have excess C cations which must be transferred to the B site, which in turn reduces the calculated Fe^{3+} content. In fact, many of the Marangudzi nepheline syenite amphiboles (e.g., for foyaites) do not have significant excess C cations and recalculation to 16 cations gives average $Fe^{3+}/\Sigma Fe$ values of 0.23 and 0.25 for column 1b (row (ii) and 1c (row (ii)) amphiboles, much closer to the chemical values. Thus, also see results for these nepheline syenite averages calculated assuming $\Delta C = 0$ (**Table 4**, 1bc, (iv)); in **Table 4** all preferred values are shown in bold.

The data for chemically analysed edenite/hastingsite amphiboles for Marangudzi quartz syenites (**Table 4**, column 2a) show compositions that have higher Si and lower Al than those from nepheline syenites; the chemically analysed valence values are $Fe^{3+}/\Sigma Fe = 0.16$ (column 2a). Column 2b shows the average EMP analysis for three Marangudzi quartz syenites (Landoll et al., 1989); the estimated '13' cation $Fe^{3+}/\Sigma Fe$ value = 0.12 (column2a, row (ii)), smaller than the value suggested by Landoll (0.14). The data in **Table 4**, column 2c is for a wider range of 14 quartz syenites from Marangudzi (this work) and the overall composition ($Fe^{3+}/\Sigma Fe$ = 0.14, column 2c, row (iii)) is closer to the data shown in column 2b, row (i). Thus, Marangudzi amphibole analyses show clear differences in major element chemistry between the silica over- and under-saturated rock types, but when the extra-O

contents are incorporated the calculated Fe-valence states are similar and suggest similar oxygen fugacities for magmatic fractionation within the main rock units for this complex.

The nepheline monzonite unit is a less-well exposed rock type but its geochemistry and mineralogy is more distinctive than for the main rock units. The composition for the amphibole from this unit is shown in **Table 4**, column 3a for the single chemically analysed amphibole from evolved sample R174; column 3b gives the average composition for R174 and for 6 more amphibole samples from mafic Ba-Ti-rich less-evolved monzonites. The chemically analysed sample R174 has a higher *mg#* value than the amphiboles from the other rock types with a slightly higher $Fe^{3+}/\Sigma Fe$ ratio of 0.21 (column 3a, row (i)); the more reliable data in column 3b show a lower average ratio of 0.13 (column 3b, row (iii)) even though the higher *mg#* of 0.39 is confirmed. The 13 cation calculated Fe valences for nepheline monzonite amphiboles columns 3a, row (ii(b)) and 3b row (ii(b)) show excellent agreement (0.29 and 0.26, respectively).

It is clear that our standard method for reporting Fe valence estimates for amphiboles using the $\Sigma^{13} - (Ca + Na + Ks) - \Delta C^{corrected}$ equation gives $Fe^{3+}/\Sigma Fe$ ratios significantly lower than the adopted chemical analyses for the nepheline syenite hastingsites but only slightly lower that those for the quartz syenite chemical analyses. Such differences are related to the former having very small or zero A group vacancies while the hastingsitic hornblendes from the latter have much larger vacancies ranging from 20% to 10% of A. No 16 cation estimates can be made for the EMP analyses of the quartz syenite amphiboles as it is impossible to deduce reliable vacancy contents. For the quartz syenite data we have assessed whether using a $^{W}O^{2-}$ value based on the 2Ti *vs* $^{W}O^{2-}$ relationship defined earlier (i.e., equation $^{W}O^{2-} = (0, 0.1473 \times \text{wt.\% } TiO_2 + 0.0051)$; this equation returns negative values which appear for very low Ti samples as zeros. The new $Fe^{3+}/\Sigma Fe$ ratios are given in **Table 4** (columns 2b, row (iv) and 2c, row (iv)). Although the improvement for the Marangudzi amphiboles is small we will use this approach for the other sources of data for oversaturated rock amphiboles to assess whether any more useful conclusions might emerge. Overall, we conclude that the complex magmatic development of the diverse Marangudzi rock suite occurred under stable redox conditions and that any post-magmatic changes showed little effect on the primary mineral assemblage.

Amphibole species present in the Coldwell magmatic complex are more varied than those at Marangudzi, particularly in the SiO_2-saturated and over-saturated ferroaugite syenite intrusive units. In **Table 5**, columns 1a-1d (centre I intrusive units) show average analyses for hornblendes (1a), ferroactinolite/edenite (1b), kataphorite (1c), and arfvedsonite/riebeckite (1d). Note that for Marangudzi syenites the presence of actinolitic amphiboles is interpreted as having formed in subsolidus conditions. Each of the four groups shows only a limited range of *mg#* values but a large variation in $Fe^{3+}/\Sigma Fe$ ratios, similar to that feature shown by Marangudzi amphiboles. In the original papers (Mitchell & Platt, 1978, 1982) Coldwell amphibole formulae were calculated to 23 O, however, the '16' cation

Table 5. Coldwell complex, Canada, amphibole EMP analyses from Centres I, II and III.

	1a	1b	1c	1d	2	3a	3b	3c
Wt.%	Hornbl. Av. 4	Eden./actinol Av.4	Kataphor Av. 4	Arf/Riebec Av. 2	Hastingsite Av. 20	Mg-Hb C2150 Av. 7	Fe-eden C812/1 Av 8	Hb sy C2213 Av 8
SiO_2	39.83	47.51	47.02	49.30	39.68	46.91	43.81	45.64
TiO_2	2.91	0.05	1.59	0.56	1.83	1.06	1.53	1.39
Al_2O_3	8.29	1.56	1.99	0.79	10.56	5.98	5.80	3.59
FeO	30.07	35.80	34.18	35.66	23.79	18.40	28.34	32.25
MnO	0.55	1.32	0.84	0.89	0.79	0.30	0.80	0.91
MgO	1.52	0.11	0.26	n.d.	5.39	10.99	3.15	1.84
CaO	10.32	9.49	5.07	1.64	10.17	10.98	9.51	7.81
Na_2O	2.61	1.21	5.34	6.93	3.05	1.43	2.16	2.64
K_2O	1.48	0.39	1.40	1.03	1.58	0.74	1.11	1.00
Total	97.75	95.92	97.69	96.83	97.31	96.77	96.72	97.07
$^{W}O^{2-}$ Li et al. (2020a)	0.417	0.007	0.143	0.044	0.258	0.128	0.176	0.193
Del C^{corr}	0.064	0.094	0.060	0.158	0.085	0.103	0.080	0.135
Cell calc.W = (OH + F + Cl + O)	X = (23 + $^{W}O^{2-}$/2) corrected to 13 cations with ΔC^{corr} 6.7/13							
Si	6.527	7.715	7.653	7.986	6.323	7.084	7.049	7.363
Al_{iv}	1.473	0.285	0.347	0.014	1.677	0.916	0.951	0.637
Ti_{iv}		-						
ΣZ	8.000	8.000	8.000	8.000	8.000	8.000	8.000	8.000
Al_{vi}	0.127	0.019	0.035	0.136	0.307	0.148	0.148	0.046
Ti_{iv}	0.358	0.006	0.194	0.068	0.220	0.120	.0.185	0.169
Fe^{3+}	0.180	0.312	0.201	0.519	0.283	0.341	0.266	0.447
Fe^{2+}	3.894	4.550	4.451	4.312	2.887	1.983	3.615	3.905
Mn	0.076	0.182	0.115	0.121	0.107	0.038	0.109	0.125
Mg	0.372	0.025	0.064	0.000	1.280	2.473	0.757	0.443
ΣC	5.054	5.094	5.060	5.156	5/086	5.102	5.080	5.135
ΔC	0.054	0.094	0.060	0.156	0.086	0.102	0.080	0.135
Ca	1.811	1.647	0.885	0.283	1.736	1.776	1.640	1.350
Na	0.828	0.379	1.686	2.177	0.942	0.418	0.674	0.824
K	0.309	0.081	0.291	0.212	0.322	0.142	0.229	0.207
Σ(A + B)	3.002	2.201	2.922	2.828	3.086	2.438	2.623	2.517
Total cats	16.001	15.205	15.922	15.828	16.086	15.438	15.623	15.515
mg#	0.08	0.005	0.013	0	0.28	0.51	0.16	0.09
(i) Fe^{3+}/Fe^{total} Σ^{13} (ΔC^{corr})	0.044	0.06	0.043	0.11	0.09	0.15	0.07	0.10
(ii) Fe^{3+}/Fe^{total} Σ^{16}					**0.17**			

Continued

(iii) Fe^{3+}/Fe^{total} (Ti calibr^{r})	0.05	0.06	0.06	0.11	0.08	0.16	0.08	0.11
Fe^{3+}/Fe^{tot}, Li et al. (2020a)	0.18	0.22	0.21	0.25	0.26	0.22	0.22	0.23
Σ^{16}_{cats}, Li et al. (2020a)	15.78	15.18	15.53	15.55	15.93	15.32	15.37	15.40
Fe^{3+}/Fe^{tot}, Ridolfi et al. (2018)	0.19	0.26	0.18	0.33	0.16	0.20	0.09	0.15
Σ^{16}_{cats}, Ridolfi et al. (2018)	15.93	15.19	15.85	15.68	15.96	15.36	15.50	15.37

Coldwell, Canada, Centre I, Silica oversat. syen. 4a hornblende; 4b edenite/actinolite; 4c kataphorite; 4d arfvedsonite/riebeckite (Mitchell & Platt (1978); Centre II, column 5, neph. syen. hastingsite (Mitchell & Platt, 1982); Centre III (Lukošius-Sanders, 1988) [#]Source Supp spreadsheet file (i) Folder III; (ii) Folder II, (iii) Folder IV, (iv) Bold typeface preferred.

totals are either < 16 or only slightly higher than the stoichiometric 16 atom formulae, reflecting the presence of significant cation vacancies as found for the Marangudzi quartz syenite amphiboles, and it is clear that only the '13' cation calculation could provide reliable Fe^{3+} estimates. Thus, all the formulae data for the Coldwell amphiboles are calculated for a (23 + $^{W}O^{2-}/2$) formula on a 13 cation basis taking account of the presence of the ΔC^{corr} components (see **Table 5**, row (i), but 13 cation $Fe^{3+}/\Sigma Fe$ with $\Delta C = 0$ are also shown in row (ii). The amphibole data in **Table 5** Columns 1a-1d are all from Centre I units. The average amphibole in Column 1a has 0.417 pfu of extra-O with Ti and Al contents typical of a hastingsite (cf. Marangudzi quartz syenites, **Table 4**, 2b, c). The average composition in column 1a is Fe-rich (*mg*# = 0.08) with a low $Fe^{3+}/\Sigma Fe$ ratio (0.04, **Table 5** 1a, row (i) or 0.09 pfu (row (ii). The second amphibole variety (column 1b) has a very small proportion of extra-O (0.007) with low Ti, Al, Na, and K typical of lower temperature, water-rich deuteric alteration conditions (cf. Mitchell, 1990); in addition, the composition is virtually Mg-free (*mg*# < 0.01) with Fe-valence (ratio 0.06, column 1b, row (i) or 0.13 (row (ii)) similar to that shown for the hastingsitic hornblendes in Column 1a. Note that 6 of the 8 samples covered in **Table 5** columns 1a and 1b are from the lower layered series but two of the actinolite-rich phases (1b) are from pegmatites in the upper series, which are associated with more sodic, peralkaline syenites (**Table 5**, 1c and d). The amphibole data in column 1c are an average of Na-Ca group amphiboles within 4 host rocks and have high Si, low Al, Ti and very high Fe (*mg*# 0.01); $^{W}O^{2-}$ contents are moderate (0.143) and the calculated $Fe^{3+}/\Sigma Fe$ is low (0.04, column 1c, row (i) or 0.05 (row (iii)). Other upper layered series rocks have Na amphiboles (column 1d) with very low Al, Ti, Ca and $^{W}O^{2-}$ (0.044); calculated $Fe^{3+}/\Sigma Fe$ is low (0.11, column 1d, row (i) or 0.22 (ii)). Most of these $Fe^{3+}/\Sigma Fe$ ratios seem low, but those obtained using the third way of estimating Fe valence (Ti vs $^{W}O^{2-}$ and lower ΔC estimate, see above) are very similar as shown in **Table 5**, equivalent columns, row (iii). However, we suggest that the row (ii) estimates might be the most reliable estimates for the Coldwell (I) Fe-valence values.

Centre II Coldwell amphibole compositions (Mitchell & Platt, 1982) are hastingsites from the nepheline syenite unit (average of 20 samples; **Table 5**, column 2). Published data for *mg*# range 0.61 to 0.08 with a smaller range for $Fe^{3+}/\Sigma Fe$ of

0.03 - 0.15; thus, we suggest that the average composition probably provides more reliable information for the calculated extra-O Fe valence, and cation sums. Thus the average data for Centre II units shown in **Table 5** (column 2) define moderate values for *mg*# (0.28) and low $Fe^{3+}/\Sigma Fe$ (0.09, column 2, row (i)) for the Σ^{13} but the 13 atom calculation with $\Delta C = 0$ gives a higher $Fe^{3+}/\Sigma Fe$ ratio of 0.18 (column 2, row (ii)) and that is the value we adopt. Although bulk compositions are similar to the values for the average amphibole in Marangudzi nepheline syenites (**Table 4**, columns 1a-c) the Fe valence ratio is slightly more-reducing. The amphibole EMP average compositions from 3 silica-saturated Centre III rocks (Lukošius-Sanders, 1988) are shown in **Table 5**. Column 3a data are magnesio-hornblende with *mg*# varying from 0.61 to 0.51 (average 0.51) with $Fe^{3+}/\Sigma Fe = 0.15$ (row (i) and 0.30 (row (ii)). Column 3b amphiboles are ferro-hornblendes with average *mg*# 0.16 and $Fe^{3+}/\Sigma Fe$ 0.07 (row (i)) and 0.14 (row (ii)). The final rock (column 3c) has winchite and kataphorite species with average *mg*# 0.09 and $Fe^{3+}/\Sigma Fe$ values for both of 0.10 (i), 0.21 (ii), and 0.11 (iii)) and we adopt the 0.21 value for comparisons for amphiboles between the three intrusive units. Thus, although the amphibole species in different Coldwell intrusive units vary with very different bulk Fe levels, the Fe valence ratios show no significant variation. Thus, amphiboles from nepheline syenites from Marangudzi and Coldwell give almost identical $Fe^{3+}/\Sigma Fe$ ratios for both the '16' and '13' cation calculations reflecting that vacancies are only present in small quantities if at all (i.e. $\Sigma^{16}_{cats} = 15.98$ for both complexes). In contrast, the magmatic amphiboles from the Coldwell amphiboles have variable proportions of A site vacancies.

Overall, *the* '13' cation calculation is the more robust method for calculating model $Fe^{3+}/\Sigma Fe$ values, especially where significant proportions of A vacancies might be present. Based on the amphibole compositions reviewed here it is clear that the Marangudzi complex syenites are firmly in the miaskite category of Mitchell (1990), whereas the Coldwell complex also includes rock types which have peralkaline (agpaitic) affinities. The Red Hill, White Mountain, USA nepheline syenites (Henderson et al., 1989) have closer similarities to those from Coldwell than to the Marangudzi undersaturated series. However, all appear to have formed under fractionation conditions close to the QFM buffer.

We have also investigated published amphibole data from a range of different world-wide localities and alkaline igneous rock types. The results are provided here in **Tables 6-8** with full data provided in the Supplementary file 1 spreadsheet, Folders II-IV.

6. Amphibole Formulae for a Wider Range of Fractionated Alkaline Igneous Rocks

In this section we recalculate representative, published amphibole compositions for a wide range of igneous rocks to assess how the Fe valence might vary within rock series ranging from: 1) basic parents to felsic differentiates, 2) within coeval quartz and nepheline syenites, 3) metasomatised upper mantle rocks (including

Table 6. Amphiboles in differentiated alkali basic rocks.

	Ditrau alkaline intr., Eastern Carpathians, Romania				Lilloise intrusion, E. Greenland		Anzemi alkaline intrusion, High Atlas, Morocco			Tamazegh alk.intrus. Morocco	
	Morogan et al. (2000)				Chambers & Brown (1995)		Lhachmi et al. (2001)			Marks et al. (2008)	
	Perid. Av 3	Alkgb/ dior Av 9	Qtz sy 1 sple	Alk gb 1 sple	Cumul Av3	Gabbro Av. 5	Gb Av 3	Mo dio Av 3	Syen Av 4	Gb mon Av 10	Neph sy Av 4
SiO_2	41.70	38.51	54.91	53.55	42.39	42.12	42.64	44.48	47.75	39.23	39.92
TiO_2	3.55	2.78	0.24	0.03	3.54	3.63	3.85	4.67	1.22	4.13	2.25
Al_2O_3	12.02	13.04	0.85	1.92	11.34	11.34	10.26	8.60	1.56	11.79	10.88
Cr_2O_3							0.04	0.06	0.05		
FeO	8.68	19.61	15.19	13.33	13.76	14.27	12.51	9.67	30.06	15.94	18.73
MnO	0.10	0.49	0.23	0.39	0.22	0.14	0.06	0.11	0.71	0.51	0.91
MgO	14.99	7.86	13.33	15.09	11.77	11.59	13.21	15.41	3.78	9.73	8.85
CaO	11.70	11.06	1.38	12.50	11.94	12.09	11.37	10.42	7.51	11.28	10.34
Na_2O	2.79	2.83	8.16	0.35	2.21	1.80	2.76	3.92	3.66	2.73	3.24
K_2O	1.17	1.69	1.68	0.08	0.88	0.99	0.74	0.46	0.85	1.90	1.88
Total	97.70	97.87	95.47	97.24	98.05	97.97	97.44	97.79	97.14	97.24	97.14
$^{W}O^{2-}$, Li et al.	0.488	0.476	0	0	0.521	0.563	0.560	0.635	0.060	0.598	0.320
ΔC^{corr}	0.089	0.117	0	*C* 0.024	0.084	0.103	0.109	0.108	0.069	0.076	0.102
Cell formulae to (23 + $^{W}O^{2-}$/2) O/13 cats corrected for ΔC^{corr}, this work											
Si	6.187	5.977	8.033	7.751	6.327	6.304	6.362	6.527	7.618	6.072	6.221
Al	1.813	2.033		0.249	1.673	1.696	1.638	1.473	0.293	1.928	1.779
Ti									0.089		
Z	8.000	8.000	8.033	8.000	8.000	8.000	8.000	8.000	8.000	8.000	8.000
Al_{IV}	0.289	0.262	0.147	0.079	0.322	0.305	0.166	0.015	-	0.222	0.219
Ti_{VI}	0.396	0.323	0.026	0.003	0.397	0.408	0.432	0.516	0.057	0.481	0.264
Cr							0.005	0.007	0.005		
Fe^{3+}	0.298	0.389	0.674	0.172	0.282	0.344	0.367	0.362	0.225	0.255	0.341
Fe^{2+}	0.779	2.156	1.195	1.441	1.436	1.442	1.194	0.824	3.786	1.807	2.101
Mn	0.013	0.065	0.029	0.049	0.028	0.017	0.008	0.013	0.096	0.067	0.120
Mg	3.314	1.818	2.907	3.256	2.619	2.585	2.938	3.371	0.898	2.244	2.101
C	5.089	5.115	5.000	5.000	5.084	5.102	5.110	5.108	5.067	5.076	5.101
ΔC^{corr}	0.089	0.115	0.000	0.000	0.084	0.102	0.110	0.108	0.067	0.076	0.101
Ca	1.860	1.840	0.216	1.939	1.910	1.939	1.818	1.639	1.284	1.871	1.727
Na	0.804	0.852	2.315	0.098	0.641	0.522	0.799	1.115	1.133	0.818	0.980
K	0.222	0.334	0.314	0.015	0.167	0.189	0.142	0.086	0.174	0.376	0.373
A + B	2.975	3.141	2.845	2.055	2.801	2.752	2.867	2.948	2.738	3.141	3.181
Total cats	15.974	16.142	15.845	15.052	15.801	15.752	15.867	15.948	15.658	16.141	16.182

Continued

mg#	0.75	0.41	0.61	0.66	0.60	0.59	0.65	0.74	0.18	0.51	0.45
#(i) $Fe^{3+}/\Sigma Fe\ \Sigma^{13}\ \Delta C^{corr}$	**0.28**	**0.15**	**0.36**	**0.11**	**0.16**	**0.19**	**0.23**	**0.31**	**0.06**	**0.12**	**0.14**
(ii) $Fe^{3+}/\Sigma Fe\ \Sigma^{16}$	0.21	0.31	0.12	-	-	-	-	0.18	-	0.32	0.36
(iii) $mFe^{3+}/\Sigma Fe\ \Sigma^{13}Ti$ cal. 6.7/13	**0.33**	**0.15**	**0.18**	**0.05**	**0.19**	**0.21**	**0.26**	**0.37**	**0.07**	**0.15**	**0.15**
Charge balance	46.49	46.48	46.00	46.00	46.52	46.56	46.56	46.64	46.06	46.60	46.32
Publ.calc	23 O/13 cat				23 O			23 O		23 O + Ti	
$Fe^{3+}/\Sigma Fe$	0.19	0.14	0.34	0.13	n.d.	n.d.	0.10	0.01	0.02	0.50	0.43
Names*	Hast	Hast	Arfv	Actinol	Hast	Hast	Hast	Hast	Kata	Hast	Hast

*Names based on Li et al. (2020a): Hast. hastingsite; Arfv. Arfvedsonite; Actinol actinolite; Kata. Kataphorite; Parg. Pargasite; K-richt. potassic richterite #Source Supp spreadsheet file (i) Folder III; (ii) Folder II, (iii) Folder IV, (iv).

MARID), and 4) for the possible partial melts of such alkali-rich mantle parents. These examples are separated into subsections with each set being calculated using the same crystal chemical approach as that used above. Note that samples with very low $^{W}O^{2-}$ and low Ti or high Na are generally best fitted with $\Delta C = 0$ (**Tables 6-8**, row (iii) and Supplementary file 1, spreadsheet Folder II, 13 cation fit). Where possible we compare our model $Fe^{3+}/\Sigma Fe$ ratios with those suggested by authors of the source papers and try to account for any consistent differences.

Table 6 shows the representative data for amphiboles in gabbro and monzonite precursors to differentiated felsic rock types (series (i)). The first set are from the Ditrau alkaline complex, Romania (Morogan et al., 2000). The main complex consists of ring-like units of felsic rocks including syenites, nepheline syenites and "granites" which have inclusions of earlier basic rocks including peridotites, alkali gabbros, and dioritic rocks. The amphibole analyses were recalculated on the basis of 23 oxygens and 13 cations and we show their calculated $Fe^{3+}/\Sigma Fe$ values at the bottom of 6 together with the amphibole species names. The hastingsites have consistently high $^{W}O^{2-}$ values > 0.4 which accounts for the Fe valence ratio reported here being higher than the values reported for the 23 O formula (Morogan et al., 2000). The group of 3 hastingsites from peridotites and the group of nine hastingsites from 5 alkali gabbros, 3 alkali diorites, one monzogabbro and one syenite have tightly defined $Fe^{3+}/\Sigma Fe$ ratios (0.11 - 0.31 for $\Sigma^{13}\ \Delta C^{corr}$ or a Σ^{16} calculation for the alkali gabbro) over a fair range of *mg#* values (0.75 - 0.41; see supplementary file 1 spreadsheet, Folder III folder for the data). Thus the redox conditions must have been fairly constant during the main magmatic differentiation process. One quartz syenite has arfvedsonite which formed during a peralkaline stage but its $Fe^{3+}/\Sigma Fe$ ratio (0.36) falls within the range of the more basic rock-type amphiboles. One alkali gabbro has actinolite which we interpret as a subsolidus or deuteric phase that formed under more-reducing conditions.

The layered rocks in the Tertiary Lilloise mafic intrusion (Chambers & Brown, 1995) contain olivine-clinopyroxene and plagioclase-amphibole cumulates which

are intruded by sheets of alkali gabbro. The amphibole compositions reported here are for these two categories. Both groups contain hastingsites showing a wide range of *mg*# values: cumulates 0.8 - 0.45; gabbros 0.71 - 0.38 and $Fe^{3+}/\Sigma Fe$ 0.1 - 0.21; 0.12 - 0.30. However, the $Fe^{3+}/\Sigma Fe$ value of 0.1 is based on a very low Fe content (~5wt.% FeO) which might lead to a very large error for $Fe^{3+}/\Sigma Fe$. We prefer to use the average values for the input oxide analyses ($Fe^{3+}/\Sigma Fe$ 0.16 and 0.19) which suggest that both cumulate and gabbro sheet amphiboles formed under the same redox conditions. The Anzemi intrusion (Morocco; Lhachmi et al., 2001) gabbro and monzodiorite hastingsites have similar average *mg*# and $Fe^{3+}/\Sigma Fe$ values suggesting stable redox conditions while the coeval quartz syenite has a less Al-rich, Fe-rich kataphorite (*mg*# = 0.18) with a very low $Fe^{3+}/\Sigma Fe$ value of 0.06. Note that the Anzemi more basic rock hastingsites have very high oxo-amphibole compositions which provides cation totals > 16 atoms and thus accounts for our $Fe^{3+}/\Sigma Fe$ ratios being much larger than the values reported by Lhachmi et al. (2001) on the basis of 23 O formulas. Finally for the differentiated complexes summarised in **Table 6**, the Tamazeght alkaline intrusion, Morocco (Marks et al., 2008) the average hastingsite compositions for the gabbro/monzonite group and the average for the hastingsitic amphiboles in nepheline syenites are very similar consistent with such different bulk rock compositions forming amphiboles under similar redox conditions. Note that our $Fe^{3+}/\Sigma Fe$ values are much smaller than those given by Marks et al. (2008) which were calculated assuming a direct relationship between the Ti content $^{W}O^{2-}$ (see above and Hawthorne et al., 1998). In fact, these amphiboles differ from many of the samples considered here by have cation totals much higher than 16, and appear to have very low vacancy counts; thus a 16 cation calculation gives $Fe^{3+}/\Sigma Fe$ of ~0.30 which might be more reliable than our 13 cation estimate in row (i); while that in row (iii) are more plausible.

Table 7 shows information for amphiboles mainly from complexes with coeval nepheline- and quartz- syenites as the main rock types exposed. The hastingsites in the Red Hill syenites (Henderson et al., 1989) and for the kataphorites in the peralkaline Kangerlussuaq complex (Riishuus et al., 2008) occur in both silica-saturated and silica undersaturated parents, with the amphibole species having closely similar low $Fe^{3+}/\Sigma Fe$ ratios ~0.10 - 0.25 averaged over the different calculation methods used; the Fe oxide ratio obtained with $\Delta C = 0$ (row iii) is preferred. The more sodic arfvedsonite in a quartz-rich syenite from Kangerlussuaq has a lower ratio (~0.07 - 0.15) but the Li et al. (and Ridolfi et al.) spreadsheets both report zero values for the $^{W}O^{2-}$ in such amphibole species. We conclude that miaskitic and more peralkaline amphibole species from both quartz- and nepheline-syenites have generally low $Fe^{3+}/\Sigma Fe$ ratios (ranging only about 0.1 to 0.25 in **Table 7**), consistent with both silica-saturated and undersaturated magmas forming and differentiating under similar redox conditions. The amphiboles from the silica undersaturated and intermediate rock types in the other complexes [Emmanuel et al. (2013); Worley & Cooper (1995); and Abu Khruq, Egypt, Mogahed (2016)]

Table 7. Amphiboles in differentiated syenite intrusions.

	Red Hill, New Hampshire, USA		Kangerlussuaq intrusion, East Greenland					Cameroon	Dismal intrusion Antarctica		Abu Khruq ring complex. Egypt		
	Henderson et al. (1989)		Riishuus et al. (2008)					Emmanuel et al. (2013)	Worley & Cooper, (1995)		Mogahed (2016)		
	Ne.sy. Av. 8	Qz sy. Av. 7	Main pul Av. 2	Trs pul Av. 2	Nord. Av. 4	Qz rich sy. 1 Av 4	Qz-rich sy 2 Av. 4	Ne sy Av. 10	Ne sy. Av. 5	Mafic ne sy. Av. 3	Mon.dior Av. 4	Alk sy Av 6	Qtz sy Av. 6
SiO_2	39.40	42.15	48.20	50.28	50.06	50.41	49.22	37.59	36.60	38.41	38.50	49.25	50.21
TiO_2	2.52	2.38	1.59	1.28	0.99	1.29	0.74	1.10	0.89	1.41	2.65	1.24	0.88
Al_2O_3	10.46	7.81	3.91	2.85	1.43	0.64	1.57	12.56	12.34	13.48	15.13	2.72	2.18
Cr_2O_3													
FeO	24.05	25.19	17.59	16.78	19.89	25.04	23.97	28.53	31.97	23.29	17.54	19.05	24.60
MnO	0.98	0.93	2.08	1.89	1.91	2.13	1.52	2.04	0.49	0.34	0.41	1.77	1.61
MgO	5.94	5.40	9.84	10.58	9.25	4.52	6.69	0.65	0.62	5.43	8.71	9.31	4.96
CaO	10.26	9.90	4.70	3.02	5.50	1.87	5.95	6.11	9.40	10.43	11.64	4.39	3.69
Na_2O	3.45	3.00	6.84	7.78	5.61	7.94	4.74	4.81	2.46	2.32	2.69	6.82	6.22
K_2O	1.70	1.23	1.38	1.38	1.15	1.36	1.00	2.54	2.14	2.00	1.52	1.50	1.75
Total	98.74	97.98	96.11	95.83	95.79	95.19	95.40	95.93	96.91	97.10	98.78	96.03	96.10
$^{W}O^{2-}$, Li et al.	0.379	0.320	0	0	0	0	0	0.192	0.299	0.301	0.485	0	0
ΔC^{corr}	0.115	0.095	0.056	0.070	0.060	0.021	0.068	0.160	0.192	0.132	0.113	0.056	0.019
Cell formulae to (23 + $^{W}O^{2-}$/2) O/13 cats corrected for ΔC^{coo} with 6.7/13, this work													
Si	6.194	6.645	7.392	7.641	7.734	8.044	7.755	6.200	6.044	6.061	5.848	7.588	7.898
Al	1.806	1.355	0.608	0.359	0.260	-	0.245	1.800	1.956	1.939	2.152	0.412	0.102
Ti					0.006	-							
Z	8.000	8.000	8.000	8.000	8.000	8.044	8.000	8.000	8.000	8.000	8.000	8.000	8.000
Al_{IV}	0.132	0.097	0.099	0.151		0.120	0.050	0.642	0.446	0.568	0.556	0.081	0.301
Ti_{VI}	0.298	0.282	0.183	0.146	0.109	0.155	0.088	0.136	0.110	0.167	0.303	0.144	0.104
Cr													
Fe^{3+}	0.381	0.317	0.185	0.233	0.196	0.069	0.226	0.529	0.642	0.438	0.377	0.165	0.062
Fe^{2+}	2.780	3.004	2.071	1.900	2.374	3.271	2.932	3.407	3.773	2.636	1.852	2.291	3.174
Mn	0.130	0.125	0.270	0.243	0.250	0.287	0.203	0.285	0.069	0.045	0.052	0.231	0.215
Mg	1.392	1.270	2.249	2.397	2.131	1.074	1.551	0.160	0.152	1.276	1.972	2.138	1.163
C	5.113	5.095	5.057	5.070	5.060	5.008	5.071	5.159	5.192	5.130	5.112	5.050	5.020
ΔC^{corr}	0.113	0.095	0.057	0.070	0.060	0.008	0.071	0.159	0.192	0.130	0.112	0.050	0.020
Ca	1.728	1.672	0.772	0.492	0.911	0.319	1.000	1.080	1.663	1.763	1.894	0.724	0.622
Na	1.097	0.916	2.033	2.293	1.680	2.457	1.450	1.538	0.788	0.710	0.792	2.037	1.898
K	0.341	0.247	0.270	0.267	0.227	0.276	0.200	0.534	0.450	0.402	0.294	0.294	0.351
A + B	3.234	2.930	3.132	3.122	2.878	3.052	2.722	3.311	3.092	3.005	3.092	3.105	2.891
Total cats	16.23	15.93	16.13	16.12	15.88	16.067	15.72	16.31	16.09	16.01	16.09	16.11	15.89

Continued

mg#	0.30	0.27	0.47	0.50	0.43	0.23	0.32	0.036	0.03	0.29	0.46	0.44	0.25
[#](i) $Fe^{3+}/\Sigma Fe$ Σ^{13} ΔC^{coo} 6.7/13	**0.12**	**0.10**	**0.08**	**0.14**	**0.08**	**0.02**	**0.07**	**0.13**	**0.14**	**0.14**	**0.17**	0.07	0.02
(ii) $Fe^{3+}/\Sigma Fe$ Σ^{16}	0.30	0.04	0.25	0.27	-	0.08	-	0.36	0.20	0.15	0.29	019	-
(iii) $Fe^{3+}/\Sigma Fe$ Σ Ti calib ΔC^{coo} 6.7/13	**0.13**	**0.14**	**0.18**	**0.20**	**0.13**	**0.07**	**0.11**	**0.17**	**0.16**	**0.17**	**0.21**	**0.14**	**0.05**
Charge balance	46.38	46.32	46	46	46	46	46	46.19	46.30	46.30	46.48	4646	
				23 O/13 cat				23 O/16cat	23 O/13 cat		23 O/13 cat		
$Fe^{3+}/\Sigma Fe$	0.17	0.13	0.17	0.22	0.18	0.12	0.15	0.31	0.23	0.20	0.16	0.23	0.04
	Hast	Hast	Kata	Kata	Kata	Arfv	Kata	Taram	Hast	Hast	Parg/Hast	Kata	Kata

[#]Source Supp spreadsheet file (i) Folder III; (ii) Folder II, (iii) Folder.

in Table 7 overall have variable $Fe^{3+}/\Sigma Fe$ ratios with an overall range of ~0.1 - 0.3 but the quartz syenite amphibole from Abu Khruq is more reduced (<0.1) as appears to be common for such silica-saturated rock types.

Table 8 shows the variation of $Fe^{3+}/\Sigma Fe$ values in different amphibole species related to upper mantle conditions. The main species described for metasomatised mantle rocks are potassic richterites or hastingsitic amphiboles (Dawson & Smith, 1973, 1977; Banerjee et al., 2018; Wagner et al., 1996; Bonadiman et al., 2021). Both species tend to show higher $Fe^{3+}/\Sigma Fe$ ratios (ranging 0.2 to 0.6) than those found in sub-volcanic alkaline complexes (0.1 - 0.2). However, the former tend to have very low Fe contents (mainly 3.4 - 4.3 wt.% FeO) which easily leads to over estimated Fe^{3+}. Any Fe valence variation could either be related to variable redox conditions or to different extents of metasomatic resetting of the pre-existing mantle geochemistry and mineralogy. Bonadiman et al. (2021) suggested that the pargasitic amphibole/phlogopite assemblage in metasomatised harzburgite mantle nodules formed under redox conditions which were more reducing (i.e., Δ(FMQ) = ~1.9) than for spinel peridotites. They compared the compositions of the amphibole and biotite in 'unreacted' and 'reacted' samples; we compare our recalculated $Fe^{3+}/\Sigma Fe$ ratios for the average amphibole compositions in Table 8 and the more reduced 'reacted' ratio (0.71) compared to 'unreacted' (0.86) is indeed consistent with that suggestion. Finally, amphibole data are given for K-richterite amphiboles from two Indian lamproites in Table 8 (Saini et al., 2022; Kaur & Mitchell, 2019); both have moderate Ti and high Fe contents and these proportions allow modelling of the Fe valence relations in these potentially primary partial melts from parental, potassic, upper-mantle rocks. Although, the *mg#* values imply that they might represent fractionated daughter compositions in both cases the $Fe^{3+}/\Sigma Fe$ ratios are low (~0.10) consistent with formation under QFM upper-mantle redox conditions. High Ti and much lower Fe contents for biotite and amphibole in 'primary' lamproites make it much more difficult to obtain reliable $Fe^{3+}/\Sigma Fe$ ratios; a common occurrence for such compositions is to give model Fe^{3+}

contents larger than the total Fe and thus large, non-physical negative Fe^{2+} contents (see above and for phlogopite in Henderson, 2025).

Table 8. Amphiboles in metasomatised upper mantle rocks and primary partial melts.

	MARID & metasomatised Upper Mantle amphiboles							Lamproites	
	Dawson & Smith (1977)	Fitzpayne (2018)	Banerjee et al. (2018)	Wagner et al. (1996)	Bonadiman et al. (2021)		Dawson & Smith (1973)	Saini et al. (2022)	Kaur & Mitchell (2019)
	Av 12	Av. 156	Av. 7	Av 5	Unreact Av. 11	Reacted Av 9	Av 8	Marapelli Av. 9	Gundra Av. 15
SiO_2	54.58	54.66	55.49	55.30	43.98	43.28	41.95	52.14	53.73
TiO_2	0.67	0.55	0.45	0.82	2.29	2.95	2.87	3.28	2.81
Al_2O_3	0.99	1.06	0.96	0.94	12.29	12.30	10.84	0.22	0.23
Cr_2O_3	0.25	0.21	0.17	0.24	1.85	1.86	0.71	-	-
FeO	4.26	3.96	3.54	4.21	3.59	4.05	7.74	17.79	14.98
MnO	0.04	0.05	0.06	0.12	0.06	0.08	0.09	0.30	0.21
MgO	21.10	21.35	21.78	20.87	18.01	17.31	16.34	11.11	13.26
CaO	6.51	6.78	6.91	6.23	10.39	10.46	11.40	3.82	3.80
Na_2O	3.73	3.54	3.58	5.45	3.61	3.61	2.74	4.74	5.13
K_2O	4.94	5.04	4.89	2.59	1.01	0.98	1.33	4.97	4.71
Total	97.08	97.17	97.82	96.79	97.08	96.88	96.02	98.35	98.67
$^{W}O^{2-}$ Li et al.	0	0.070	0	0	0.108	0.196	0.324	0.315	0.230
ΔC^{corr}	0.036	0.044	0.031	0.022	0.077	0.069	0.111	0.046	0.038
Cell formulae to (23 + $^{W}O^{2-}$/2) O/13 cats corrected for ΔC, this work									
Si	7.777	7.780	7.812	7.833	6.285	6.238	6.226	7.859	7.909
Al	0.167	0.177	0.159	0.157	1.715	1.762	1.774	0.039	0.039
Ti	0.056	0.043	0.029	0.010				0.102	0.052
Z	8.000	8.000	8.000	8.000	8.000	8.000	8.000	8.000	8.000
Al_{VI}	-	-	-	-	0.355	0.328	0.123	-	-
Ti_{VI}	0.015	0.015	0.018	0.077	0.246	0.320	0.321	0.269	0.259
Cr	0.027	0.022	0.018	0.026	0.201	0.204	0.080	-	-
Fe^{3+}	0.120	0.146	0.102	0.072	0.254	0.229	0.367	0.152	0.127
Fe^{2+}	0.388	0.325	0.315	0.427	0.175	0.259	0.594	2.090	1.717
Mn	0.004	0.006	0.007	0.014	0.007	0.010	0.011	0.039	0.026
Mg	4.482	4.529	4.570	4.406	3.837	3.719	3.614	2.495	2.909
C	5.037	5.043	5.031	5.022	5.075	5.069	5.110	5.045	5.038
ΔC^{corr}	0.037	0.043	0.031	0.022	0.075	0.069	0.110	0.045	0.038
Ca	0.994	1.034	1.043	0.945	1.591	1.615	1.813	0.616	0.599
Na	1.030	0.977	0.978	1.504	1.000	1.009	0.790	1.385	1.465
K	0.900	0.914	0.878	0.467	0.184	0.180	0.252	0.956	0.884

Continued

A + B	2.961	2.968	2.929	2.938	2.852	2.873	2.965	3.002	2.986
Total cats	15.960	15.970	15.929	15.938	15.852	15.873	15.964	16.002	15.987
mg#	0.90	0.91	0.92	0.90	0.90	0.88	0.79	0.52	0.61
#(i) $Fe^{3+}/\Sigma Fe\ \Sigma^{13}$ ΔC^{corr} 6.7/13	**0.24**	**0.31**	**0.24**	**0.14**	**0.59**	**0.47**	**0.38**	**0.07**	**0.07**
(ii) $Fe^{3+}/\Sigma Fe\ \Sigma^{16}$	0.09	0.12	-	-	-	-	0.27	0.07	0.05
(iii) $Fe^{3+}/\Sigma Fe\ \Sigma^{13}$ Ti calib. ΔC^{corr} 6.7/13	**0.30**	**0.30**	**0.30**	**0.22**	**0.13**	**0.07**	**0.41**	**0.16**	**0.17**
Charge balance	46.00	46.07	46.00	46.00	46.11	46.20	46.32	46.32	46.23
Publ. calc.	23O/8cat							23 O	
$Fe^{3+}/\Sigma Fe$	0.18	n.d.	n.d.	n.d.	n.d.	n.d	n.d.	0-0.03	n.d.
	K-richt	K-richt	K-richt	K-richt	Parg/Hast		Hast	Kata/Richt	K-richt

*D & S, Dawson & Smith (1977); D & S, Dawson & Smith (1973); Kaur/Mitch Kaur & Mitchell (2019); #Source Supp spreadsheet file (i) Folder III; (ii) Folder II, (iii) Folder IV, (iv).

Representative data from these sets of data are plotted in Figure 1.

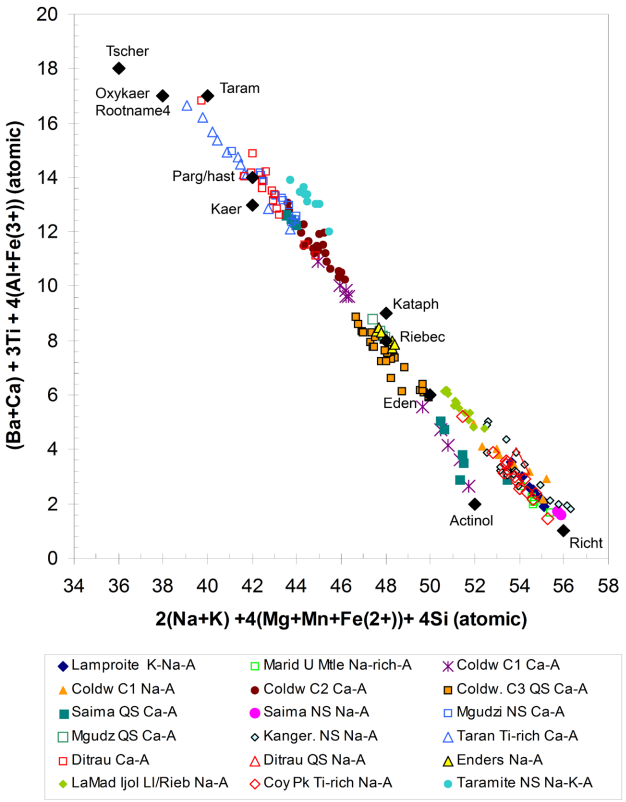

Figure 1. Mixed valence and intersite atomic substitution reaction for $2^{A,B}(Na^{+} + K^{+}) + 4^{C}(Mg^{2+} + Mn^{2+} + Fe^{2+}) + 4^{T}Si^{4+} \leftrightarrow {}^{B}Ca^{2+} + 3^{C}Ti^{4+} + 4^{C,T}(Al_{total} + Fe^{3+})^{3+}$ in Ca-, Na-Ca, and Na amphiboles in alkaline igneous rocks together with ideal labelled species end-member names (see text).

7. Multi-Site and Multi-Valence Trends for the Alkali-Rock Amphibole Database

For Ba-Ti-rich biotites Henderson (2025) used the Guo & Green (1990) atomic exchange model to display compositional trends for coupled multi-site, mixed-valence atomic substitutions occurring in Ba-, Ti-rich micas in alkaline igneous rocks. Amphiboles in the same rock-types also show similar interactions with Ca replacing Ba and Na mainly replacing K in the equivalent structural sites and we write the exchange reaction here as $2^{A,B}(Na^{+} + K^{+}) + 4^{C}(Mg^{2+} + Mn^{2+} + Fe^{2+}) + 4^{T}Si^{4+} \leftrightarrow {}^{B}Ca^{2+} + 3^{C}Ti^{4+} + 4^{CT}(Al_{total} + Fe^{3+})^{3+}$. Representative data for our amphibole database are plotted with different coloured symbols in **Figure 1**, with sources of published data identified as follows: Lamproite K-Na-amphiboles (A) (Saini et al., 2022); Marid Na-rich-A (Wagner et al., 1996); Coldwell Centre 1 Ca-A and Na-A, (Mitchell & Platt, 1978; this work); Coldwell Centre 2 Ca-A, (Mitchell & Platt, 1982; this work); Coldwell Centre 3 Ca-A, (Lukošius-Sanders, 1988; this work); Saima Ca-A and Na-A (Zhu et al., 2016); Mgudzi, Marangudzi Ca-A (Henderson, 1968, this work); Kangerlussuaq Na-A (Riishuus et al., 2008); Ti-rich Ca-A (Taran et al., 1999); Ditrau Ca-A and Na-A (Morogan et al., 2000); Na-A (Enders et al., 2000); La Madera Na-A (Galliski et al., 2004); Coyote Park, Na-A (Hawthorne et al., 1998); Taramite, Ca-A (Emmanuel et al., 2013). In addition, end-member amphibole compositon points are given for Tschermakite; Taramite, Oxykaersutite, Rootname4; Pargasite/Hastingsite; Kaersutite; Kataphorite; Riebeckite; Edenite; Actinolite; and Richterite.

In this variation diagram Mg and Fe^{2+} plot in the same manner, thus the normal magmatic differentiation evolution of the Fe/(Fe + Mg) ratio is not depicted. The main trend for most amphiboles investigated here is effectively a coupled, inter-site exchange between ${}^{B}Na + {}^{T}Si$ and ${}^{B}Ca + {}^{T}Al$. together with a Tschermak-type interaction simplified as ${}^{C}Mg + {}^{T}Si = {}^{C}Al + {}^{T}Al$; with Ti (particularly) and Fe^{3+} playing more important roles in some cases; especially for oxoamphiboles. The main trend for the Ca amphiboles is initially a simple, linear trend from an X-axis value of 39 to 46 which steepens to a maximum X of 52. As expected the amphiboles with the highest Y axis values are Ti- and Al-rich kaersutites (see the 'Taran' and 'Ditrau' data points), although these compositions also vary from having low-to-moderate Fe^{3+} varieties ($Fe^{3+}/\Sigma Fe$ 0.2 - 0.5). Hastingsitic amphiboles occupy the middle of the Ca-amphibole trend and the steeper trend is represented by less Al-rich species including hornblendes and ultimately actinolite. Clearly the trend from top to bottom (decreasing Y) is represented by amphiboles with increasing vacancies in A. The Ca-amphiboles from the Coldwell complex mainly fall within the bottom half of the main trend. The main trend shows clusters of points with a vertically limited scatter; note particularly the upward displacement of the taramite-rich sample from Cameroon (Emmanuel et al., 2013). The Marangudzi (Mgudzi points) for nepheline syenites show a clear trend from X 41 - 44 with those from the quartz syenites plotting at lower Y values reflecting lower Al, and higher Si contents, thus matching the compositions of the bulk rocks.

The Na-amphibole species trend is displaced to higher X values (51 - 56) compared to the Ca-Na-amphibole trend (X 50 - 52) over similar Y values (5 - 2). The former samples also show a clear trend with some scatter for different complexes with the slope being more similar to that at the top of the Ca-amphibole trend (i.e. *Y* 12 - 14). Note that amphiboles from Kangerlussuaq ('Kanger' points) and those from Coyote Peak ('Coy Pk') both cover much of the trend, which in both cases matches the Ti variation trend. Very Ti-rich (up to 7.4 wt.%) kaersutites define the upper part of the same trend leading to an intersection with the Ca-amphibole trend at about X = 48. Indeed, very Na-Al-rich glaucophane-riebeckite solid solutions plot at the intersection with the Ca-amphibole trend, effectively marking the 'end-point' of the Na amphibole series (**Figure 1**, 'Enders' points). Note that quartz syenites at Saima and Coldwell complexes have Ca-amphiboles whereas the coeval nepheline syenites both have Na-amphiboles consistent with their peralkaline affinities as compared with the miaskitic natures of the former.

8. Conclusion

(1) Ideally, **amphiboles should be reliably analysed for H_2O, H or (OH), and separately for Fe^{3+} and Fe^{2+} which would provide direct determination of the extra-O ($^{W}O^{2}$) present** in the sample. In addition, a wide range of minor elements should be determined including Sr, Ba, Mn, Zn, Ni, V, Cr, and Li.

(2) Most amphiboles have W anions totalling 2.0 apfu with $^{W}O^{2-}$ = (2.0–(OH)–F– Cl). Thus, the 'die is cast' ("Alea iest est", Julius Caesar, January 10th, 49 BC) and any attempt to estimate Fe^{3+} must take into account the possibility of vacant cation sites.

(3) The work of Li et al. (2020a) is used to predict $^{W}O^{2-}$ values from conventional EMP amphibole analyses.

(4) An anhydrous EMP analysis with all Fe reported as FeO can now be calculated on the basis of a (23 O + $^{W}O^{2-}$/2) formula.

(5) Formula correction protocols are checked against compositions of hypothetical stoichiometric amphiboles with chosen values for proportions of vacant sites and fixed values for Fe^{3+} and Fe^{2+} (Supplementary excel file 1). For any content of vacant sites in the A or B groups, a reliable estimate for Fe^{3+} should be possible with normalisation to 13 cations.

(6) The preferred $Fe^{3+}/\Sigma Fe$ ratio calculation protocol is assessed for published amphibole compositions for which Fe-valence has been determined by Mössbauer spectroscopy. A scheme is developed to quantify a value for any excess of cations in the C group (ΔC), giving the relationship $\Sigma^{13}_{cations} = \Sigma^{16}_{cations} - \Sigma(Ca + Na + K) - \Delta C$.

(7) The calculation protocol using a (23 + $^{W}O^{2-}$/2) O basis, followed by recalculation to a 13 cation formula is applied to a database of published EMP analyses for Ca-Na igneous rock amphiboles from: 1) differentiated sub- alkaline basic volcanics; 2) coeval quartz syenites and nepheline syenites; 3) metasomatised upper mantle rock types and their possible potassic partial melts (lamproites).

(8) Supplementary file 1 is an EXCEL spreadsheet with four folders for carrying

out (23 O + $^{W}O^{2-}$/2) calculations on the basis of: Folder I. 24 anion, 16 cation calculations for analyses which include values for H_2O, Fe_2O_3 and FeO; Folder (II) 23 O, 16 cation ($\Sigma16$) and 13 cation ($\Sigma^{13} = \Sigma^{16} - (Ca + Na + K)$) calculations to obtain formulae and Fe^{3+} estimates where $\Delta C = 0$); Folder (III) 23 O, 13 cation ($\Sigma^{13} = \Sigma^{16} - (Ca + Na + K) - \Delta C^{corrected}$), where $\Delta C^{corrected}$ deals with more than 5 atoms in C); and Folder (IV) 23 O, 13 cations based on the $^{W}O^{2-} = 2Ti$ relationship (Hawthorne et al., 1998; Henry & Daighe, 2018) using that version of the estimated $^{W}O^{2-}$ and equivalent $\Delta C^{corrected}$. This method uses the equation fitted to the wt. % TiO_2 *vs* atomic $^{W}O^{2-}$ values from 'training set' input data in Li et al. (2020a); the fitted equation slope is applied to our amphibole sample data using the excel relationship [$^{W}O^{2-} = MAX(0, 0.1473 \times (wt.\%TiO_2) + 0.0051)$], which sets negative values to zero (this work). Calculations obtained using folders (III) and (IV) give similar results and individual users could choose which one to use or could vary the value for the correction parameter in the attached spreadsheet.

Acknowledgements

Dr Kofi Owusu and Dr Fred Markanday kept CMBH on the right track with computer matters. Access to digital reference information was provided via the University of Manchester free of charge.

Declaration of Interests

The authors have no known competing financial interests or personal relationships that could appear to have influenced the work reported in this paper; both are Emeritus Professors and have not held any paid employment or received any specific grant from funding agencies in the public, commercial or not-for-profit sectors to support this work.

Data Availability

All analytical data are taken from published scientific publications and are attached here in Supplementary spreadsheet file 1. This file is accessible via Figshare at: https://doi.org/10.6084/m9.figshare.32446224. Download the excel spreadsheet on-to your computer and select Enable editing if necessary. Enter your EMP ana-lytical data into the appropriate columns (e.g., in Folder III use columns D to P and copy the **numerical** value for the conversion factor in column AP into column AQ). If necessary contact CMBH by email at michael.henderson@manchester.ac.uk.

CRediT Authorship Contribution Statement

C.M.B. Henderson: Data assembly, Conceptualization, Calculations. Writing original draft, Review and Editing. **R.H. Mitchell**: Review and Editing.

Conflicts of Interest

The authors declare no conflicts of interest regarding the publication of this paper.

References

Abdu, Y. A., & Hawthorne, F. C. (2009). Crystal Structure and Mossbauer Spectroscopy of Tschermakite from the Ruby Locality at Fiskenaesset, Greenland. *The Canadian Mineralogist, 47,* 917-926. https://doi.org/10.3749/canmin.47.4.917

Andersen, T., & Sørrensen, H. (1993). Crystallization and Metasomatism of Nepheline Syenite Xenoliths in Quartz-Bearing Intrusive Rocks in the Permian Oxlo rifr, SE Norway. *Norsk Geologisk Tidsskrift, 73,* 250-266.

Banerjee, S., Kyser, T. K., & Mitchell, R. H. (2018). Oxygen and Hydrogen Isotopic Composition of Phlogopites and Amphiboles in Diamond-Bearing Kimberlite Hosted MARID Xenoliths: Constraints on Fluid-Rock Interaction and Recycled Crustal Material in the Deep Continental Lithospheric Mantle. *Chemical Geology, 479,* 272-285. https://doi.org/10.1016/j.chemgeo.2018.01.022

Bernardini, S., Ventura, G. D., Schlüter, J., & Mihailova, B. (2023). Thermally-Activated Electron Hopping in Fe-Rich Amphiboles: Implications for the High-Conductivity Anomalies in Subduction Zones. *Geochemistry, 83,* Article ID: 125942. https://doi.org/10.1016/j.chemer.2022.125942

Berry, A. J., Yaxley, G. M., Woodland, A. B., & Foran, G. J. (2010). A XANES Calibration for Determining the Oxidation State of Iron in Mantle Garnet. *Chemical Geology, 278,* 31-37. https://doi.org/10.1016/j.chemgeo.2010.08.019

Binns, R. A. (1965). The Mineralogy of Metamorphosed Basic Rocks from the Willyama Complex, Broken Hill District, New South Wales. Part I. Hornblendes. *Mineralogical Magazine and Journal of the Mineralogical Society, 35,* 306-326. https://doi.org/10.1180/minmag.1965.035.270.05

Bonadiman, C., Brombin, V., Andreozzi, G. B., Benna, P., Coltorti, M., Curetti, N. et al. (2021). Phlogopite-Pargasite Coexistence in an Oxygen Reduced Spinel-Peridotite Ambient. *Scientific Reports, 11,* Article No. 11829. https://doi.org/10.1038/s41598-021-90844-w

Bonadiman, C., Nazzareni, S., Coltorti, M., Comodi, P., Giuli, G., & Faccini, B. (2014). Crystal Chemistry of Amphiboles: Implications for Oxygen Fugacity and Water Activity in Lithospheric Mantle beneath Victoria Land, Antarctica. *Contributions to Mineralogy and Petrology, 167,* Article No. 984. https://doi.org/10.1007/s00410-014-0984-8

Borley, G., & Frost, M. T. (1963). Some Observations on Igneous Ferrohastingsites. *Mineralogical Magazine and Journal of the Mineralogical Society, 33,* 646-662. https://doi.org/10.1180/minmag.1963.033.263.03

Chambers, A. D., & Brown, P. E. (1995). The Lilloise Intrusion, East Greenland: Fractionation of a Hydrous Alkali Picritic Magma. *Journal of Petrology, 36,* 933-963. https://doi.org/10.1093/petrology/36.4.933

Colombo, F., Rius, J., Molins, E., Biglia, H., Galliski, M. Á., Márquez-Zavalía, M. F. et al. (2023). Ferro-Ferri-Katophorite, a New Clinoamphibole from the Silicocarbonatite Dykes in Sierra De Maz, La Rioja, Argentina. *Mineralogical Magazine, 87,* 324-330. https://doi.org/10.1180/mgm.2023.2

Cosca, M. A., Essene, E. J., & Bowman, J. R. (1991). Complete Chemical Analyses of Metamorphic Hornblendes: Implications for Normalizations, Calculated H_2O Activities, and Thermobarometry. *Contributions to Mineralogy and Petrology, 108,* 472-484. https://doi.org/10.1007/bf00303451

Dawson, J. B., & Smith, J. V. (1973). Alkalic Pyroxenite Xenoliths from the Lashaine Volcano, Northern Tanzania. *Journal of Petrology, 14,* 113-131. https://doi.org/10.1093/petrology/14.1.113

Dawson, J. B., & Smith, J. V. (1977). The MARID (Mica-Amphibole-Rutile-Ilmenite-Di-

opside) Suite of Xenoliths in Kimberlite. *Geochimica et Cosmochimica Acta, 41,* 309-323. https://doi.org/10.1016/0016-7037(77)90239-3

Deer, W. A. (1938). Note on a Pegmatitic Hornblende from the Carsphairn Complex. *Geological Magazine, 74,* 359-361. https://doi.org/10.1017/s0016756800087756

Deer, W. A., Howie, R. A., & Zussman, J. (1966). *An Introduction to the Rock-Forming Minerals.* Longmans Group.

Deer, W. A., Howie, R. A., & Zussman, J. (1997). *Rock-Forming Minerals, Double-Chain Silicates, Volume 2B* (2nd ed., pp. i-xi, 1-764). The Geological Society.

Della Ventura, G., Bernardini, S., J. Redhammer, G., Galdenzi, F., Radica, F., Marcelli, A. et al. (2024). The Oxidation of Iron in Amphiboles at High Temperatures: A Review and Implications for Large-Scale Earth Processes. *Rendiconti Lincei. Scienze Fisiche e Naturali, 35,* 893-906. https://doi.org/10.1007/s12210-024-01280-7

Della Ventura, G., Galdenzi, F., Cibin, G., Oberti, R., Xu, W., Macis, S. et al. (2018). Iron Oxidation Dynamics *vs.* Temperature of Synthetic Potassic-Ferro-Richterite: A XANES Investigation. *Physical Chemistry Chemical Physics, 20,* 21764-21771. https://doi.org/10.1039/c8cp04249g

Della Ventura, G., Redhammer, G. J., Robert, J., Sergent, J., Iezzi, G., & Cavallo, A. (2016). Crystal-Chemistry of Synthetic Amphiboles along the Richterite-Ferro-Richterite Join: A Combined Spectroscopic (FTIR, Mössbauer), XRPD, and Microchemical Study. *The Canadian Mineralogist, 54,* 97-114. https://doi.org/10.3749/canmin.1500076

Droop, G. T. R. (1987). A General Equation for Estimating Fe^{3+} Concentrations in Ferromagnesian Silicates and Oxides from Microprobe Analyses, Using Stoichiometric Criteria. *Mineralogical Magazine, 51,* 431-435. https://doi.org/10.1180/minmag.1987.051.361.10

Dyar, M. D., Breves, E. A., Emerson, E., Bell, S. W., Nelms, M., Ozanne, M. V. et al. (2012). Accurate Determination of Ferric Iron in Garnets by Bulk Mossbauer Spectroscopy and Synchrotron Micro-Xanes. *American Mineralogist, 97,* 1726-1740. https://doi.org/10.2138/am.2012.4107

Dyar, M. D., Breves, E. A., Gunter, M. E., Lanzirotti, A., Tucker, J. M., Carey, C. J. et al. (2016). Use of Multivariate Analysis for Synchrotron Micro-Xanes Analysis of Iron Valence State in Amphiboles. *American Mineralogist, 101,* 1171-1189. https://doi.org/10.2138/am-2016-5556

Dyar, M. D., Mackwell, S. J., McGuire, A. V., Cross, L. R., & Robertson, J. D. (1993). Crystal Chemistry of Fe^{3+} and H^{+} in Mantle Kaersutites: Implications for Mantle Metsomatism. *American Mineralogist, 78,* 968-979.

Emmanuel, N. N., Rigobert, T., Anne, N., Roberto, S., André, P., & Jérôme, B. (2013). Structure and Petrology of Pan-African Nepheline Syenites from the South West Cameroon; Implications for Their Emplacement Mode, Petrogenesis and Geodynamic Significance. *Journal of African Earth Sciences, 87,* 44-58. https://doi.org/10.1016/j.jafrearsci.2013.07.008

Enders, M., McCammon, C. A., Maresch, W. V., & Speer, D. (2000). Ferric/ferrous Iron Ratios in Sodic Amphiboles: Mössbauer Analysis, Stoichiometry-Based Model Calculations and the High-Resolution Microanalytical Flank Method. *Contributions to Mineralogy and Petrology, 140,* 135-147. https://doi.org/10.1007/s004100000179

Fitzpayne, A., Giuliani, A., Hergt, J., Phillips, D., & Janney, P. (2018). New Geochemical Constraints on the Origins of MARID and PIC Rocks: Implications for Mantle Metasomatism and Mantle-Derived Potassic Magmatism. *Lithos, 318,* 478-493. https://doi.org/10.1016/j.lithos.2018.08.036

Galliski, M. A., Lira, R., & Dorais, M. J. (2004). Low-Pressure Differentiation of Melaneph-

elinitic Magma and the Origin of Ijolite Pegmatites at La Madera, Cordoba, Argentina. *The Canadian Mineralogist, 42,* 1799-1823. https://doi.org/10.2113/gscanmin.42.6.1799

Gatta, G. D., McIntyre, G. J., Oberti, R., & Hawthorne, F. C. (2017). Order of $^{[6]}Ti^{4+}$ in a Ti-Rich Calcium Amphibole from Kaersut, Greenland: A Combined X-Ray and Neutron Diffraction Study. *Physics and Chemistry of Minerals, 44,* 83-94. https://doi.org/10.1007/s00269-016-0839-0

Graham, C. M., Harmon, R. S., & Sheppard, S. M. F. (1984). Experimental Hydrogen Isotop Studies: Hydrogen Isotope Exchange between Amphibole and Water. *American Mineralogist, 69,* 128-138.

Guo, J., & Green, T. H. (1990). Experimental Study of Barium Partitioning between Phlogopite and Silicate Liquid at Upper-Mantle Pressure and Temperature. *Lithos, 24,* 83-95. https://doi.org/10.1016/0024-4937(90)90018-v

Hallimond, A. F. (1941). On the Graphical Representation of the Calciferous Amphiboles. *American Mineralogist, 28,* 65-87.

Han, K., Yi, L., Wang, D., Zhang, R., & Chen, P. (2024). Experimental Study on the Kinetics of Magnesiohornblende Dehydration and Its Implications. *American Mineralogist, 109,* 502-509. https://doi.org/10.2138/am-2022-8692

Harris, C., Marsh, J. S., & Milner, S. C. (1999). Petrology of the Alkaline Core of the Messum Igneous Complex, Namibia: Evidence for the Progressively Decreasing Effect of Crustal Contamination. *Journal of Petrology, 40,* 1377-1397. https://doi.org/10.1093/petroj/40.9.1377

Hawthorne, F. C. (1983). The Crystal Chemistry of the Amphiboles. *Canadian Mineralogist, 16,* 37-480.

Hawthorne, F. C., & Harlow, G. E. (2008). The Crystal Chemistry of Al-Rich Amphiboles: Sadanagaite and Potassic-Ferrisadanagaite. *The Canadian Mineralogist, 46,* 151-162. https://doi.org/10.3749/canmin.46.1.151

Hawthorne, F. C., & Oberti, R. (2007). Amphiboles: Crystal Chemistry. *Reviews in Mineralogy and Geochemistry, 67,* 1-54. https://doi.org/10.2138/rmg.2007.67.1

Hawthorne, F. C., Oberti, R., Harlow, G. E., Maresch, W. V., Martin, R. F., Schumacher, J. C. et al. (2012). Nomenclature of the Amphibole Supergroup. *American Mineralogist, 97,* 2031-2048. https://doi.org/10.2138/am.2012.4276

Hawthorne, F. C., Oberti, R., Zanetti, A., & Czamamnske, G. K. (1998). The Role of Ti in Hydrogen-Deficient Amphiboles: Sodic-Calci and Sodic Amphiboles from Coyote Peak, California. *Canadian Mineralogist, 36,* 1253-1265.

Henderson, C. M. B. (1968). Chemistry of Hastingsitic Amphiboles from the Marangudzi Igneous Complex, Southern Rhodesia. In *5th General Meeting, Cambridge 1966* (pp. 291-304). Mineralogical Society.

Henderson, C. M. B. (2025). Ti- and Ba-Rich Phlogopitic Micas in Alkaline Basic and Upper Mantle Igneous Rocks; Stoichiometry, Stability, and Fe Valence Estimation Reassessed and Rationalised. *Geochimica et Cosmochimica Acta, 406,* 57-81. https://doi.org/10.1016/j.gca.2024.10.011

Henderson, C. M. B., & Foland, K. A. (1996). Ba- and Ti-Rich Primary Biotite from the Brome Alkaline Igneous Complex. Monteregian Hills, Quebec: Mechanisms of Substitution. *Canadian Mineralogist, 34,* 1241-1252.

Henderson, C. M. B., Pearce, C. I., Charnock, J. M., Harrison, R. J., & Rosso, K. M. (2016). An X-Ray Magnetic Circular Dichroism (XMCD) Study of Fe Ordering in a Synthetic $MgAl_2O_4$-Fe_3O_4 (Spinel-Magnetite) Solid-Solution Series: Implications for Magnetic Properties and Cation Site Ordering. *American Mineralogist, 101,* 1373-1388.

https://doi.org/10.2138/am-2016-5612

Henderson, C. M. B., Pendlebury, K., & Foland, K. A. (1989). Mineralogy and Petrology of the Red Hill Alkaline Igneous Complex, New Hampshire, U.S.A. *Journal of Petrology, 30,* 627-666. https://doi.org/10.1093/petrology/30.3.627

Henry, D. J., & Daigle, N. M. (2018). Chlorine Incorporation into Amphibole and Biotite in High-Grade Iron-Formations: Interplay between Crystallography and Metamorphic Fluids. *American Mineralogist, 103,* 55-68. https://doi.org/10.2138/am-2018-6143

Hezel, D. C., Höfer, H. E., & Fichtner, A. (2024). A Fast Open Data Reduction Workflow for the Electron Microprobe Flank Method to Determine $Fe^{3+}/\sigma Fe$ Contents in Minerals. *American Mineralogist, 109,* 1387-1393. https://doi.org/10.2138/am-2023-9122

Höfer, H. E., Weinbruch, S., Mccammon, C. A., & Brey, G. P. (2000). Comparison of Two Electron Probe Microanalysis Techniques to Determine Ferric Iron in Synthetic Wüstite Samples. *European Journal of Mineralogy, 12,* 63-71. https://doi.org/10.1127/0935-1221/2000/0012-0063

Ishida, K., Hawthorne, F. C., & Ando, Y. (2002). Fine Structure of Infrared Oh-Stretching Bands in Natural and Heat-Treated Amphiboles of the Tremolite-Ferro-Actinolite Series. *American Mineralogist, 87,* 891-898. https://doi.org/10.2138/am-2002-0712

Kitamura, M., Tokonami, M., & Morimoto, N. (1975). Distribution of Titanium Atoms in Oxy-Kaersutite. *Contributions to Mineralogy and Petrology, 51,* 167-172. https://doi.org/10.1007/bf00372077

Kaur, G., & Mitchell, R. H. (2019). Mineralogy of the Baotite-Bearing Gundrapalli Lamproite, Nalgonda District, Telangana, India. *Mineralogical Magazine, 83,* 401-411. https://doi.org/10.1180/mgm.2018.169

Landoll, J. D., Foland, K. A., & Henderson, C. M. B. (1989). Excess Argon in Amphiboles from Fluid Interaction and Short Intrusion Interval at the Epizonal Marangudzi Complex, Zimbabwe. *Journal of Geophysical Research: Solid Earth, 94,* 4053-4069. https://doi.org/10.1029/jb094ib04p04053

Leake, B. E., Woolley, A. R., Arps, C. E. S., Birch, W. D., Gilbert, M. C., Grice, J. D. et al. (1997). Nomenclature of Amphiboles; Report of the Subcommittee on Amphiboles of the International Mineralogical Association Commission on New Minerals and Mineral Names. *Mineralogical Magazine, 61,* 295-310. https://doi.org/10.1180/minmag.1997.061.405.13

Lhachmi, A., Lorand, J. P., & Fabries, J. (2001). Pétrologie de l'intrusion alcaline mésozoïque de la région d'Anemzi, Haut Atlas Central, Maroc. *Journal of African Earth Sciences, 32,* 741-764. https://doi.org/10.1016/s0899-5362(02)00052-0

Li, X., Zhang, C., Almeev, R. R., Zhang, X., Zhao, X., Wang, L. et al. (2019). Electron Probe Microanalysis of $Fe^{2+}/\sigma Fe$ Ratios in Calcic and Sodic-Calcic Amphibole and Biotite Using the Flank Method. *Chemical Geology, 509,* 152-162. https://doi.org/10.1016/j.chemgeo.2019.01.009

Li, X., Zhang, C., Behrens, H., & Holtz, F. (2020a). Calculating Amphibole Formula from Electron Microprobe Analysis Data Using a Machine Learning Method Based on Principal Components Regression. *Lithos, 362,* Article ID: 105469. https://doi.org/10.1016/j.lithos.2020.105469

Li, X., Zhang, C., Behrens, H., & Holtz, F. (2020b). Corrigendum to "Calculating Biotite Formula from Electron Microprobe Analysis Data Using a Machine Learning Method Based on Principal Components Regression" [Lithos 356-357 (2020) 105371]. *Lithos, 362,* Article ID: 105506. https://doi.org/10.1016/j.lithos.2020.105506

Locock, A. J. (2014). An Excel Spreadsheet to Classify Chemical Analyses of Amphiboles

Following the IMA 2012 Recommendations. *Computers & Geosciences, 62,* 1-11. https://doi.org/10.1016/j.cageo.2013.09.011

Lukošius-Sanders, J. (1988). Petrology of Syenites from Centre III of the Coldwell Alkaline Complex, Northweatern Ontario. Master's Thesis, Lakehead University.

Marks, M. A. W., Schilling, J., Coulson, I. M., Wenzel, T., & Markl, G. (2008). The Alkaline-Peralkaline Tamazeght Complex, High Atlas Mountains, Morocco: Mineral Chemistry and Petrological Constraints for Derivation from a Compositionally Heterogeneous Mantle Source. *Journal of Petrology, 49,* 1097-1131. https://doi.org/10.1093/petrology/egn019

Mitchell, R. H. (1990). A Review of the Compositional Variation of Amphiboles in Alkaline Plutonic Complexes. *Lithos, 26,* 135-156. https://doi.org/10.1016/0024-4937(90)90044-2

Mitchell, R. H., & Platt, R. G. (1978). Mafic Mineralogy of Ferroaugite Syenite from the Coldwell Alkaline Complex, Ontario, Canada. *Journal of Petrology, 19,* 627-651. https://doi.org/10.1093/petrology/19.4.627

Mitchell, R. H., & Platt, R. G. (1982). Mineralogy and Petrology of Nepheline Syenites from the Coldwell Alkaline Complex, Ontario, Canada. *Journal of Petrology, 23,* 186-214. https://doi.org/10.1093/petrology/23.2.186

Mogahed, M. M. (2016). Petrogenesis of Cogenetic Silica-Oversaturated and -Undersaturated Syenites of Abu Khruq Ring Complex, South Eastern Desert, Egypt. *Journal of African Earth Sciences, 124,* 44-62. https://doi.org/10.1016/j.jafrearsci.2016.09.010

Möller, V., & Williams-Jones, A. E. (2016). Petrogenesis of the Nechalacho Layered Suite, Canada: Magmatic Evolution of a REE-Nb-Rich Nepheline Syenite Intrusion. *Journal of Petrology, 57,* 229-276. https://doi.org/10.1093/petrology/egw003

Moreau, C., Ohnenstetter, D., Demaiffe, D., & Robineau, B. (1996). The Los Archipelago Nepheline Syenite Ring-Structure: A Magmatic Marker of the Evolution of the Central and Equatorial Atlantic. *Canadian Mineralogist, 34,* 281-299.

Morogan, V., Upton, B. G. J., & Fitton, J. G. (2000). The Petrology of the Ditrau Alkaline Complex, Eastern Carpathians. *Mineralogy and Petrology, 69,* 227-265. https://doi.org/10.1007/s007100070023

Nasir, S., & Al-Rawas, A.D. (2006). Mossbauer Characterization of Upper Mantle Ferrikaersutite. *American Mineralogist, 91,* 1163-1169. https://doi.org/10.2138/am.2006.2128

Oberti, R., Boiocchi, M., Hawthorne, F. C., & Ciriotti, M. E. (2018). Magnesio-Hornblende from Lüderitz, Namibia: Mineral Description and Crystal Chemistry. *Mineralogical Magazine, 82,* 1253-1259. https://doi.org/10.1180/minmag.2017.081.093

Oberti, R., Boiocchi, M., Hawthorne, F. C., Ball, N. A., & Chiappino, L. (2016). Magnesio-ferri-Fluoro-Hornblende from Portoscuso, Sardinia, Italy: Description of a Newly Approved Member of the Amphibole Supergroup. *Mineralogical Magazine, 80,* 269-275. https://doi.org/10.1180/minmag.2016.080.008

Oberti, R., Boiocchi, M., Smith, D. C., & Medenbach, O. (2007a). Aluminotaramite, Alumino-Magnesiotaramite, and Fluoro-Alumino-Magnesiotaramite: Mineral Data and Crystal Chemistry. *American Mineralogist, 92,* 1428-1435. https://doi.org/10.2138/am.2007.2529

Oberti, R., Hawthorne, F. C., Cannillo, E., & Camara, F. (2007b). Long-Range Order in Amphiboles. *Reviews in Mineralogy and Geochemistry, 67,* 125-171. https://doi.org/10.2138/rmg.2007.67.4

Oberti, R., Boiocchi, M., & Smith, D. C. (2003). Fluoronyböite from Jianchang (Su-Lu, China) and Nyböite from Nybö (Nordfjord, Norway): A Petrological and Crystal-Chem-

ical Comparison of These Two High-Pressure Amphiboles. *Mineralogical Magazine, 67,* 769-782. https://doi.org/10.1180/0026461036740133

Oberti, R., Ungaretti, L., Cannillo, E., & Hawthorne, F. C. (1992). The Behaviour of Ti in Amphiboles: I. Four- and Six-Coordinate Ti in Richterite. *European Journal of Mineralogy, 4,* 425-440. https://doi.org/10.1127/ejm/4/3/0425

Popp, R. K., Hibbert, H. A., & Lamb, W. M. (2006). Oxy-Amphibole Equilibria in Ti-Bearing Calcic Amphiboles: Experimental Investigation and Petrologic Implications for Mantle-Derived Amphiboles. *American Mineralogist, 91,* 54-66. https://doi.org/10.2138/am.2006.1838

Prider, R. T. (1939). Some Minerals from the Leucite-Rich Rocks of the West Kimberley Area, Western Australia. *Mineralogical Magazine and Journal of the Mineralogical Society, 25,* 373-387. https://doi.org/10.1180/minmag.1939.025.166.01

Ridolfi, F., & Renzulli, A. (2012). Calcic Amphiboles in Calc-Alkaline and Alkaline Magmas: Thermobarometric and Chemometric Empirical Equations Valid up to 1,130°C and 2.2 GPA. *Contributions to Mineralogy and Petrology, 163,* 877-895. https://doi.org/10.1007/s00410-011-0704-6

Ridolfi, F., Zanetti, A., Renzulli, A., Perugini, D., Holtz, F., & Oberti, R. (2018). AMFORM, a New Mass-Based Model for the Calculation of the Unit Formula of Amphiboles from Electron Microprobe Analyses. *American Mineralogist, 103,* 1112-1125. https://doi.org/10.2138/am-2018-6385

Righter, K., Dyar, M. D., Delaney, J. S., Vennemann, T. W., Hervig, R. L., & King, P. L. (2002). Correlations of Octahedral Cations with OH^-, O^{2-}, Cl^-, and F^- in Biotite from Volcanic Rocks and Xenoliths. *American Mineralogist, 87,* 142-153. https://doi.org/10.2138/am-2002-0115

Riishuus, M. S., Peate, D. W., Tegner, C., Wilson, J. R., & Brooks, C. K. (2008). Petrogenesis of Cogenetic Silica-Oversaturated and -Undersaturated Syenites by Periodic Recharge in a Crustally Contaminated Magma Chamber: The Kangerlussuaq Intrusion, East Greenland. *Journal of Petrology, 49,* 493-522. https://doi.org/10.1093/petrology/egm090

Robinson, G. W., Grice, J. D., Gault, R. A., & Lalonde, A. E. (1997). Potassicpargasite, a New Member of the Member Group from Pargas, Turku-Pori, Finland. *Canadian Mineralogist, 35,* 1535-1540.

Robinson, P., Spear, F. S., Schumacher, J. C., Laird, J., Klein, C., Evans, B. W. et al. (1982). Chapter 1. Phase Relations of Metamorphic Amphiboles: Natural Occurrence and Theory. In D. R. Veblen, & P. H. Ribbe (Eds.), *Amphiboles* (pp. 1-228). De Gruyter. https://doi.org/10.1515/9781501508196-005

Saini, J., Kaur, P., Mitchell, R. H., & Kaur, G. (2022). Mineralogy of the Marepalli Lamproite Dyke from the Nalgonda District, Telangana, Southern India. *Mineralogical Magazine, 86,* 799-813. https://doi.org/10.1180/mgm.2022.49

Satoh, H., Yamaguchi, Y., & Makino, K. (2004). Ti-Substituion Mechamism in Plutonic Oxy-Kaersutite from the Larvik Alkaline Complex, Oslo Rift, Norway. *Mineralogical Magazine, 68,* 687-697.

Schumacher, J. C. (1991). Empirical Ferric Iron Corrections: Necessity, Assumptions, and Effects on Selected Geothermobarometers. *Mineralogical Magazine, 55,* 3-18. https://doi.org/10.1180/minmag.1991.055.378.02

Schumacher, J. C. (2007). Metamorphic Amphiboles: Composition and Coexistence. *Reviews in Mineralogy and Geochemistry, 67,* 359-416. https://doi.org/10.2138/rmg.2007.67.10

Stout, J. H. (1972). Phase Petrology and Mineral Chemistry of Coexisting Amphiboles from

Telemark, Norway. *Journal of Petrology, 13,* 99-145. https://doi.org/10.1093/petrology/13.1.99

Taran, M. N., Andrut, M., Polshin, E. V., & Matsyuk, S. S. (1999). Optical Spectroscopy Study of Natural Fe, Ti-Bearing Calcic Amphiboles. *Physics and Chemistry of Minerals, 27,* 59-69. https://doi.org/10.1007/s002690050241

Tiepolo, M., Zanetti, A., & Oberti, R. (1999). Detection, Crystal-Chemical Mechanisms and Petrological Implications of [6]Ti^{4+} Partitioning in Pargasite and Kaersutite. *European Journal of Mineralogy, 11,* 345-354. https://doi.org/10.1127/ejm/11/2/0345

Tilley, C. E., & Vincent, H. C. G. (1937). The Paragenesis of Kyanite-Amphibolites (with Plate xx.). *Mineralogical Magazine and Journal of the Mineralogical Society, 24,* 555-568. https://doi.org/10.1180/minmag.1937.024.158.02

Tindle, A. G., & Webb, P. C. (1994). Probe-AMPH—A Spreadsheet Program to Classify Microprobe-Derived Amphibole Analyses. *Computers & Geosciences, 20,* 1201-1228. https://doi.org/10.1016/0098-3004(94)90071-x

Underwood, S. J., Feeley, T. C., & Clynne, M. A. (2012). Hydrogen Isotope Investigation of Amphibole and Biotite Phenocrysts in Silicic Magmas Erupted at Lassen Volcanic Center, California. *Journal of Volcanology and Geothermal Research, 227,* 32-49. https://doi.org/10.1016/j.jvolgeores.2012.02.019

Underwood, S. J., Feeley, T. C., & Clynne, M. A. (2013). Hydrogen Isotope Investigation of Amphibole and Glass in Dacite Magmas Erupted in 1980-1986 and 2005 at Mount St. Helens, Washington. *Journal of Petrology, 54,* 1047-1070. https://doi.org/10.1093/petrology/egt005

Uvarova, Y., Sokolova, E., Hawthorne, F. C., McCammon, C. A., Kazansky, V. I., & Lobanov, K. V. (2007). Amphiboles from the Kola Superdeep Borehole: Fe^{3+} Contents from Crystal-Chemical Analysis and Mössbauer Spectroscopy. *Mineralogical Magazine, 71,* 651-669. https://doi.org/10.1180/minmag.2007.071.6.651

Ventruti, G., Caggianelli, A., Festa, V., & Langone, A. (2020). Crystal Chemistry of Barian Titanian Phlogopite from a Lamprophyre of the Gargano Promontory (Apulia, Southern Italy). *Minerals, 10,* Article 766. https://doi.org/10.3390/min10090766

Virgo, D., & Popp, R. k. (2000). Hydrogen Deficiency in Mantle-Derived Phlogopites. *American Mineralogist, 85,* 753-759. https://doi.org/10.2138/am-2000-5-614

Wagner, C., Deloule, E., & Mokhtari, A. (1996). Richterite-bearing Peridotites and Marid-Type Inclusions in Lavas from North Eastern Morocco: Mineralogy and D/H Isotopic Studies. *Contributions to Mineralogy and Petrology, 124,* 406-421. https://doi.org/10.1007/s004100050200

Whittaker, E. J. W. (1981). *Crystallography: An Introduction for Earth Science (and Other Solid State) Students* (pp. xii, 254). Pergamon Press.

Wilke, M., Farges, F., Petit, P., Brown, G. E., & Martin, F. (2001). Oxidation State and Coordination of Fe in Minerals: An Fe *k*-XANES Spectroscopic Study. *American Mineralogist, 86,* 714-730. https://doi.org/10.2138/am-2001-5-612

Woolley, A. R., & Garth Platt, R. (1986). The Mineralogy of Nepheline Syenite Complexes from the Northern Part of the Chilwa Province, Malawi. *Mineralogical Magazine, 50,* 597-610. https://doi.org/10.1180/minmag.1986.050.358.05

Worley, B. A., & Cooper, A. F. (1995). Mineralogy of the Dismal Nepheline Syenite, Southern Victoria Land, Antarctica. *Lithos, 35,* 109-128. https://doi.org/10.1016/0024-4937(94)00049-8

Zaitsev, A. N., Avdontseva, E. Y., Britvin, S. N., Demény, A., Homonnay, Z., Jeffries, T. E. et al. (2013). Oxo-Magnesio-Hastingsite, $NaCa_2(Mg_2Fe^{3+}{}_3)(Al_2Si_6)O_{22}O_2$, a New Anhy-

drous Amphibole from the Deeti Volcanic Cone, Gregory Rift, Northern Tanzania. *Mineralogical Magazine, 77,* 2773-2792. https://doi.org/10.1180/minmag.2013.077.6.06

Zhu, Y. S., Yang, J. H., Sun, J., Zhang, J. G., & Wu, F. Y. (2016). Petrogenesis of Coeval Silica-Saturated and Silica-Undersaturated Alkaline Rocks: Mineralogical and Geochemical Evidence from the Saima Alkaline Complex, NE China. *Journal of Asian Earth Sciences, 117,* 184-207. https://doi.org/10.1016/j.jseaes.2015.12.014

Appendix

https://doi.org/10.6084/m9.figshare.32446224